

Glutamatergic Involvement in Ethanol Withdrawal Convulsion Susceptibility and Resistance

by
Jennifer F. Buckman

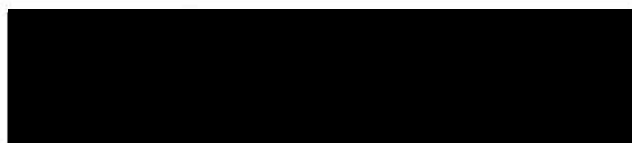
A DISSERTATION

Presented to the Department of Behavioral Neuroscience
And the Oregon Health Sciences University
School of Medicine
in partial fulfillment of
the requirements for the degree of
Doctor of Philosophy
September 1998

School of Medicine
Oregon Health Sciences University

CERTIFICATE OF APPROVAL

This is certify that the Ph.D. thesis of
Jennifer F. Buckman
has been approved



Charles K. Meshul, Mentor

John C. Crabbe, Member



Deborah A. Finn, Member



Aaron Janowsky, Member



William Woodward, Chair

Richard Maurer, Associate Dean for Graduate Studies

TABLE OF CONTENTS

Tables and Figures	iv
List of Abbreviations	vii
Acknowledgments	ix
Abstract	x
Introduction	1
Glutamate Transporters	3
Seizures	6
Ethanol	8
Glutamine Synthetase and Glial Fibrillary Acidic Protein	9
Seizures	10
Ethanol	10
Cytochrome Oxidase	12
Seizures	14
Ethanol	15
Behavior and Animal Model	17
Behavior	17
Genetics	18
Animal Model	19
Rationale	23
Overall Aim	23
Anatomical Considerations	24
Specific Aim #1: To determine glutamate transporter activity and protein density in WSP and WSR mice in their naive state	25
Specific Aim #2: To determine glutamate transporter activity in WSP and WSR mice following exposure to EtOH or HICs	26

Specific Aim #3: To determine the density of glutamine synthetase and glial fibrillary acidic protein in naive WSP and WSR mice	27
Specific Aim #4: To determine the amount of cytochrome oxidase activity in naive WSP and WSR mice	29
Material and Methods	30
Chemicals and Reagents	30
Animals	30
Procedures	31
Handling and HICs	31
Acute EtOH intoxication	31
<i>In vitro</i> EtOH	31
EtOH withdrawal	32
Glutamate Uptake	32
Crude Synaptosomal Preparation	32
Synaptosomal L-[³ H]glutamate uptake	33
Blood Ethanol Measurements	33
Immunocytochemistry and Histochemistry	34
Slice Preparation	34
Immunoperoxidase Reaction	34
Histochemical Reaction	35
Optical Density Measurements	36
Statistics	37
Kinetic and statistical analysis of glutamate uptake experiments	37
Statistical analysis of immunocytochemical and histochemical experiments	37

Results	40
Glutamate Uptake Experiments	40
Effect of handling on [³ H]glutamate uptake	40
Effect of acute HIC activity on [³ H]glutamate uptake	40
Effect of EtOH intoxication on [³ H]glutamate uptake	41
Effect of <i>in vitro</i> EtOH exposure on [³ H]glutamate uptake	41
Effect of EtOH withdrawal on [³ H]glutamate uptake	42
Glutamate Transporter Immunolabeling	43
GLAST	43
GLT-1	43
EAAC1	44
Glutamine Synthetase Immunolabeling	44
Glial Fibrillary Acidic Protein Immunolabeling	44
Cytochrome Oxidase Activity	45
Discussion	46
Naive Glutamate Uptake and Transporter Subtype Immunolabeling	46
Glutamate Uptake in WSP and WSR mice following HICs or EtOH	49
Glutamine Synthetase and Glial Fibrillary Acidic Protein Immunolabeling	53
Cytochrome Oxidase Activity	57
Summary and Conclusions	61
References	64

TABLES AND FIGURES

<u>Table 1</u>	Data supporting involvement of glutamate uptake and metabolism in seizures	87
<u>Table 2</u>	Evidence for a role of glutamate uptake and metabolism in EtOH-related behaviors	89
<u>Table 3</u>	Scale for measuring severity of handling-induced convulsions	90
<u>Table 4</u>	Summary of results from experiments performed in drug- and convulsion-naïve WSP and WSR mice	117
<u>Table 5</u>	Summary of results from L-[³ H] glutamate uptake experiments	118
<u>Figure 1</u>	Cartoon of glutamatergic neurotransmission: neuronal and glial roles in synthesis and metabolism	91
<u>Figure 2</u>	Regional analysis of the density of immunoperoxidase labeling	92
<u>Figure 3</u>	L-[³ H] glutamate uptake into hippocampal synaptosomes from colony raised (CR) and specially raised (SR) WSP and WSR mice	93
<u>Figure 4</u>	L-[³ H] glutamate uptake into cortical synaptosomes from colony raised (CR) and specially raised (SR) WSP and WSR mice	94
<u>Figure 5</u>	L-[³ H] glutamate uptake into hippocampal synaptosomes from naïve and handled WSP and WSR mice	95
<u>Figure 6</u>	L-[³ H] glutamate uptake into cortical synaptosomes from naïve and handled WSP and WSR mice	96
<u>Figure 7</u>	L-[³ H] glutamate uptake into hippocampal synaptosomes following injection of saline or a hypnotic dose of EtOH in WSP and WSR mice	97
<u>Figure 8</u>	L-[³ H] glutamate uptake into cortical synaptosomes from following injection of saline or a hypnotic dose of EtOH in WSP and WSR	98

mice

<u>Figure 9</u>	Dose-dependent inhibition of L-[³ H]glutamate uptake by <i>in vitro</i> exposure to EtOH, PDC or kainic acid	99
<u>Figure 10</u>	Effect of withdrawal from exposure to 72 hour EtOH vapor on L-[³ H]glutamate uptake in hippocampal synaptosomes	100
<u>Figure 11</u>	L-[³ H]glutamate uptake into hippocampal synaptosomes from WSP and WSR mice during peak withdrawal from chronic EtOH inhalation	101
<u>Figure 12</u>	Correlation of uptake parameters and blood-ethanol concentration (BEC)	102
<u>Figure 13</u>	Immunoperoxidase staining for GLAST in naive WSP and WSR mice	103
<u>Figure 14</u>	Density of the glial transporter GLAST immunolabeling in hippocampus and cortex	104
<u>Figure 15</u>	Immunoperoxidase staining for GLT-1 in naive WSP and WSR mice	105
<u>Figure 16</u>	Density of the glial transporter GLT-1 immunolabeling in hippocampus and cortex	106
<u>Figure 17</u>	Immunoperoxidase staining for EAAC1 in naive WSP and WSR mice	107
<u>Figure 18</u>	Density of the glial transporter EAAC1 immunolabeling in hippocampus and cortex	108
<u>Figure 19</u>	Immunoperoxidase staining for glutamine synthetase in naive WSP and WSR mice	109
<u>Figure 20</u>	Density of glutamine synthetase (GS) immunolabeling in hippocampus and cortex	110
<u>Figure 21</u>	Low magnification immunoperoxidase staining for GFAP in naive WSP and WSR mice	111

<u>Figure 22</u>	High magnification immunoperoxidase staining for GFAP in naive WSP and WSR mice	112
<u>Figure 23</u>	Density of GFAP immunolabeling in hippocampus and cortex	113
<u>Figure 24</u>	GFAP immunoreactivity within single glial cells from the CA1 of the hippocampus	114
<u>Figure 25</u>	Cytochrome oxidase activity assessed by peroxidase reactivity in naive WSP and WSR mice	115
<u>Figure 26</u>	Cytochrome oxidase activity in hippocampus and cortex	116

LIST OF ABBREVIATIONS

ANOVA	analysis of variance
ATP	adenosine triphosphate
BEC	blood ethanol concentration
CA1	CA1 subfield of the hippocampus
CA3	CA3 subfield of the hippocampus
CNS	central nervous system
CONT	control
DAB	3',3-diaminobenzidine
DG	dentate gyrus
EAAC1	excitatory amino acid carrier 1
EAAT	excitatory amino acid transporter
EBSS	Earles balanced salt solution
EM	electron microscopy
EtOH	ethanol
GABA	gamma aminobutyric acid
GEPR	genetically epilepsy prone rats
GFAP	glial fibrillary acidic protein
GLAST	glutamate/aspartate transporter
GLT-1	glutamate transporter 1
GS	glutamine synthetase
HIC	handling-induced convulsion
i.p.	intraperitoneal
K_m	affinity of the transporter for glutamate
NMDA	N-methyl-d-aspartate
PDC	L-trans-pyrrolidine-2,4-dicarboxylic acid
PYR	pyrazole

SAL	saline
SEM	standard error of the mean
SSC	somatosensory cortex
V_{\max}	maximal glutamate uptake
WSP	Withdrawal Seizure-Prone
WSR	Withdrawal Seizure-Resistant
2-DG	2-deoxyglucose

ACKNOWLEDGMENTS

I gratefully acknowledge the support and guidance of my advisor, **Charlie Meshul**. His enthusiasm and patience created the optimal training environment for me.

I would also like to thank **Aaron Janowsky**, for giving me the opportunity to work in his laboratory and learn the techniques necessary for the glutamate uptake experiments and for functioning as a co-advisor for the past two years; **John Crabbe**, for his support and assistance in developing this project as well as for the contribution of the animals used in these experiments; **Amy Eshleman**, for her technical assistance in the glutamate uptake experiments in the Janowsky lab; **Christina Lessov**, for assisting with the animal handling and treatment for the glutamate uptake assays; **Janet Dorow** and **Deb Finn**, for helping with the ethanol chamber studies; **Bill Woodward**, for his assistance with the light microscopic immunolabeling data analysis; and **Cindy Allen**, for her support and technical assistance that made the successful completion of the light and electron microscopic studies possible.

ABSTRACT

Withdrawal Seizure-Prone (WSP) and Withdrawal Seizure-Resistant (WSR) mice exhibit differences in handling-induced convulsion (HIC) severity during ethanol (EtOH) withdrawal. EtOH- and HIC-naïve WSP mice have a greater density of hippocampal nerve terminal glutamate immunoreactivity than naïve WSR mice. Stimuli eliciting convulsions in EtOH-naïve WSP mice decrease the density of presynaptic glutamate immunolabeling in the hippocampus. When exposed to the same stimuli, EtOH-naïve WSR mice do not exhibit convulsions or changes in glutamate immunoreactivity. Thus, the glutamatergic system may underlie the behavioral differences observed between the WSP and WSR mice.

To test the role of the glutamatergic system in susceptibility to and expression of EtOH-withdrawal convulsions, L-[³H]glutamate uptake and the immunolabeling density of the glutamate transporters and glutamine synthetase in the hippocampus and cortex of WSP and WSR mice were measured. To determine whether structural differences in glial cells exist between the selected lines, the immunolabeling density of glial fibrillary acidic protein (GFAP) was assessed. To ascertain whether differences in neuronal activity exist, cytochrome oxidase activity was characterized.

L-[³H]glutamate uptake into hippocampal and cortical synaptosomes was characterized in mice that were handling- and EtOH-naïve or in mice following exposure to handling, repeated HICs, acute EtOH intoxication, acute *in vitro* EtOH exposure or withdrawal following chronic EtOH exposure. The density of immunolabeling of glutamine synthetase and GFAP and of the sodium-dependent, high affinity glutamate transporters, GLAST, GLT-1 and EAAC1, was assessed in the hippocampus and cortex of naïve mice. In addition, cytochrome oxidase activity was measured in these regions.

Hippocampal and cortical synaptosomal L-[³H]glutamate uptake did not differ between naïve WSP and WSR mice, nor did it differ following exposure to handling, convulsions, a hypnotic dose of EtOH (4g/kg) or *in vitro* exposure to EtOH (5-320mM).

However, withdrawal from 72 hours of EtOH exposure significantly increased L-[³H]glutamate uptake in both mouse lines as compared to EtOH-naive controls. The observed increases in glutamate uptake during withdrawal may be associated with compensatory adaptations to chronic intoxication which are independent of the selected differences for withdrawal severity.

The immunoreactivity of the glial transporter, GLAST, was significantly greater in CA1 of the hippocampus of naive WSP-2 mice than in WSR-2 mice. No differences in the glial transporter, GLT-1, or the neuronal transporter, EAAC1, were observed between the mouse lines in CA1, although a trend towards a greater GLT-1 immunolabeling was observed in CA3 of the hippocampus of naive WSP mice. The density of glutamine synthetase immunolabeling in naive WSP and WSR mice was not significantly different, but naive WSP-2 mice tended to exhibit more labeling than WSR-2 mice in the CA1. A trend toward lower GFAP labeling in naive WSP (versus WSR) mice was observed in all brain regions tested. Analysis of cytochrome oxidase activity revealed no differences between naive WSP and WSR mice. Taken together, these data offer modest evidence that alterations in glutamate uptake and metabolism may be responsible for the differences between the lines in the nerve terminal pool of glutamate in CA1 and that glia may play a pivotal role in susceptibility to drug-naive and -withdrawal convulsions observed in WSP mice.

INTRODUCTION

Glutamate is the predominant excitatory neurotransmitter in the central nervous system (Fonnum, 1984). It is an amino acid that is neurotoxic at high extracellular concentrations. Being both ubiquitously distributed in the brain and potentially damaging to neurons, extracellular glutamate concentrations must be stringently controlled to prevent overstimulation of postsynaptic glutamate receptors (Choi, 1988). Glutamate receptor hyperactivity has been implicated as an underlying mechanism in Alzheimer's disease, Huntington's disease, amyotrophic lateral sclerosis, epilepsy, ischemia, hypoglycemia, anoxia and drug dependence (for review, see Lipton and Rosenberg, 1994).

Normal glutamatergic neurotransmission is maintained by balancing transmitter availability, release and uptake (Bradford et al., 1978; Hamberger et al., 1979b; Attwell et al., 1993). Pre- and postsynaptic neuronal structures as well as astrocytes are involved in regulating the function of the glutamate system (Fig. 1). Although numerous biosynthetic pathways for glutamate are known, glutamine is thought to be a major precursor for vesicular glutamate (Bradford et al., 1978; Hamberger et al., 1979a, b; Ward et al., 1983). Glutamine is converted to glutamate presynaptically by the mitochondrial enzyme, glutaminase (Bradford et al., 1978). Once released, a complex system of transporters is responsible for removing glutamate from the synaptic cleft (Pines et al., 1992, Storck et al., 1992; Kanai and Hediger, 1992; Fairman et al., 1994; Arriza et al., 1997). These transporters are found on astroglial cell processes and postsynaptic structures, such as dendritic shafts and spines (Rothstein et al., 1994, Lehre et al., 1995). The majority of glutamate uptake occurs into glial processes located in close apposition to glutamatergic nerve terminals (Rothstein et al., 1996; Derouiche and Rauen, 1995). Astrocytes contain the enzyme, glutamine synthetase, which metabolizes glutamate into glutamine. This glutamine can be released perisynaptically, taken up into nerve terminals and converted back into glutamate (Hamberger et al., 1979b). Direct associations between astrocytic

glutamate uptake and metabolism (Norenberg, 1979; Derouiche and Rauen, 1995), glutamate metabolism (by glutamine synthetase) and glutamate synthesis (Hamberger et al., 1979b), glutamate synthesis and glutamate release (Bradford et al., 1978; Hamberger, 1979b), and glutamate release and uptake (Mennerick and Zorumski, 1994) have been reported. Thus, each step in this neuron-glia cycle must be precisely balanced to ensure normal CNS excitatory activity.

The stability of excitatory activity is highly dependent on adenosine triphosphate (ATP) and depletion of ATP is associated with massive glutamate overflow and hyperactivation of glutamate receptors (Lipton and Rosenberg, 1994). The majority of ATP in the brain is utilized to drive the Na^+/K^+ ATPases that regulate neuronal resting membrane potential (Erecinska and Silver, 1989). Electrogenic glutamate transporters use the Na^+ and K^+ gradients to drive uptake (Madl and Burgesser, 1993; Pellerin and Magistretti, 1997). In addition, the astrocytic metabolic enzyme, glutamine synthetase, is ATP dependent and may be compromised by energy disruption (Lipton and Rosenberg, 1994). Thus, the removal of glutamate from the synaptic cleft and the metabolism of glutamate by glial cells are dependent on sufficient energy availability and may become impaired during states of energy disruption.

Seizures are observed as periods of intense CNS activity, and energy availability may become insufficient during these episodes (Glass and Dragunow, 1995). Ethanol (EtOH) is a CNS depressant, and withdrawal following chronic exposure is associated with a rebound increase in CNS activity (Michaelis et al., 1980; Lovinger, 1993). Singh et al. (1994) reported that exposing cortical cultures to EtOH results in neuronal damage, inhibition of astrocytic glutamate uptake and increased glutamate efflux. These EtOH-induced alterations are similar to those seen during states of glucose deprivation (Singh et al., 1994). Additionally, EtOH and EtOH-withdrawal exert direct effects on Na^+/K^+ ATPases (Swann, 1990; Rangaraj and Kalant, 1978). Therefore, the ATP-dependent components of the glutamatergic system (i.e. the glutamate transporters and glutamine

synthetase) may offer the greatest opportunity to reveal the underlying neurochemical basis of drug-dependent and drug-independent convulsions.

Glutamate Transporters

Glutamate transporters are critical for the maintenance of normal glutamatergic activity. They are ATP-dependent and utilize the Na^+ and K^+ gradients to drive uptake (Madl and Burgesser, 1993; Pellerin and Magistretti, 1997). Therefore, they are prone to inhibition and/or reversal during states of intense stimulation, such as seizure activity, and during states of energy impairment, such as EtOH intoxication (Szatkowski et al., 1990; Attwell et al., 1993; Madl and Burgesser, 1993). Alterations in transporter function may be associated with increased susceptibility to seizures, alcoholism and other disease states (Lipton and Rosenberg, 1994).

Characterization of the glutamate transporter system has led to the cloning of five transporters: the glutamate transporter-1, GLT-1 (Pines et al., 1992), the glutamate/aspartate transporter, GLAST (Storck et al., 1992), the excitatory amino acid carrier 1, EAAC1 (Kanai and Hediger, 1992), the excitatory amino acid transporter 4, EAAT4 (Fairman et al., 1994), and the excitatory amino acid transporter 5, EAAT5 (Arriza et al., 1997). GLAST and GLT-1 have been localized to glial cells (Danbolt et al., 1992; Levy et al., 1993; Lehre et al., 1995) and EAAC1 and EAAT4 are considered neuronal transporters (Kanai and Hediger, 1992; Rothstein et al., 1994). Recent evidence suggests, however, that this classification based on glial/neuronal localization may be an oversimplification (Mennerick et al., 1998; Conti et al., 1998).

Glial glutamate transporter activity is responsible for the majority of glutamate uptake following stimulation (Rothstein et al., 1996). GLAST transporter protein and mRNA expression is highest in cerebellum whereas GLT-1 transporter protein and mRNA predominate in cerebrum, especially in regions that receive dense glutamatergic innervations such as the hippocampus, striatum and cortex (Torp et al., 1994; Rothstein

et al., 1994; Lehre et al., 1995; Chaudhry et al., 1995). Rosenberg et al. (1992) found that neurons cultured with few astrocytes are considerably more sensitive to the neurotoxic effects of glutamate than are neurons cultured with many astrocytes, suggesting that glia are responsible for the termination of excitatory activity. Inhibition of glial transporters using antisense deoxyoligonucleotides results in increased extracellular glutamate concentrations and excitotoxic cell damage (Rothstein et al., 1996). A progressive motor dysfunction following chronic intraventricular administration of either GLAST or GLT-1 specific antisense oligonucleotides has also been reported (Rothstein et al., 1996).

Unlike the glial transporters, loss of the neuronal transporter EAAC1 activity does not increase extracellular glutamate or lead to excitotoxicity (Rothstein et al., 1996; Peghini et al., 1997). EAAC1 is observed predominantly in dendritic spines and shafts and has a perisynaptic distribution [i.e. away from the area of synaptic contact (Rothstein et al., 1994; Coco et al., 1997; Furuta et al., 1997)]. The kinetics and localization of EAAC1 suggest that it functions to limit glutamate diffusion to nearby synapses as opposed to terminating the glutamatergic signal within a single synaptic cleft (Coco et al., 1997). Rothstein et al. (1996) reported that inhibition of EAAC1 activity by chronic intraventricular antisense administration leads to epileptic seizure activity in rats. Seizures result from synchronous neuronal firing; thus, failure or reversal of EAAC1 function could increase glutamate diffusion and activate glutamatergic receptors on adjacent cells. EAAC1 protein has been detected on non-glutamatergic neurons, such as the GABAergic cerebellar Purkinje cells (Rothstein et al., 1994; Furuta et al., 1997). Although the role for these neuronal transporters is somewhat unclear, it has been proposed that they sequester glutamate into cells to be used as a precursor for GABA synthesis [(Rothstein et al., 1996); for review of GABAergic involvement in seizures, see Horton, 1991]. Alternatively, the location of these transporters may be associated with glutamatergic nerve terminals and not necessarily with the type of cell making the

postsynaptic contact. Rapid removal of glutamate from the synapse to avoid diffusion is critical to maintaining normal glutamatergic activity and dendrites would provide a large cytoplasmic pool for glutamate diffusion. With so many roles in the CNS, glutamate should be readily utilizable by most neuronal or glial structures.

EAAT4 has a distributional profile similar to EAAC1 but is pharmacologically distinct (Fairman et al., 1994; Furuta et al., 1997; Dehnes et al., 1998). EAAT5 has been localized to retina and kidney (Arriza et al., 1997), but its unique functional significance remains unknown. Characterization of these more recently cloned transporters is preliminary, so the physiological significance of glutamate transporter heterogeneity remains to be elucidated. Moreover, the existence of a presynaptic transporter, based on ultrastructural analysis of aspartate uptake, has been suggested but thus far no transporter subtypes have been observed presynaptically (Gundersen et al., 1993). Therefore it is possible that other, uncloned glutamate transporters exist.

The glutamate transporters exhibit differences in their levels of expression (Rothstein et al., 1994) and anatomical localization (Rothstein et al., 1994; Torp et al., 1994; Fairman et al., 1994; Arriza et al., 1997) as well as in their pharmacological (Arriza et al., 1994) and kinetic (Wadiche et al., 1995) profiles. They are differentially modulated by second messengers, such as arachidonic acid (Zerangue et al., 1995), and *in vivo* treatments, such as kindling (Prince Miller et al., 1997), and may serve different functions in glutamate neurotransmission (Rothstein et al., 1996). Furthermore, the glutamate transporter system is dynamically affected by changes in glutamate availability and release (Mennerick and Zorumski, 1994). Therefore, the rate of glutamate uptake and the level of transporter protein can be influenced by the amount of excitatory neurotransmission occurring within distinct regions of the brain (Gundersen et al., 1995).

Decreased GLT-1 and GLAST protein levels that parallel decreases in glutamate uptake have been observed following cortical lesions and traumatic brain injury (Levy et al., 1995; Raghavendra et al., 1998). In addition, decreased glutamate transport activity

that is associated with a profound and specific loss of EAAT2 protein (human analogue of GLT-1) has been reported in patients with amyotrophic lateral sclerosis (Rothstein et al., 1992, 1995; Lin et al., 1998). A decrease in GLT-1 protein, but not in GLAST protein, also has been observed in motor neuron degeneration mutant (*Mnd*) mice (Mennini et al., 1998). Thus, glutamate uptake and extracellular glutamate concentrations can be regulated at the level of protein expression, although more rapid alterations in neuronal excitatory activity may lead to alterations in the rate or affinity of uptake.

Seizures

Excitotoxic disorders, such as seizure-related disorders, also influence glutamate transporter activity and protein levels. Following a subcutaneous injection of the convulsant soman (an acetylcholinesterase inhibitor), rats show an increase in extracellular glutamate levels in the CA1 region of the hippocampus, as measured by *in vivo* microdialysis, as well as an increase in L-[³H]glutamate uptake in hippocampal homogenates (Lallement et al., 1991). Cordero et al. (1994), on the other hand, reported that mice bred to be absence seizure-prone (C57BL/10Bg SPS/sps mice) have significantly less hippocampal synaptosomal [³H]glutamate uptake than their seizure-resistant counterparts. GLT-1 mRNA expression in Genetically Epilepsy Prone rats (GEPR) is significantly increased in the CA1 region of the hippocampus, cortex, striatum, and inferior colliculus, as compared to control, non-seizure prone rats, 7 days following intense seizure activity. EAAC1 mRNA is also lower than control levels within the striatum. These differences in mRNA expression are not associated with alterations in protein levels (Akbar et al., 1998).

The use of genetic animal models, such as knockouts, is particularly useful for determining factors that lead to susceptibility or resistance to specific disease states. Tanaka et al. (1997) created GLT-1 knockout mouse lines that exhibited limbic seizure

susceptibility. Crude cortical synaptosomal glutamate uptake in homozygous GLT-1 mutants is reduced to 5.8% of control levels and excitotoxic cell damage is observed in some homozygous mutants. Thus, GLT-1 appears responsible for the majority of glutamate uptake into synaptosomes and plays a role in enhanced sensitivity to seizure activity. In contrast, EAAC1 knockout mice display no convulsive activity or abnormal morphology (Peghini et al., 1997). From these data, it appears that altered glial, but not neuronal, transporter activity may be an underlying cause of some seizure-related disorders. However, Rothstein et al. (1996) reported the opposite when using chronic antisense oligonucleotide treatment to temporarily “knockout” the individual glutamate transporter subtypes. The latter observations indicate that glial transporters are critical for maintaining low extracellular glutamate concentrations, but that epileptic-type seizures are only observed following EAAC1 antisense treatment.

Prince Miller et al. (1997) tracked GLAST, GLT-1 and EAAC1 protein levels, using Western blotting, during the development of amygdala-kindled seizures. A decrease in GLAST protein in piriform cortex is observed before the animal is fully kindled. In contrast, EAAC1 transporter protein levels are increased in piriform cortex and hippocampus only after kindling is complete. When Akbar et al. (1997) tested GLT-1 and GLAST mRNA and protein levels 28 days after rats are fully kindled, no changes in mRNA or protein are seen. Additionally, kainic acid-induced seizures, but not kainic acid itself, are capable of increasing GLAST mRNA in a time-dependent manner. GLAST mRNA is elevated by 12 hours following kainic acid administration and peak at 48 hours post-injection (Nonaka et al., 1998). Overall, although data indicate a functional role for glutamate transporters in susceptibility to and expression of seizures, the nature of that role may be dependent on the type of seizure, type of animal model and the time point tested (Table 1).

Ethanol

Acute EtOH administration to cell cultures and synaptosomes prepared from rats may affect glutamate uptake; however, involvement of specific glutamate transporter subtypes in increased susceptibility to drug dependence has not been explored.

Incubation of rat whole brain synaptosomes *in vitro* with EtOH for 10 minutes results in a decrease in [^3H]glutamate uptake (Roach et al., 1973b). [^3H]Glutamate uptake also is decreased in rat cortical astrocytic cultures exposed to 50 or 100 mM EtOH *in vitro* for 6 hours (Singh et al., 1994). Conversely, a small but significant increase in [^3H]glutamate uptake in rat cortical astrocytic cultures is seen following a 15 minute *in vitro* exposure to 100 mM EtOH (Smith and Zsigo, 1996). Four days of EtOH exposure results in a larger increase in uptake (Smith and Zsigo, 1996). Finally, following a single i.p. EtOH injection (4 g/kg) or a 2 hour *in vitro* EtOH exposure (56 mM), no changes in glutamate uptake into rat slices and synaptosomes from cortex, hippocampus or striatum are seen (Keller et al., 1983). The variability in these results, although potentially due to differences in incubation time or tissue preparation, makes it difficult to draw conclusions about the effect of acute EtOH on glutamate uptake.

Likewise, the effect of chronic EtOH exposure on glutamate uptake is inconsistent. Keller et al. (1983) gave rats a liquid EtOH (or control) diet for 21-25 days and tested [^3H]glutamate uptake during intoxication or following 36 hours of withdrawal. Chronic EtOH treatment does not alter glutamate uptake in cortical synaptosomes or slices, but an increase in uptake is observed in hippocampal slices while the rats are intoxicated. During withdrawal, however, glutamate uptake is comparable in EtOH-treated and control rats. Roach et al. (1973a), on the other hand, reported that whole brain [^3H]glutamate uptake is decreased in rats exposed to EtOH vapor for 7 days and withdrawn for 12 hours. This latter report measured uptake in only those rats that exhibited severe withdrawal symptoms, which included "convulsions when suspended by the tail" (Roach et al., 1973a). In conclusion, it appears that the effects of EtOH on

glutamate uptake are regulated by the duration of EtOH exposure, route of EtOH administration as well as tissue preparation (Table 2).

Glutamine Synthetase and Glial Fibrillary Acidic Protein

Glial cells are involved in a number of processes that are critical to normal neural activity (Barres, 1991). They express membrane-bound ion channels, neurotransmitter receptors and transporters, and have complex interactions with neurons. In addition, they contain the ATP-dependent enzyme, glutamine synthetase (GS, L-glutamate:ammonia ligase, EC 6.3.1.2) (Martinez-Hernandez et al., 1977). Glutamine synthetase converts glutamate into glutamine, a nontoxic glutamate metabolite. Glutamine synthesized by glutamine synthetase also serves as the major precursor for the releasable pool of glutamate (Bradford et al., 1978; Hamberger et al., 1979a & b; Ward et al., 1983, Rothstein and Tabakoff, 1984). Reduction in nerve terminal glutamate immunoreactivity has been observed following blockade of glutamine synthetase by L-methionine sulfoximine (Laake et al., 1995). These data indicate that glutamine synthetase is directly responsible for glutamate metabolism and indirectly tied to glutamate synthesis. In fact, glutamate synthesized from glutamine appears to be more critical to the maintenance of vesicular glutamate concentrations than de novo synthesis or presynaptic glutamate reuptake (Laake et al., 1995).

The highest density of glutamine synthetase protein is observed in regions rich in glutamatergic innervation. At the ultrastructural level, glutamine synthetase labeling is observed in astrocytic processes in close proximity to asymmetric, presumably excitatory, synapses and is associated with GLAST immunoreactivity in rat retina (Derouiche & Frotscher, 1991; Derouiche & Rauen, 1995). Glutamine synthetase activity and protein density are influenced by local glutamatergic activity (Norenberg, 1979) and, due to its ATP dependence, can be used to identify the general metabolic capacities of glial cells.

Seizures

Identifying a role for astroglia in susceptibility or resistance to convulsions may be possible using glutamine synthetase as a marker. GEPR-9 rats have less glutamine synthetase activity than seizure-resistant Sprague Dawley rats (Carl et al., 1993). However, when these "normal" Sprague Dawley rats (i.e. seizure resistant) are convulsed using maximal electroshock treatments, no change in glutamine synthetase is observed. This suggests that glutamine synthetase may be involved in susceptibility to convulsions, but not necessarily in seizure-related excitotoxicity. Laming et al. (1989) reported that seizure-prone Mongolian gerbils display less cerebral glutamine synthetase activity as compared to their nonseizure-prone counterparts following seizure-inducing stimuli. This depressed glutamine synthetase activity is not associated with a decreased density of astrocytes. Conversely, Abdul-Ghani et al. (1989) observed no alterations in glutamine synthetase activity in rat cortical brain homogenates from animals with insulin- or picrotoxin-induced seizures. Sherwin et al. (1984) observed no differences in glutamine synthetase activity between human tissue removed from the epileptic focus and tissue removed from the surrounding cortical areas. However, these data were collected in human subjects who display a wide variety of epilepsy-induced morphological alterations. In addition, the non-focal cortical regions used were "not normal, but (did) differ electrographically from the focus" (Sherwin et al., 1984). Interestingly, direct inhibition of glutamine synthetase by L-methionine sulfoximine results in seizures (Svenneby and Torgner, 1987; Carl et al., 1992). Thus, glutamine synthetase may represent one of many pathways underlying susceptibility to, or expression of, certain types of seizure activity (Table 1).

Ethanol

In addition to being a marker for glial metabolic activity and glutamatergic uptake and biosynthesis, glutamine synthetase is a sensitive measure of oxidative stress

(Bondy and Guo, 1994). Long-term EtOH exposure can lead to tissue damage; thus, glutamine synthetase has been employed as an indirect means of characterizing how EtOH produces cell death. Cell cultures exposed to *in vitro* EtOH (for 4 to 15 days) show a dose-dependent decrease in glutamine synthetase levels (Davies and Vernadakis, 1984; Ledig et al., 1991). This decrease is not explained by a simple reduction in protein content. Moreover, *in vivo* exposure to acute EtOH causes a transient increase in glutamine synthetase activity whereas *in vivo* exposure to chronic EtOH results in decreased glutamine synthetase in rat cortical tissue (Bondy and Guo, 1994). Thus, glutamine synthetase appears to be directly influenced by the dose and duration of EtOH exposure (Table 2).

Sakellaridis et al. (1989) examined glutamine synthetase activity during development in mouse lines selectively bred for different sensitivities to EtOH. A trend for higher glutamine synthetase activity throughout the brains of Long Sleep mice, as compared to Short Sleep mice, is seen during development. Long Sleep mice exhibit a longer duration of the loss of righting reflex following acute exposure to a hypnotic dose of EtOH than Short Sleep mice. This same report measured glutamine synthetase activity in Mild-, Control-, and Severe- Ethanol Withdrawal (MEW, CEW, SEW) mice, that show differences in withdrawal severity (measured using multiple withdrawal symptoms). Line differences between MEW and SEW mice are observed in late development (30-46 days) in the forebrain, but not in the cerebellum. These data suggest that glutamine synthetase may be associated with susceptibility to and/or expression of EtOH-induced hypnosis or -withdrawal symptoms (Table 2).

The concentration of glutamine synthetase can be affected by alterations in translation or with proliferation of glutamine synthetase-positive glial cells. Glial hypertrophy frequently is observed following intense neuronal activity (Steward et al., 1991; Torre et al., 1993). This reactive gliosis can be easily observed following seizure

activity using the glial marker, glial fibrillary acidic protein (GFAP) (Brigande et al., 1992; Torre et al., 1993). GFAP is a structural protein associated with intermediate filaments in astrocytes (Eng et al., 1971). Although is it a useful marker for assessing damage incurred by seizure activity, it does not identify alterations in glial activity that may be associated with susceptibility to seizures. However, assessment of glial cell structure can be valuable when interpreting the significance of other functional changes in glial cells.

Astrocytes are responsible for maintaining normal excitatory tone in the CNS (Rothstein et al., 1996). Glutamine synthetase, a glial specific enzyme, is essential for both glutamate metabolism and synthesis. Because glutamine synthetase activity can be influenced by changes in glutamatergic activity and by changes in energy availability, it may be responsible for conferring susceptibility or resistance to seizure activity and/or drug dependence.

Cytochrome Oxidase

Cytochrome oxidase (CO; ferrocytochrome *c* oxygen oxidoreductase, E.C. 1.9.3.1) is a mitochondrial enzyme that catalyzes the terminal oxidative reaction for the conversion of glucose to ATP. Since nearly all (95+ %) ATP in the brain is derived from oxidative metabolism, neuronal functioning is highly dependent on the activity of CO. As neurons become more active, glucose utilization and oxidative metabolism increase and can be observed as increased cytochrome oxidase activity (Kageyama and Wong-Riley, 1982). Thus, cytochrome oxidase histochemistry is frequently used as a measure of cellular respiration and local energy metabolism of neurons (Wong-Riley, 1989) and may be indicative of the level of activity in a given brain region or cell.

Cytochrome oxidase is heterogeneously distributed throughout the brain, showing significant variability between anatomical structures and within individual cells (Kageyama and Wong-Riley, 1982). Comparison of protein levels with enzymatic

activity suggests that cytochrome oxidase activity is controlled primarily by protein levels which, in turn, are regulated by local energy demands (Hevner and Wong-Riley, 1989). Because its activity is regulated by protein synthesis and/or degradation, changes in cytochrome oxidase activity are typically observed following long-term alterations in neuronal functioning (on the order of days) (Hevner and Wong-Riley, 1990).

The majority of energy utilized by the brain drives the Na^+/K^+ -ATPases which regulate neuronal membrane potential (Erecinska and Silver, 1989). Since restoration of the resting membrane potential following depolarization requires more active ion transport than required after hyperpolarization, it follows that the intensity of cytochrome oxidase labeling is influenced more by changes in excitatory activity than by changes in inhibitory activity. Co-localization of Na^+/K^+ -ATPases and cytochrome oxidase have been observed (Hevner et al., 1992; Wong-Riley et al., 1998) and several lines of evidence suggest that cytochrome oxidase activity is greater in neurons receiving excitatory inputs.

Cytochrome oxidase activity tends to be highest in dendrites making asymmetric (presumably excitatory) contacts (Carroll and Wong-Riley, 1984; Nie and Wong-Riley, 1995; Nie and Wong-Riley, 1996). It is correlated to the type of synaptic contact (asymmetric/excitatory versus symmetric/inhibitory; see Gray, 1959) more than it is associated with the cell type (Kageyama and Wong-Riley, 1982; Carroll and Wong-Riley, 1985; Nie and Wong-Riley, 1995; Nie and Wong-Riley, 1996). However, co-localization of N-methyl-d-aspartate (NMDA) glutamate receptor subtype immunoreactivity and cytochrome oxidase staining has been reported (Zhang and Wong-Riley, 1996; Wong-Riley et al., 1998). Finally, Mjaatvedt and Wong-Riley (1988) analyzed the density of cytochrome oxidase staining in rat Purkinje cell bodies as excitatory climbing fibers were displaced by inhibitory basket cell terminals and found a progressive decrease in histochemical reactivity. Thus, cytochrome oxidase activity also is associated with excitatory synaptogenesis. Taken together, these data suggest that

excitatory activity is positively correlated with cytochrome oxidase activity and that deviations from normal functioning can result in altered cytochrome oxidase activity that is measurable using histochemistry.

Seizures

Seizure activity is associated with increased NMDA receptor activation and neuronal hyperexcitability (Meldrum, 1994). Norbrega et al. (1993a) measured the intensity of cytochrome oxidase histochemical staining following eight electroconvulsive shock-induced tonic-clonic seizures and found a trend towards increased cytochrome oxidase activity in numerous regions at 24 hours and a significant increase in limbic regions (i.e. hypothalamus) 28 days after the last seizure. However, rats that are kindled using subconvulsive electrical stimulation to the entorhinal cortex (Norbrega et al., 1993b) or subconvulsant doses of pentylenetetrazol (Schunzel et al., 1992) show no changes in cytochrome oxidase activity at any time point tested. Furthermore, cytochrome oxidase activity in human hippocampal tissue from patients with temporal lobe epilepsy is lower than in autopsied, non-epileptic controls (Brines et al., 1995). These data suggest that cytochrome oxidase activity may be influenced by certain types of seizure activity, depending on the type of seizure induced (i.e. tonic versus clonic), the mode of induction (i.e. electrical versus chemical) and/or the severity (duration and frequency) of the resulting convulsions (Norbrega et al., 1993b).

The 2-deoxyglucose (2-DG) technique (Sokoloff et al., 1977) is another measure of neuronal activity (Schwartz et al., 1979). Although similar to cytochrome oxidase histochemistry, determination of glucose utilization results in a measure of acute (vs. long-term) neuronal activity. As outlined by Norbrega et al. (1993b), the 2-DG method suggests a complex time course of neuronal activity during and following a seizure, with acute increases observed during the ictal state, acute decreases observed during the post-ictal state and no changes from baseline observed during the interictal state. Therefore, it

is likely that neuronal activity is transiently affected by seizure activity, and, under some conditions, may be permanently altered.

Ethanol

As with seizure activity, withdrawal from chronic EtOH exposure results in CNS hyperexcitability and an increase in NMDA receptor activation (Lovinger, 1993). To the best of our knowledge, cytochrome oxidase activity during EtOH withdrawal has not been assessed. However, cytochrome oxidase activity has been reported to be unchanged during intoxication. Spectrophotometric analysis of cytochrome oxidase activity in purified liver and brain mitochondrial extracts from rats that were made dependent on EtOH found no changes in cytochrome oxidase activity (Thayer and Rottenberg, 1992). Rubio et al. (1996) assessed cytochrome oxidase activity in rat mamillary bodies following approximately 6 weeks of intragastric EtOH administration. During intoxication, no changes from baseline are observed. Diazepam, on the other hand, does significantly increase cytochrome oxidase activity in the mamillary bodies (Rubio et al., 1996).

The 2-DG method has been used to assess changes in neuronal activity during acute and chronic EtOH exposure. Glucose utilization in a variety of brain regions (mostly in auditory pathway) decreases following gastric administration of 3.2 g/kg EtOH (Grunwald et al., 1993) and dose-dependently following an intraperitoneal (i.p.) administration of EtOH (Eckhardt et al., 1988; Williams-Hemby and Porino, 1994). However, after three weeks of exposure to EtOH in the drinking water, rats do not show decreased glucose utilization in the same structures (Grunwald et al., 1993). Rats in this group are likely to be in early withdrawal stages (no EtOH was administered for at least 2 hours before 2-DG assessment) and thus compensatory mechanisms may be involved.

These data suggest that transient changes in neuronal activity may occur during EtOH intoxication. The cytochrome oxidase experiments, though, do not support long-

term changes. However, it should be noted that Thayer and Rottenberg (1992) used spectrophotometry, which lacks the anatomical resolution possible with histochemistry and Rubio et al. (1996) looked at only one brain region, which receives an excitatory input from the subiculum, but is not a region frequently associated with withdrawal symptoms.

Evidence indicating that EtOH exposure alters neuronal activity via an effect on Na^+/K^+ ATPase function (for review, see Tabakoff et al., 1987) does suggest, however, that neuronal activity is altered during EtOH withdrawal. This conclusion is supported by the recent finding that there is extensive overlap in the distribution of cytochrome oxidase activity and Na^+/K^+ ATPase immunoreactivity (Hevner et al., 1992). *In vitro* exposure to EtOH has been reported to inhibit Na^+/K^+ ATPase activity. Swann (1990) reported that *in vitro* exposure to physiologically relevant doses of EtOH influences Na^+/K^+ ATPase function by altering the selectivity of the ATPase for Na^+ and K^+ . Rangaraj and Kalant (1978) reported a significant increase in Na^+/K^+ ATPase activity in rat whole brain homogenates during withdrawal from chronic EtOH (liquid diet) or from an acute injection (5 g/kg). Although inconclusive, there is data suggesting that ethanol alters neuronal activity.

In summary, using cytochrome oxidase histochemistry, local changes in neuronal activity may be observed following treatments that result in long-term changes in CNS excitability and glutamate receptor activation (Norbrega et al., 1993a; Brines et al., 1995; Zhang and Wong-Riley, 1996; Wong-Riley et al., 1998). Moreover, Norbrega et al. (1998) reported differences in cytochrome oxidase histochemical staining between mutant dystonic hamsters and their wild-type counterparts prior to any treatment. This suggests that cytochrome oxidase histochemistry can be used to assess inherent differences in excitatory neuronal activity.

Behavior and Animal Model

Behavior

Neuronal hyperexcitability has been implicated as an underlying factor in numerous disease states (Rothman and Olney, 1987). This CNS hyperactivity has been associated with increased glutamatergic activity and decreased GABAergic activity. Although extensive evidence supports a role for both neurotransmitter systems in increased neuronal activation, the involvement of glutamate in diseases ranging from epilepsy to ischemia to amyotrophic lateral sclerosis to alcoholism has been widely researched (Lipton and Rosenberg, 1994).

Seizures are associated with synchronous neuronal firing of structures rich in excitatory synaptic contacts (Dingledine et al., 1990). It is estimated that up to 10% of the population can experience a seizure during his/her lifetime (Engel, 1989). Seizure activity can result from a variety of triggers including trauma, ischemia and drug abuse (Hesdorffer and Verity, 1997). Although a number of drugs act directly as convulsants, withdrawal from depressant drugs also can result in seizure activity. In fact, alcohol is a leading cause of non-epileptic seizures in patients admitted to hospitals (Earnest and Yarnell, 1976; Aminoff and Simon, 1980).

Alcohol (EtOH) is a CNS depressant to which the body develops rapid tolerance. Lovinger et al. (1989) observed that EtOH directly decreases glutamatergic synaptic activity. Consumption of EtOH in large quantities or over long periods of time can induce compensatory mechanisms in the brain (i.e. NMDA receptor hypersensitivity) that, upon cessation of EtOH exposure, can lead to excitatory hyperactivity (Michaelis et al., 1980; Lovinger, 1993). Clinical reports from epileptic patients suggest that EtOH may intensify seizure activity and that anti-epileptic drugs reduce an individual's tolerance to EtOH (Gumnit, 1995). Moreover, convulsions are among the most common symptoms observed during withdrawal from alcohol (Kosobud and Crabbe, 1986). They have been reported in nearly every species tested. In addition, withdrawal seizures may

be progressive; reports have indicated a kindling-like phenomenon following repeated binge-withdrawal episodes (Ballenger and Post, 1978; Ulrichsen et al., 1992; Becker, 1994).

Excessive glutamatergic activity can lead to severe morphological damage and abnormal behavior (Rothman and Olney, 1987; Mathern et al., 1997). Determining the underlying mechanisms by which glutamate leads to structural and behavioral change is of critical importance. The complexity of this transmitter system suggests that multiple neurochemical components may be involved. In the present study, glutamate uptake and metabolism have been examined in mice that are prone or resistant to EtOH-dependent and -independent handling-induced convulsions (HICs). The use of genetically bred mice allows evaluation of the involvement of glutamate in predisposing animals to severe convulsive activity, in both their drug-naïve state and during withdrawal from EtOH.

Genetics

Selective breeding is a valuable tool for assessing the underlying genetic factors associated with complex, polygenic traits. Numerous selected lines have been developed to study the heritable components of drug and alcohol abuse (Crabbe et al., 1994b). Selective breeding of the Withdrawal Seizure-Prone (WSP) and Withdrawal Seizure-Resistant (WSR) mouse lines was accomplished by taking a heterogeneous population of mice, exposing them to 72 hours of EtOH vapor, removing the EtOH and observing the severity of convulsions exhibited during withdrawal (Crabbe et al., 1983, 1985). Mice with the most severe convulsions were bred together to develop the WSP line and mice that exhibited mild or no convulsive activity were bred together to develop the WSR line. This experiment was performed twice, in two separate heterogeneous populations and resulted in replicate lines of both the WSP and the WSR phenotypes (Crabbe et al., 1983).

During the artificial selection process, genes associated with the drug effect of interest (i.e. EtOH withdrawal convulsions) become homozygously fixed with alleles that confer susceptibility or resistance to that effect. The ability of the selection process to manipulate allelic frequencies is essential for elucidating the underlying neurochemical and genetic basis for the selection behavior. This is because non-selected traits that differ between the selected lines, called correlated phenotypes, are most likely associated with the same set or a subset of the same genes fixed during the selection process (Crabbe et al., 1990). Thus, if a selected line exhibits increased susceptibility to the selected behavior and is more sensitive to an agonist of a given transmitter, then it may be suggested that this transmitter system represents a neurochemical mechanism by which increased susceptibility to the selected behavior occurs. However, due to differences in the founding populations, genetic drift or inadvertent trait-irrelevant inbreeding, the possibility of observing erroneous correlations between the selected trait and an unselected trait is high. To decrease risk of these types of errors, replicates of selected lines are developed. Differences observed between replicates suggest the involvement of trait-irrelevant factors and decrease the likelihood of a true genetic correlation (for complete review, see Crabbe et al., 1990).

Animal Model

The WSP and WSR mouse lines exhibit differences in their sensitivity to HICs during EtOH withdrawal (Crabbe et al., 1983). These mouse lines also exhibit differences in HIC severity prior to drug exposure, during administration of proconvulsant drugs and during withdrawal from hypnotic drugs (Kosobud and Crabbe, 1986; Belknap et al., 1987, 1988, 1989; Feller et al., 1988; Crabbe et al., 1991a, b, Buckman et al., *submitted*). In all cases, WSP mice are more susceptible to HICs than are WSR mice. However, latency to clonic or tonic hindlimb extension seizures following a

tail infusion of NMDA is significantly shorter in EtOH-naïve WSR mice as compared to EtOH-naïve WSP mice (Kosobud and Crabbe, 1993). Following an intraperitoneal (i.p.) injection of NMDA, though, an exacerbation of HICs in EtOH-naïve WSP mice is observed (Crabbe et al., 1993). Olfactory bulb kindling rates in drug-naïve WSP and WSR mice are not significantly different at 2 months, whereas at 8 months of age, WSP mice are significantly less prone to kindling as compared to WSR mice (Green et al., 1993). In addition, when tested for audiogenic seizure susceptibility, mild to no seizure activity is observed in WSP mice but HIC severity increased following auditory stimuli exposure (Feller et al., 1994). Taken together, these data suggest factors specific to HICs, as opposed to convulsions in general, have been influenced by selection.

HICs are easily observed and rated for severity and are therefore useful measures of EtOH withdrawal severity. It appears that in addition to EtOH withdrawal severity differences, the selection of WSP and WSR mouse lines has resulted in phenotypic differences in HICs and to those stimuli that alter sensitivity to HICs. It is plausible that a common set of genes is responsible for conferring sensitivity to EtOH withdrawal as well as to susceptibility to HICs (i.e. EtOH-dependent and EtOH-independent HICs are correlated phenotypes). EtOH withdrawal and convulsive activity are both associated with central nervous system (CNS) hyperexcitability potentially resulting from excessive glutamatergic activity, insufficient GABAergic activity as well as increased voltage-gated calcium channel activity (for reviews, see Lovinger, 1993; Meldrum, 1995; Crews et al., 1995). Thus genes associated with glutamatergic or GABAergic neurotransmission may have been impacted by selection.

The NMDA receptor-ion complex has been implicated in the differences in EtOH withdrawal symptoms and HIC susceptibility observed between WSP and WSR mice. Assessment [³H]MK-801 binding to NMDA receptors in EtOH-naïve and EtOH-withdrawn WSP and WSR mice has yielded conflicting results (Valverius et al., 1990; Carter et al., 1995). Systemic administration of NMDA and kainate receptor agonists

exacerbates the severity of HICs in naive and acutely withdrawn WSP mice. Conversely, the NMDA receptor antagonist, MK-801, decreases the severity of HICs in naive and acutely withdrawn WSP mice without influencing all other withdrawal symptoms (Crabbe et al., 1993, Crabbe et al., 1994a). These data indicate that differences may exist at the NMDA receptor-ion complex. However, due to the number of genes potentially involved in ethanol withdrawal HICs, receptor differences may be subtle and coupled with inherent presynaptic alterations.

EtOH- and HIC-naive WSP mice exhibit a higher density of presynaptic glutamate immunoreactivity in the CA1 region of the hippocampus than naive WSR mice (Buckman and Meshul, 1997). This line difference is observed in the hippocampus but not in the somatosensory cortex. It is specific to glutamate (there were no line differences in GABA immunoreactivity). These mice were not exposed to EtOH or to any other convulsive stimuli, suggesting that the genes associated with glutamatergic functioning were influenced by selection. In addition, when EtOH-naive WSP and WSR mice are exposed to handling stimuli that induce HIC activity in WSP mice, the density of glutamate immunoreactivity in hippocampal axon terminals does not differ between the lines (Buckman and Meshul, 1998). Thus, convulsions decrease the labeled nerve terminal pool of glutamate, indicating that the greater density of glutamate observed in naive WSP animals is associated with the releasable pool and is therefore of functional relevance.

In conclusion, WSP mice exhibit EtOH withdrawal-induced and drug-naive convulsive activity. It has been well established that the glutamatergic and GABAergic systems, as well as numerous ion channels, are influenced by EtOH and by seizure activity (Lovinger, 1993; Crews et al., 1996; Glass and Dragunow, 1995). We have recently reported that differences in the density of presynaptic glutamate immunoreactivity exist in the CA1 subfield of the hippocampus of naive WSP and WSR mice. Therefore, the

focus of this study is to examine the functional components of the glutamatergic system, which may play a role in predisposing WSP mice to HICs and severe EtOH withdrawal and lead to increased presynaptic glutamate immunolabeling. Particular attention has been paid to components of this transmitter system which are ATP-dependent, and therefore, susceptible to damage by increased excitatory activity.

RATIONALE

Overall Aim

The goal of this thesis is to characterize the components of the glutamatergic system involved in alcohol withdrawal convulsion susceptibility using the selectively bred WSP and WSR mice. ATP-dependent glutamatergic components have been assessed for their involvement in the phenotypic differences between the WSP and WSR mouse lines. L-[³H]glutamate uptake have been tested in the hippocampus and cortex of WSP and WSR mice in their naive state and following a number of treatments. The density of glutamate transporter subtype immunolabeling and glutamine synthetase labeling in several regions of the hippocampus and cortex have been compared in naive WSP and WSR mice. Cytochrome oxidase activity in several regions of the hippocampus and cortex of naive WSP and WSR mice also has been analyzed as a measure of energy utilization in the brain.

Based on the previously reported ultrastructural immunocytochemical observations (Buckman and Meshul, 1997; 1998), it was hypothesized that WSP mice would exhibit greater glutamatergic activity than WSR mice. In the naive state, it was predicted that the heightened activity in WSP mice would be reflected by greater glutamate availability, release *and* uptake, such that the system would remain “balanced”. Exposure to alcohol or other convulsion-inducing stimuli was expected to disrupt this balance, leading to glutamate accumulation in the synaptic cleft and overactivation of glutamate receptors in WSP mice.

Anatomical Considerations

The hippocampus is innervated via the perforant path with the initial synaptic contact being made in the molecular layer of the dentate gyrus. The neurons associated with these excitatory contacts (granule cells) project mossy fiber terminals into the stratum radiatum of the CA3 subfield of the hippocampus. These CA3 neurons (pyramidal cells)

innervate the CA1 subfield of the hippocampus (in the stratum radiatum) via the Schaffer collaterals. CA1 neurons then project out of the hippocampal formation to the subiculum. Each synaptic contact in this well-defined trisynaptic circuit is glutamatergic and extremely sensitive to excitatory hyperactivity.

A connection between hippocampal damage and seizure activity has been recognized since the early 1800's. It has been established that the pattern of hippocampal damage (called sclerosis) associated with seizures follows the excitatory trisynaptic circuit. The hippocampus also may be critically involved in predisposing and/or propagating alcohol withdrawal seizures (Gulya et al., 1991). Furthermore, alcohol, independent of seizure activity, may also influence the morphology of the hippocampus. Pathological evaluation of a middle aged alcoholic, who had no known history of seizures and died of alcohol-induced liver failure, was found to have major hippocampal atrophy (Mathern et al., 1997). Thus, although the anatomical pathway regulating the specific expression of alcohol withdrawal seizures has not been fully elucidated, this evidence does support hippocampal involvement in alcohol withdrawal seizures. These data further support the hypothesis that the WSP and WSR mouse lines may exhibit differences in glutamatergic activity specifically within the hippocampus.

Recent studies from this laboratory have observed glutamatergic differences between the WSP and WSR mouse lines within the CA1 of the hippocampus, but not within the somatosensory cortex (Buckman and Meshul, 1997). Thus, several regions of the hippocampus (Fig.2) associated with the trisynaptic excitatory circuit have been analyzed in the present experiments. In addition, the somatosensory cortex has been examined to determine whether differences are specific to hippocampus and are consistent with our earlier ultrastructural immunocytochemical observations (Buckman and Meshul, 1997).

Specific Aim #1: To determine glutamate transporter activity and protein density in WSP and WSR mice in their naive state

Glutamate uptake and transporter immunolabeling density were compared between naive WSP and WSR mice in order to assess whether these components of the glutamatergic system were involved in conferring susceptibility or resistance to severe EtOH withdrawal and HICs. L-[³H]glutamate uptake into crude hippocampal and cortical synaptosomes prepared from EtOH-naive WSP and WSR mice was measured. The density of the glutamate transporters in hippocampal slices from EtOH-naive WSP and WSR mice also was assessed. Maximal uptake and the affinity of the transporters for glutamate were calculated to determine the characteristics of glutamate transporter activity. The density of the glial glutamate transporters, GLAST and GLT-1, was characterized in the stratum radiatum of the CA1 and CA3, the molecular layer of the dentate gyrus and layers II – VI of the somatosensory cortex. The density of the neuronal transporter, EAAC1, was assessed within individual pyramidal cells in the stratum pyramidale of the CA1.

L-[³H]glutamate uptake in naive WSP and WSR mice was assessed and, based on our previous finding (Buckman and Meshul, 1997), naive WSP mice were expected to show greater maximal uptake than naive WSR mice. The density of glutamate transporter immunolabeling using antibodies against three transporter subtypes, GLAST, GLT-1 and EAAC1, was determined in naive WSP and WSR mice. Alterations in GLAST, GLT-1 and EAAC1 are associated with seizure activity in different animal models, with a loss of transporter expression being associated with an increase in seizure susceptibility (Rothstein et al., 1996; Tanaka et al., 1997; Prince Miller et al., 1997; Akbar et al., 1998). Therefore, it was predicted that subtle differences between naive WSP and WSR mice would be detected in one or several glutamate transporter subtypes. Naive WSP mice were expected to express a lower density of immunolabeling for at least one of the glutamate transporter subtypes as compared to naive WSR mice. However,

greater glutamate uptake was expected in naive WSP mice. To reconcile these discrepant hypotheses, it was suggested that alterations in the ratio (i.e. neuronal to glial uptake) or localization of GLAST, GLT-1 and EAAC1 would lead to increased uptake observed in synaptosomes, but a decrease in protein levels observed in slice preparations.

Specific Aim #2: To determine glutamate transporter activity in WSP and WSR mice following exposure to EtOH or HICs

WSP and WSR mice respond differently to handling and exposure to EtOH. The activity of the glutamate transporters may be associated with these behavioral differences. HICs and withdrawal from EtOH may increase glutamatergic activity, thereby increasing glutamate uptake. Alternatively, a failure of the transporters to increase uptake following these treatments may result in an accumulation of glutamate in the extracellular cleft. It was of interest to assess whether exposure to handling, acute EtOH intoxication or chronic EtOH withdrawal would alter L-[³H]glutamate uptake, and whether the selected lines would differ in the amount and rate of glutamate uptake. L-[³H]glutamate uptake into crude hippocampal and cortical synaptosomes were tested and maximal glutamate uptake and the affinity of the transporters for glutamate was determined using non-linear regression.

Alterations in L-[³H]glutamate uptake following convulsions were assessed and in accordance with our immunocytochemical experiments (Buckman and Meshul, 1998), WSP mice were expected to show significant decreases in L-[³H]glutamate uptake as a result of drug-naïve HIC activity. Decreased uptake would result in an accumulation of glutamate in the synaptic cleft and lead to a decrease in glutamate-glutamine cycling. This could account for increased susceptibility to HICs in WSP mice and the depletion of glutamate immunolabeling observed in WSP mice following HIC activity. In addition, L-[³H]glutamate uptake in WSP and WSR mice was tested during peak intoxication following a single hypnotic dose of EtOH and during peak withdrawal following 72

hours of EtOH vapor. Glutamate uptake during peak withdrawal from chronic EtOH was compared to blood EtOH concentrations collected at the end of the 72 hours of EtOH exposure. Significant differences in [3 H]glutamate uptake between the mouse lines during intoxication and withdrawal and a positive correlation between uptake and blood EtOH concentrations were expected. In particular, EtOH intoxication was expected to decrease glutamate uptake in both selected lines because of the depressant effects of this drug. Withdrawal following chronic EtOH was expected to increase uptake in both selected lines. However, it was predicted that WSR mice would exhibit a greater increase in uptake, thereby suggesting that they were more efficiently “compensating” for the increased glutamatergic activity during the rebound CNS hyperexcited state observed during withdrawal.

Specific Aim #3: To determine the density of glutamine synthetase and glial fibrillary acidic protein in naive WSP and WSR mice

The density of glutamine synthetase immunolabeling was determined in naive WSP and WSR mice to ascertain whether inherent differences exist in glutamate metabolism. Glutamine synthetase is an ATP-dependent glial enzyme found in abundance in astrocytes, especially within small diameter astrocytic processes (Derouiche and Frotscher, 1991). EtOH-naive WSP and WSR mice were perfused and hippocampal slices from these mice were incubated with an antibody against glutamine synthetase. The density of immunolabeling for this protein was determined in the stratum radiatum of the CA1 and CA3, the molecular layer of the dentate gyrus and layers II-VI of the somatosensory cortex using light microscopic optical density analysis.

GFAP is a glial cell marker that labels structural elements in glial cell bodies and their large processes (Derouiche et al., 1993). The density of GFAP immunolabeling was assessed at low (62.5x) and high (400x) magnification. Low magnification was used to measure whether overall differences in the structure of glial cells existed between naive

WSP and WSR mice; in particular, this analysis would offer information about glial cell arborization. GFAP immunoreactivity was assessed in the stratum radiatum of the CA1 and CA3, the molecular layer of the dentate gyrus and layers II-VI of the somatosensory cortex. The number of astroglia and the area and density of immunolabeling within single cell bodies was determined using high magnification analysis. GFAP-positive glial cell bodies were analyzed specifically within the stratum radiatum of the CA1. These data would indicate whether glial hypertrophy (by the number, size or amount of GFAP within the cells) was present.

Alterations in glutamine synthetase activity have been observed in other genetic models of alcohol withdrawal severity (Sakellaridis et al., 1989). These data, taken together with previous morphological studies (Buckman and Meshul, 1997), offer indirect support for that hypothesis that glutamate immunoreactivity in the CA1 region of the hippocampus of naive WSP mice would be significantly greater than in naive WSR mice. Alternatively, no differences in GFAP immunolabeling between naive WSP and WSR mice were expected. If, however, selected line differences in other glial proteins were observed (i.e. glial glutamate transporters or glutamine synthetase), assessment of GFAP labeling would clarify whether these protein levels were associated with the number or structure of glia.

Specific Aim #4: To determine the amount of cytochrome oxidase activity in naive WSP and WSR mice

Cytochrome oxidase is the terminal enzyme in the electron transport chain and assessment of cytochrome oxidase activity is indicative of the amount of ATP being generated and utilized in the CNS. Cytochrome oxidase activity can be determined in tissue slices using a histochemical reaction. Hippocampal slices from naive WSP and WSR mice were incubated with cytochrome c (the substrate for the cytochrome oxidase-mediated reaction) and diaminobenzidine (a visualizing agent).

The amount of cytochrome oxidase activity (using optical density) in the stratum radiatum of the CA1 and CA3, the molecular layer of the dentate gyrus and layers II – VI of the somatosensory cortex was determined using light microscopic image analysis.

Cytochrome oxidase is a measure of energy utilization and can reflect whether there are inherent differences in neuronal activity between the WSP and WSR mouse lines. If nerve terminal glutamate immunolabeling is correlated with higher glutamate activity, naive WSP mice should show increased cytochrome oxidase staining in the CA1 region of the hippocampus. Convulsions and EtOH withdrawal may lead to increased neuronal activity. Therefore, the differences that WSP and WSR mice exhibit in their susceptibility to HICs and severe EtOH withdrawal symptoms lend additional support for the hypothesis that cytochrome oxidase histochemistry will be different between the selected lines.

MATERIALS AND METHODS

Chemicals and Reagents

L-[³H]glutamate (30-60 Ci/mmol) was purchased from American Radiolabeled Chemicals (St. Louis, MO). L-trans-pyrrolidine-2,4-dicarboxylic acid (PDC) was obtained from RBI (Natick, MA). Pyrazole hydrochloride, cytochrome c from horse heart, 3,3'-diaminobenzidine, acrolein and normal goat serum were obtained from Sigma Chemicals (St. Louis, MO). Electron microscope (EM) grade glutaraldehyde (50%) was purchased from Electron Microscopy Sciences (Fort Washington, PA). Biotinylated goat anti-rabbit IgG, *Elite* avidin-biotin complex (ABC) kits and peroxidase substrate kits were purchased from Vector Laboratories, Inc. (Burlingame, CA). The GLAST, GLT-1, EAAC1 antibodies against the glutamate transporters were purchased from Chemicon International, Inc. (Temecula, CA). The antibody against GFAP was purchased from Dako Corporation (Carpinteria, CA). The antibody against glutamine synthetase was a generous gift from Dr. Masaya Oda from Tokyo Metropolitan Neurological Hospital, Tokyo, Japan.

Animals

Male WSP and WSR mice (ages: 60-110 days) from both replicate lines (WSP-1, WSP-2, WSR-1, WSR-2) were a generous gift from Dr. John Crabbe at the Portland Veteran's Administration Medical Center. Mice were given free access to standard lab chow and water and maintained on a 12:12 light-dark cycle. Prior to the experiments, all animals were group housed and handled twice per week for cage cleaning only. Experiments were not performed within 24 hours of cage cleaning. All animals were acclimated to the procedure room by being left undisturbed for 1 hour prior to initiating the experiments.

Procedures

Handling and HICs

Handling-induced convulsions (HICs) are elicited by lifting a mouse by the tail and suspending it in the air or, in some cases, by spinning the mouse gently by the tail while suspending it in the air. The severity of HICs can be rated based on a scale developed by Goldstein (1972) and modified by Crabbe et al. (1991b) (Table 3). The “handled” group was handled once per ten minutes, for a total of 10 trials. HICs were avoided in control groups by using a special handling procedure: each mouse was gently scooped into a small cup, transferred and gently poured out onto fresh bedding.

Acute EtOH intoxication

Mice were given a single intraperitoneal (i.p.) injection of 0.9% saline or 4 g/kg EtOH (20% v/v in saline). Five minutes later, mice were euthanized. No HICs were elicited in these mice.

In vitro EtOH

Inhibition of glutamate uptake into hippocampal synaptosomes from naive WSP mice was tested following *in vitro* exposure to EtOH (5 – 320 mM), PDC (0.05 – 100 μ M; a nonspecific inhibitor of glutamate uptake) or kainic acid [15 μ M – 8 mM; a moderately selective inhibitor of the glial glutamate transporter GLT-1 (Arriza et al., 1994)]. Synaptosomes were preincubated in EtOH for 15 minutes at 37°C in covered wells prior to addition of the L-[³H]glutamate. No preincubation was necessary to observe inhibition of uptake by PDC or kainic acid.

EtOH withdrawal

Mice were separated into three groups (Air/Saline, Air/Pyrazole, EtOH/Pyrazole), weighed and given a priming dose of saline, pyrazole hydrochloride (an alcohol

dehydrogenase inhibitor) or EtOH and pyrazole. They were then placed in inhalation chambers containing stainless steel 1/4 inch hardware cloth cages inside a large Plexiglas enclosure (temperature maintained at 28-30°C). Mice were given free access to food and water. Two groups were exposed only to air for 72 hours and injected with either saline or pyrazole every 24 hours. A third group was exposed to EtOH vapor for 72 hours and injected with pyrazole every 24 hours. Doses of EtOH (priming injection and vapor) were varied for each line due to small differences in EtOH metabolism. Doses of pyrazole also were varied in order to stabilize blood ethanol concentration (BEC) throughout exposure. At the 24 and 48 hour time points, before injections were given, tail blood samples from a subset of EtOH-exposed mice were taken to monitor BEC (see below). Tail blood samples were also taken from all EtOH-exposed mice immediately upon removal from the inhalation chambers at 72 hours. Air exposed animals had their tails snipped, but no blood was taken. Mice were then placed in fresh cages, transferred to a procedure room and euthanized during peak withdrawal, which occurs 7-8 hours after removal from the inhalation chambers (Kosobud and Crabbe, 1986; Crabbe and Phillips, 1993). No convulsions were induced in these mice.

Glutamate Uptake

Crude Synaptosomal Preparation

Mice were cervically dislocated and brains were immediately harvested and placed on ice. Hippocampi and cortices from 3-4 mice were dissected and placed in 20 volumes of ice cold Earles Balanced Salt Solution (EBSS containing 1.8 mM CaCl_2 , 0.8 mM MgSO_4 , 5.4 mM KCl , 26.2 mM NaHCO_3 , 80 mM NaCl , 1 mM NaH_2PO_4 and 5.5 mM L-glucose (pH 7.4). Tissue was homogenized with a Teflon-glass homogenizer and the crude homogenate was centrifuged at 800x g for 10 minutes. The resulting supernatant was centrifuged at 12,000x g for 20 minutes. The pellet (containing synaptosomes, mitochondria and other membranous structures) from this final

centrifugation was resuspended in 50 volumes of EBSS. Protein content was determined as described by Lowry et al. (1951).

Synaptosomal L-[³H] glutamate uptake

Uptake assays were performed with triplicate determinations in 96-well plates. Uptake was initiated by the addition of 100 μ l of hippocampal or cortical synaptosomal suspension (10-30 μ g protein) to wells containing 50 μ l of radioligand (100 nM L-[³H]glutamate) and 50 μ l of unlabeled glutamate of various concentrations (0.3 μ M – 60 μ M) in a total volume of 250 μ l. Specific uptake was defined as the difference in uptake observed in the presence and absence of PDC (40 μ M). Samples were incubated at 37°C for 2 minutes and the reaction was terminated using a Tomtech 96-well cell harvester by filtration over Whatman GF/C filters. Filters were rinsed twice with 4 mls of cold EBSS and the radioactivity remaining on the filters was determined using a Wallac beta-plate reader.

For the *in vitro* experiments, the assays were performed as detailed above with the following exceptions. Tissue was preincubated with the inhibitor (EtOH, PDC or kainic acid). Uptake was initiated by the addition of 100 nM L-[³H]glutamate. 50 μ l of the inhibitor was added in place of unlabeled glutamate thus keeping the total assay volume at 250 μ l.

Blood EtOH Measurement

BEC was determined according to Roach and Creaven (1968). Briefly, 20 μ l of blood were taken from the tip of the tail and mixed with 50 μ l ZnSO₄, 50 μ l of 0.3N Ba(OH)₂ and 300 μ l of distilled water. Samples were centrifuged at 12,000 rpm for 5 minutes and the resulting supernatant was analyzed for EtOH concentration by gas chromatography. Standards of known EtOH concentrations were run with the samples.

Immunocytochemistry and Histochemistry

Slice Preparation

Mice were overdosed with an anesthetic containing 5 % ketamine, 2 % xylazine and 1 % acepromazine (0.1 – 0.2 mls/animal) and transcardially perfused with 6 mls of 1000 units/ml heparin in 0.1M phosphate buffer followed immediately by 10 mls of fixative containing 2 % paraformaldehyde, 3.75 % acrolein in 0.1M phosphate buffer and 40 mls 2 % paraformaldehyde in 0.1M phosphate buffer using a peristaltic pump (Cole Parmer, Vernon Hills, IL) at a rate of 25 mls/minutes. Brains were harvested and post-fixed for 1 hour in cold fixative containing 2 % paraformaldehyde, washed with cold 0.1M phosphate buffer overnight. Up to 10 adjacent sections (50 μ m, coronal) were cut from anterior regions of the hippocampus from each mouse using a vibratome (System 1000, Ted Pella, Redding, CA). Sections were placed in 0.1M phosphate buffer for several days (at 4°C).

Immunoperoxidase Reaction

On the day of the experiment, excess aldehyde groups still present in the tissue were reacted with 0.1 % sodium borohydride in 0.1M phosphate buffer. Tissue was extensively washed in 0.1M phosphate buffer and then preincubated in a blocking solution containing 1 % normal goat serum and 0.01 % Triton X-100 in 0.1M phosphate buffer for 1 hour at 4°C. Primary antibodies were diluted with this blocking solution and tissue was incubated overnight at 4°C.

Tissue slices from each animal were incubated with either primary polyclonal antibodies against glial fibrillary acidic protein (GFAP, 1:25), glutamine synthetase (GS, 1:32,000) or one of the three glutamate transporters (GLAST, 1:3500; GLT-1, 1:3000; EAAC1, 1:1000). Control slices were exposed to the blocking solution (with no primary antibody) overnight at 4°C. The antibody against GFAP was characterized by the Dako Corporation. The glutamine synthetase antibody also has been previously characterized

(Oda et al., 1983). The antibodies against the glutamate transporters have not yet been characterized for specificity. However, based on the pattern of staining (i.e EAAC1 is localized to pyramidal cell bodies) observed in pilot experiments, it appears that these antibodies are at least specific for the structures to which they have been localized.

Tissue was rinsed with the blocking solution and exposed to the secondary antibody (biotinylated goat anti-rabbit IgG diluted to 0.44 % in 0.1M phosphate buffer) for 30 minutes at room temperature. This was followed by exposure to an avidin-biotin complex (standard protocol with Vector ABC Elite kit) for 30 minutes at room temperature, and several washes. The reaction product was visualized using nickel-enhanced diaminobenzidine (DAB; standard protocol using Vector Peroxidase Substrate kit). Tissue was exposed to the nickel/DAB solution for 2 minutes for all antibodies except the glutamate transporter EAAC1 (5 minutes). All tissue slices were mounted on gelatin-coated slides, air dried overnight and coverslipped.

Histochemical Reaction

Mice were anesthetized and perfused as detailed above (see Immunoperoxidase section) with the following exceptions. Animals were perfused with 10 mls of 0.1M sodium phosphate buffer with 4% sucrose followed immediately by 100 mls of fixative containing 2.5% paraformaldehyde, 1.5% glutaraldehyde and 4% sucrose in 0.1M phosphate buffer (pH 7.4). Brains were harvested and post-fixed for 1 hour in cold fixative. Brains were then washed with cold 0.1M phosphate buffer containing 4% sucrose and rinsed overnight at 4°C.

Two 100 μ m thick coronal sections were cut from anterior regions of the hippocampus from each mouse using a vibratome (System 1000, Ted Pella, Redding, CA). Tissue sections were incubated in 0.02% cytochrome c and 0.05% DAB in warmed phosphate buffered saline for 15 minutes at 37°C. Incubated tissue was washed in 0.1M

phosphate buffer with 4% sucrose twice and in 0.1M phosphate buffer three times. Tissue was then mounted on glass slides, dried overnight and coverslipped.

Optical Density Measurements

Tissue slices were visualized using a Zeiss Axioplan light microscope (Carl Zeiss Inc., West Germany) and images were captured with a 5x objective (final magnification of 62.5x) for GLAST, GLT-1, GS, cytochrome oxidase and low magnification GFAP experiments or with a 20x objective (final magnification of 400x) for EAAC1 and high magnification GFAP experiments using a Polaroid Digital Microscope Camera (Cambridge, MA) and saved onto recordable compact discs. All images from a given experiment were captured in one session to minimize differences due to potential variations in light source intensity. Optical density measurements were calculated using the Image-Pro Plus software (Version 3.01, Media Cybernetics, Silver Springs, MD). One slice containing both hemispheres was analyzed for each animal except for the cytochrome oxidase experiments in which two slices containing both hemispheres were analyzed. The light intensity of a region of a slide that contained no tissue was assigned an optical density value of zero. Optical densities for the regions of interest were calculated. Larger values of optical density correlated with areas of darker immunoreaction on the slides. The regions of interest included the stratum radiatum and stratum pyramidale of the CA1 region of the hippocampus, the stratum radiatum of the CA3 of the hippocampus, the molecular layer of the dentate gyrus and layers II – VI of the somatosensory cortex (Franklin and Paxinos, 1997).

For low magnification analysis, the entire area of each brain region of interest was analyzed in each animal (Fig. 2). A computer generated mean optical density for each hemisphere of each region was collected. Data from both hemispheres of each animal were averaged and used in the statistical analysis. For high magnification analysis, cells immunolabeled above background were circled, counted and the optical

density within each cell was determined by the image analysis program. The mean area and optical density for each animal was calculated and used in the final statistical analysis. For the GFAP experiment, the number of cells, the cell body area and the mean optical density for all labeled cells within a $280 \times 140 \mu\text{m}$ area of the stratum radiatum of the CA1 region of the hippocampus of each animal was used in the analysis. For the EAAC1 experiment, the number of labeled pyramidal cells and the mean optical density of these cells was calculated in the stratum pyramidale of the CA1 region of the hippocampus. The optical density within cells was subtracted from background labeling. All labeled cells within the CA1 region of the hippocampus were analyzed. A mean optical density for each animal was generated and used in the statistical analysis.

Statistics

Kinetic and statistical analysis for glutamate uptake experiments

Specific L-[^3H]glutamate uptake was calculated as nmol uptake per mg protein per 2 minutes. Maximal L-[^3H]glutamate uptake (V_{max}) and apparent affinity of the transporter for glutamate (K_{m}) were estimated using the non-linear curve fitting program, Prism (GraphPAD Software, San Diego, CA). Statistical analysis of V_{max} and K_{m} was done using analysis of variance (ANOVA). Each experiment was performed at least three times.

When necessary, replicate lines within each selected line and treatment group were compared first using a one-way ANOVA or t-test (i.e. WSP-1 vs. WSP-2 controls were compared, etc.). Data were collapsed across replicate lines when no significant difference existed. For withdrawal experiments, data from the two control groups (saline and pyrazole) were compared using a two-way ANOVA (line x control treatment). Data were collapsed across control treatments when no significant differences were detected. Finally, differences between selected lines and treatment groups were assessed using a two-way ANOVA (selected line x treatment group).

Correlations between BEC and V_{\max} or K_m were computed using a linear regression model from Prism (GraphPAD Software, San Diego, CA). Hippocampi from 3–4 mice were combined for the L-[^3H]glutamate uptake assay and a single V_{\max} and K_m value were obtained. Blood samples were collected from all mice exposed to EtOH in the inhalation chambers and a mean BEC value was calculated from animals that were pooled for assessment of glutamate uptake. The V_{\max} and K_m values obtained from each experiment were regressed on the mean BEC calculated from all mice.

Statistical Analysis for immunocytochemical and histochemical experiments

For low magnification analyses, data from each brain region and each experiment were analyzed separately. The mean optical density from both hemispheres of each animal were collected and averaged, resulting a mean density for each animal. Data from each animal in each mouse line (i.e. WSP-1, WSP-2, WSR-1, WSR-2) were then combined to generate a mean optical density for each line and replicate. These means were then analyzed using a two-way ANOVA (selected line x replicate line). If no significant differences were observed between the replicate mouse lines, the data were combined and a one-way ANOVA was performed. When significant interactions were observed, a post-hoc analysis of simple effects was performed.

For the high magnification analysis of the EAAC1 experiment, the mean optical density within each cell was subtracted from the mean optical density of an adjacent region (representing background). Cells from each animal were combined and averaged. The mean optical density for each mouse line was then calculated and analyzed using a two-way ANOVA.

For high magnification analysis of the GFAP experiments, the number of immunolabeled glial cells, the area of those cell bodies and the mean optical density from each cell body was computed. Three separate two-way ANOVAs were then performed (comparing number, area and optical density between mouse lines). All cells analyzed

from each hemisphere were averaged and the mean from both hemispheres was averaged. This resulted in a single mean value (for each parameter analyzed) for each animal, which was used in the statistical analysis.

RESULTS

Glutamate Uptake Experiments

Effect of handling on [3 H]glutamate uptake

Drug-naïve WSP mice may exhibit HICs throughout life as a result of routine handling. To determine whether this HIC activity altered glutamate uptake, V_{\max} and K_m of L-[3 H]glutamate uptake were measured in synaptosomes prepared from naïve WSP and WSR mice that were either handled in a normal manner by trained animal care technicians (colony raised, CR) or handled using a special protocol that avoided the possible induction of convulsions (specially raised, SR). [3 H]Glutamate uptake was assessed in hippocampal and cortical synaptosomes. Glutamate uptake was dose-dependent and saturable and is expressed as nmol per mg protein per 2 minutes. No significant differences in hippocampal (Fig. 3) or cortical (Fig. 4) V_{\max} or K_m values were observed between mouse lines or treatment groups.

Effect of acute HIC activity on [3 H]glutamate uptake

Drug-naïve HICs that occur in WSP mice during routine handling had no apparent effect on glutamate uptake (Figs. 3 and 4). It was unclear how often and how severely these WSP mice convulsed. To ascertain the effect of frequent tonic convulsions on glutamate uptake, EtOH-naïve WSP-2 and WSR-2 mice were exposed to ten handling trials that resulted in at least 8 HIC non-zero scores in WSP mice and no HIC activity in WSR mice. WSP-2 mice were used in this experiment because these mice have more consistent drug-naïve HIC activity as compared to WSP-1 mice (Buckman et al., *submitted*).

One hour following the final handling trial, [3 H]glutamate uptake was assessed in hippocampal and cortical synaptosomes (this time point was chosen to correspond to other experiments). Again, uptake was dose-dependent and saturable. No differences in

hippocampal (Fig. 5) or cortical (Fig. 6) V_{\max} or K_m values were observed between mouse lines or treatment groups.

Effect of EtOH intoxication on [3 H]glutamate uptake

WSP and WSR mice exhibit differences in the severity of their withdrawal from acute and chronic EtOH (Kosobud and Crabbe, 1986; Crabbe et al., 1991). It is not known whether these differences result from chronic exposure to EtOH *per se* or to compensatory mechanisms triggered by withdrawal from chronic EtOH. In order to determine whether glutamate uptake was altered by EtOH exposure *in vivo*, WSP-2 and WSR-2 mice were injected with saline or EtOH (4 g/kg) and euthanized 5 minutes later. Peak brain EtOH concentrations are expected within 10 minutes of an i.p., injection (Goldstein, 1983). Hippocampal and cortical L-[3 H]glutamate uptake was dose-dependent and saturable. Analysis of V_{\max} and K_m values in hippocampal (Fig. 7) and cortical (Fig. 8) preparations revealed no significant effect of line or treatment group.

Effects of *in vitro* EtOH exposure on [3 H]glutamate uptake

L-[3 H]Glutamate uptake did not appear to be altered by acute *in vivo* EtOH exposure (Figs. 6 and 7). To ascertain whether glutamate transporter activity was influenced by direct exposure to EtOH, hippocampal synaptosomes prepared from naive WSP mice were exposed *in vitro* to various concentrations of EtOH. Synaptosomes were also exposed to PDC or kainic acid. PDC and kainic acid are known inhibitors of glutamate uptake and were used to confirm that inhibition of uptake could be observed using this assay technique. Dose-dependent inhibition of L-[3 H]glutamate uptake was observed for PDC and kainic acid (Figs. 9B and C). No inhibition of L-[3 H]glutamate uptake was observed following a 15 minute exposure to EtOH (Fig. 9A). Similar observations were observed in WSR mice (data not shown).

Effect of EtOH withdrawal on [3 H]glutamate uptake

To assess the effect of withdrawal from chronic EtOH on glutamate uptake, hippocampal synaptosomes were prepared from both replicate lines of WSP and WSR mice that were (1) exposed to air in inhalation chambers and injected with saline (SAL), (2) exposed to air in inhalation chambers and injected with pyrazole (PYR), or (3) exposed to EtOH vapor and injected with pyrazole (ETOH) (Fig. 10). [3 H]Glutamate uptake was tested during peak withdrawal. Initial analysis compared V_{\max} and K_m values from the replicate WSP and WSR lines. Since there were no significant differences between WSP-1 and WSP-2 or between WSR-1 and WSR-2 lines, data were pooled across replicate lines for further analysis (Fig. 11).

To determine whether pyrazole treatment altered [3 H]glutamate uptake, WSP and WSR mice from the SAL and PYR groups were compared using a two-way ANOVA. There were no differences in hippocampal V_{\max} or K_m values between mouse lines or between saline and pyrazole treatments. Therefore, data from the SAL and PYR groups were collapsed for further analysis.

Direct comparisons were made between animals exposed to control treatments (SAL + PYR = CONT groups) and those exposed to chronic EtOH (EtOH groups). Withdrawal from chronic EtOH significantly increased maximal glutamate uptake (i.e. V_{\max}) in both WSP and WSR mice versus the EtOH-naive controls. Hippocampal V_{\max} values were not different between the lines. No differences in K_m values were observed between lines or treatments.

To determine whether the tissue concentration of EtOH was related to alterations in glutamate uptake, BECs taken after 72 hours of EtOH exposure were regressed on withdrawal V_{\max} and K_m values (Fig. 12). V_{\max} and K_m values were calculated for each synaptosomal preparation (containing hippocampi from 3-4 mice) used in each experiment. All mice receiving EtOH vapor were analyzed for BEC and animals with BECs in the range of 1.0 – 2.0 mg/ml were chosen for use in this experiment. BECs

from each mouse used in a synaptosomal preparation were averaged and the mean BEC was regressed on the corresponding V_{\max} and K_m values. The overall mean BEC was 1.16 mg/ml. The mean BEC achieved in the WSP mice was 1.10 mg/ml and the mean BEC for WSR mice was 1.22 mg/ml. There was no significant correlation between either the V_{\max} or K_m for glutamate uptake and BEC.

Glutamate Transporter Immunolabeling

GLAST

The density of immunolabeling was analyzed in the stratum radiatum of the CA1 and CA3, the molecular layer of the dentate gyrus and the somatosensory cortex (Fig. 2). GLAST immunoreactivity were assessed in naive WSP and WSR mice from both replicate lines to determine whether differences in specific glutamate transporter subtypes were altered during the selection of WSP and WSR mice (Fig. 13). GLAST is a glial glutamate transporter and the phenotypic differences between WSP and WSR mice may be reflected by differences in GLAST immunolabeling. A significant interaction between selected and replicate line data was observed in the stratum radiatum of the CA1 region of the hippocampus. Post-hoc analysis revealed that this difference was the result of WSP-2 mice exhibiting a significantly greater density of GLAST immunolabeling as compared to WSR-2 mice ($p < 0.01$). No mouse line differences were observed in the CA3 of the hippocampus, the molecular layer of the dentate gyrus or the somatosensory cortex (Fig. 14).

GLT-1

Naive WSP and WSR mice from both replicate lines were assessed for GLT-1 protein levels using light microscopic immunoperoxidase (Fig. 15). GLT-1 is a glutamate transporter located on glial cells and may have been influenced by the selection process used to develop the WSP and WSR mouse lines. No significant

differences in the density of GLT-1 immunolabeling in the stratum radiatum of the CA1 and CA3, the molecular layer of the dentate gyrus and the somatosensory cortex were observed between the mouse lines (Fig. 16). However, since no replicate line differences were observed, data were collapsed and reanalyzed using a one-way ANOVA (WSP vs. WSR). In the CA3 subfield of the hippocampus, GLT-1 immunolabeling approached significance ($p = 0.0625$).

EAAC1

The density of the neuronal glutamate transporter, EAAC1, immunoreactivity was assessed in naive WSP and WSR mice from both replicate lines (Fig. 17). It is much less abundant, than the glial transporters but may function in a different manner to control glutamatergic activity. The density of EAAC1 immunolabeling within pyramidal cells in the stratum pyramidale of the CA1 was analyzed. No significant differences in any region were observed between the mouse lines (Fig. 18).

Glutamine Synthetase Immunolabeling

The density of glutamine synthetase labeling in glial cells was determined in naive WSP and WSR mice from both replicate lines (Fig. 19). Glutamine synthetase is responsible for the metabolism of glutamate. No significant differences were observed between the selected lines the hippocampus or somatosensory cortex (Fig. 20). However, due to similarities between the pattern of results for GLAST and glutamine synthetase, a post-hoc unpaired t-test compared only replicate line 2 mice was performed. The mean optical density of WSP-2 and WSR-2 mice in the CA1 ($t=1.87$; $p = 0.091$) and the somatosensory cortex ($t=1.88$, $p=0.087$) approached significance.

Glial Fibrillary Acidic Protein Immunolabeling

A subset of naive WSP and WSR mice from both replicate lines (3 animals/group) were analyzed for the density of GFAP labeling in glial cells (Figs. 21 and 22). GFAP is associated with the intermediate filaments in glial cells and differences in GFAP immunolabeling between the selected lines may be indicative of altered glial cell structure. The density of GFAP immunolabeling in the stratum radiatum of the CA1 and CA3, the molecular layer of the dentate gyrus and the somatosensory cortex was determined at low power. Although significant differences were observed only between the replicate lines in the CA1 region of the hippocampus (i.e. replicate 1 > replicate 2; Fig. 23), differences between the selected lines approached significance in all brain regions (CA1: $p=0.11$; CA3: $p=0.09$; DG: $p=0.054$; SSC: $p=0.08$).

The number, area and optical density of GFAP immunolabeled glial cells in the stratum radiatum of the CA1 visualized at high power was computed. Analysis of individual glial cell numbers and area in the CA1 revealed no significant differences between the selected lines (Fig. 24). A significant difference in the mean optical density of GFAP-immunopositive cell bodies was observed, with replicate 2 mice exhibiting lower GFAP immunolabeling as compared to replicate line 1 mice.

Cytochrome Oxidase Activity

Naive WSP and WSR mice from both replicate lines were assessed for cytochrome oxidase activity using histochemistry (Fig. 25). Cytochrome oxidase reflects the activity of the CNS, especially of neuronal structures. The optical density of the cytochrome oxidase reaction was analyzed in the stratum radiatum of the CA1 and CA3, the molecular layer of the dentate gyrus and the somatosensory cortex but no significant differences in any region were observed between the mouse lines (Fig. 26).

DISCUSSION

Naive Glutamate Uptake and Transporter Subtype Immunolabeling

To assess the functional significance of the differences observed in the density of nerve terminal glutamate immunoreactivity between naive WSP and WSR mice (Buckman and Meshul, 1997), synaptosomal L-[³H]glutamate uptake and the density of GLAST, GLT-1 and EAAC1 immunoreactivity were analyzed in the naive hippocampus and cortex of these mouse lines. Under normal physiological conditions, nerve terminal transmitter content should be indicative of the amount of transmitter available for release (Aas et al., 1993). Likewise, transmitter uptake should vary with the amount of transmitter released. A functional relationship between availability, release and uptake is necessary to maintain low extracellular concentrations of glutamate (Attwell et al., 1993; Fig. 1).

No differences in V_{max} or K_m values were detected between drug- and convulsion-naive WSP and WSR mice suggesting that genes encoding the glutamate transporters were not affected by genetic selection. Glutamate transporters in WSP and/or WSR mice may function normally under basal conditions but may not compensate for treatment-induced perturbations in glutamate release. Alternatively, changes in glutamate uptake may be too subtle to be detected using the assay employed for these experiments. There are a number of reasons to suspect the latter explanation. Crude synaptosomes (rich in presynaptic terminals) were used to assess glutamate uptake, but only indirect evidence suggests the presence of glutamate transporters presynaptically (Gundersen et al., 1993). The uptake of glutamate into synaptosomal preparations may be the result of glial contamination (Gegelashvili and Schousboe, 1998) and a heterogeneity of transporters that are found in these preparations (Dowd et al., 1996). In addition, the synaptosomes used in these experiments were prepared from whole hippocampi, but different regions of the hippocampal formation (i.e. CA1, CA3, dentate gyrus) are differentially sensitive to excitotoxic perturbations. Heterogeneity of transporter expression within specific

subfields also has been reported (Rothstein et al., 1994). Thus, it may be that one subtype of glutamate transporter or transport in only one region of the hippocampus is influenced by genetic selection. Unaffected transporters or insensitive hippocampal regions also present in our synaptosomal preparation could dilute treatment effects.

In order to test this, the density of glutamate transporter subtype immunolabeling in hippocampal slices from naive WSP and WSR mice was analyzed. The glutamate transporters, GLT-1, GLAST and EAAC1 have been localized to the hippocampus and antibodies against them are commercially available. Using light microscopic immunocytochemistry, assessment of transporter subtype immunolabeling within discrete regions and layers of the hippocampus was possible (Fig. 2). The analysis of the density of GLAST immunolabeling revealed a significant interaction between selected and replicate lines in the CA1 region of the hippocampus. Post-hoc analysis indicated that this was due to significant differences between mice from replicate line 2 ($p < 0.01$). WSP-2 mice had significantly more GLAST immunoreactivity (146%) as compared to WSR-2 mice in the CA1 region of the hippocampus (Fig. 14). No other significant differences existed. No differences in the density of GLT-1 immunolabeling in any brain region tested were observed between naive WSP and WSR mice (Fig. 16). However, when the replicate lines were combined, differences between WSP and WSR GLT-1 protein density did approach significance in the CA3 ($p = 0.0625$) with naive WSP mice exhibiting modestly greater GLT-1 labeling (110%) than naive WSR mice. Analysis of EAAC1 immunoreactivity within hippocampal and cortical pyramidal cells revealed no significant selected line differences (Fig. 18). Therefore, WSP mice, especially WSP-2 mice, exhibit a greater density of glial glutamate transporters as compared to WSR mice but these differences are modest and localized to discrete regions of the hippocampus.

L-[³H]glutamate uptake does not appear to differ between naive WSP and WSR mice but WSP-2 mice have greater GLAST immunolabeling in the CA1 region of the hippocampus and a trend toward greater GLT-1 immunoreactivity in the CA3 of the

hippocampus. These data may suggest that the differences in immunoreactivity are not associated with alterations in transporter activity. Alternatively, the glutamate uptake assays performed with crude synaptosomal preparations may not be sensitive enough to detect subtle differences in transporter function resulting from slight differences in transporter number. The majority of L-[³H]glutamate uptake that occurs into synaptosomes is considered to be glial (Gegelashvili and Schousboe, 1998) and GLT-1 is thought to be responsible for the majority of glutamate uptake in the CNS (Tanaka et al., 1997). GLT-1 immunoreactivity in the selected lines was similar in the CA1 and dentate gyrus and modestly different in the CA3. GLAST immunoreactivity was similar in the CA3 and dentate gyrus. Consequently the combination of subtle and region specific differences in transporter density may not have been sufficient to result in detectable differences in glutamate uptake as measured using whole hippocampal L-[³H]glutamate uptake assays.

The number of animals per group in these immunohistochemical experiments was relatively low which may be the reason for the lack of significant mouse line differences detected. However, the data presented here do suggest that repeating this experiment using a larger number of animals is warranted. Moreover, it is unlikely that a single protein or gene was profoundly altered during selection and therefore, due to the number of genes potentially involved in ethanol withdrawal HICs, only subtle differences between the selected lines should be observed. Thus, analysis of glutamate transporter subtype immunolabeling using a more specific immunochemical technique (i.e. immunogold) or at the ultrastructural level may improve resolution sufficiently to detect subtle differences that exist between the selected lines. Furthermore, preliminary characterization of EAAT4, a neuronal transporter, suggests that low concentrations of this transporter may be present in the hippocampus (Fairman et al., 1994; Futura et al., 1997). The density of EAAT4 immunolabeling could be associated with the behavioral differences observed between WSP and WSR mice as well.

In conclusion, the density of the glutamate transporter subtypes GLAST, in the stratum radiatum of the CA1, and GLT-1, in the stratum radiatum of the CA3, were slightly greater in naive WSP mice as compared to naive WSR mice (Table 4). These data, although merely suggestive, do indicate that the glial glutamate transporters may have been affected by selection and may be associated with the selected line differences in susceptibility to drug-naive and/or ethanol withdrawal HICs. Further assessment of these glial transporters is warranted.

Glutamate Uptake in WSP and WSR mice following HICs or EtOH

Postsynaptic activation and/or excitotoxicity resulting from increased extracellular glutamate availability can inactivate or reverse the ATP-, Na^+ -, K^+ -, and voltage-dependent glutamate transporters (Szatkowski et al., 1990, Madl and Burgesser, 1993). Both convulsions and withdrawal from EtOH may result in glutamatergic hyperexcitability; therefore line differences in glutamate uptake may be observable after treatments that stimulate the release of glutamate and lead to different behavioral responses in the WSP and WSR mouse lines.

L-[^3H]glutamate uptake was assayed in hippocampal and cortical synaptosomes prepared from drug-naive WSP-2 and WSR-2 mice that were handled in a manner that would elicit HICs in sensitive WSP mice. Uptake was assessed one hour after ten handling trials to determine the effect of acute HIC activity. The WSP-2 mice tested in these experiments displayed a range of convulsion severity and duration, but each mouse exhibited at least 8 tonic convulsions during the 10 handling trials. No HIC activity was seen in WSR mice. No differences between mouse lines in V_{\max} or K_m values were observed in either brain region. Thus, handling *per se* (and acute HIC activity in WSP mice) did not alter V_{\max} or K_m values (Figs. 5 and 6; Table 5). However, these convulsions might not be sufficiently severe to impact glutamate uptake. It is also possible that these HICs alter uptake in discrete regions of the hippocampus [i.e. CA1

(for evidence of regional effects see Prince Miller et al., 1997; Akbar et al., 1998)] or in only a subset of glutamate transporters [i.e. GLAST, GLT-1 or EAAC1 (Prince Miller et al., 1997; Akbar et al., 1998)]. Furthermore, the effect of HICs on glutamate uptake may be too transient to be detected using this assay technique. This last explanation seems unlikely because separate studies assessed glutamate uptake immediately following a single handling trial, but did not detect line differences or changes from baseline (data not shown).

The effect of a single intoxicating dose of EtOH on glutamate transporter activity in WSP and WSR mice was assessed at 5 minutes, a time corresponding to peak brain EtOH concentrations. EtOH intoxication suppresses HIC activity (Kosobud and Crabbe, 1986) and no convulsions were observed during this experiment. No line differences in V_{\max} or K_m values were observed in hippocampal or cortical synaptosomes (Figs. 7 and 8). In addition, glutamate uptake following acute *in vivo* EtOH exposure was not different than uptake following a saline injection. Because injections were given 5 minutes prior to sacrifice, handling and/or injection stress may have masked an effect of EtOH. To test this, L-[^3H]glutamate uptake was also measured at a 60 minute post-injection time point and during peak withdrawal (7-8 hours following injection) but no differences between lines or treatments were observed (data not shown). Therefore, these data suggest that a hypnotic dose of EtOH (4 g/kg) does not alter glutamate uptake in WSP and WSR mice. These data are in agreement with Keller et al. (1983), who reported that a 4 g/kg EtOH injection was not sufficient to alter glutamate uptake in rat hippocampal slices or synaptosomes.

Valverius et al. (1990) reported an upregulation of the NMDA subtype of glutamate receptors in WSP and WSR mice during chronic EtOH intoxication. This was evidenced by an increase in the number of [^3H]MK-801 binding sites following 6-7 days of a liquid diet containing EtOH. A basal difference in [^3H]MK-801 binding sites in the hippocampus was observed, but it did not appear that EtOH influenced binding

differently in the selected lines. Carter et al. (1995), on the other hand, did not observe basal differences in the number of [3 H]MK-801 binding sites in WSP and WSR mice. In addition, no changes in [3 H]MK-801 binding were observed in WSP or WSR mice after 24 hours of EtOH vapor exposure (tested during intoxication and withdrawal) (Carter et al., 1995). These data indicate that the effects of EtOH on NMDA receptors are independent of selection and also raise the possibility that long term exposure (> 24 hours) is necessary to induce compensatory changes that can be observed using binding or uptake assays.

Acute exposure to convulsions or EtOH may not be sufficient to alter L-[3 H]glutamate uptake (Figs. 3-7; Table 5). The direct effect of acute EtOH exposure was tested in hippocampal synaptosomes from naive WSP mice. These synaptosomes were exposed to various concentrations of EtOH *in vitro*. No dose-dependent inhibition of glutamate uptake was observed following 15 minutes of exposure (Fig. 9A). No inhibition of glutamate uptake was observed until concentrations of 1M were achieved and at this concentration, uptake was almost completely abolished (data not shown). Similar results were obtained using synaptosomes prepared from naive WSR mice (data not shown). Conversely, exposure of hippocampal synaptosomes from naive WSP mice to PDC, a nonspecific uptake inhibitor, or kainic acid, a moderately selective inhibitor of the glial transporter GLT-1, resulted in a dose-dependent inhibition (Figs. 9B & C). This further suggests that acute exposure to EtOH does not impact synaptosomal glutamate uptake.

Compensatory changes in uptake may be observed only after long-term exposure to EtOH. To test this, hippocampal synaptosomes were prepared from WSP and WSR mice and glutamate uptake was tested during peak withdrawal. Exposure to 72 hours of EtOH vapor significantly increased maximal L-[3 H]glutamate uptake in both lines when compared to their air exposed controls (Fig. 11). K_m values were not different during withdrawal.

Animals can exhibit a wide range in their metabolic response to EtOH. Differences in BEC often can be observed between mice following exposure to the same concentration of EtOH. Since the duration and concentration of EtOH exposure can influence the severity of withdrawal (Crabbe et al., 1985), it is essential to test whether animals experience different tissue concentrations of EtOH. In the case of the WSP and WSR mouse lines, BECs are routinely taken during exposure to EtOH vapor. The concentration of EtOH vapor and the dose of pyrazole can be varied to ensure that mice are exposed to similar concentrations of EtOH (Crabbe and Phillips, 1993). In addition, BECs are determined upon removal from the inhalation chambers thereby making it possible to specifically choose animals from each selected line that have been exposed to similar concentrations of EtOH. For each of experiment assessing the effect of chronic EtOH withdrawal on glutamate uptake, mice exhibiting similar BECs were chosen (mean WSP BEC = 1.10 mg/ml, mean WSR BEC = 1.22 mg/ml). However, there was some variability in the average EtOH exposure (i.e. average BEC) between experiments. Therefore, BECs taken after 72 hours of EtOH exposure were regressed on withdrawal V_{\max} and K_m values. No correlation between glutamate uptake and BEC (following 72 hours of EtOH vapor exposure) was found (Fig. 12). These observations indicate that glutamate uptake is not directly influenced by the amount of alcohol in the blood.

Taken together, these data suggest that maximal L-[^3H]glutamate uptake is increased during withdrawal from chronic EtOH, regardless of BEC or inherent sensitivity to EtOH. The observed withdrawal-induced increase in uptake may be associated with compensatory changes resulting from chronic EtOH exposure that occur regardless of the animal's genetic predisposition towards withdrawal severity. These data are in agreement with the observation that the effect of EtOH on NMDA receptor binding activity was independent of selection (Valverius et al., 1990; Carter et al., 1995). However, they contradict those previously reported by Roach et al. (1973a), who found a decrease in [^3H]glutamate uptake in rats that exhibited severe withdrawal symptoms

(such as convulsions) following 7 days of EtOH inhalation. The methods used in the present experiment differ from those previously reported (Roach et al., 1973a) in that the present study utilized synaptosomes prepared from hippocampus (versus whole brain) from selectively bred mice (versus rats) and HICs were not elicited during withdrawal. WSP mice consistently exhibit HICs during EtOH withdrawal, whereas the WSR mice display mild, if any, HIC activity (Crabbe et al., 1985; Kosobud and Crabbe, 1986; Crabbe and Phillips, 1993). Thus, these mouse lines are useful models for characterizing the effect of EtOH withdrawal on glutamate uptake without confounding the analysis with convulsive activity.

In conclusion, it appears that withdrawal from chronic EtOH alters L-[³H]glutamate uptake into hippocampal synaptosomes prepared from WSP and WSR mice (Table 5). This withdrawal-induced increase in glutamate uptake does not appear to be related to selection (Fig. 11), direct effects of EtOH (Fig. 9A) nor to BECs taken after 72 hours of EtOH exposure (Fig. 12). Modest differences in glial glutamate transporter immunoreactivity were detected between naive WSP and WSR mice suggesting that more pronounced selected line differences in glial transporter immunoreactivity should be observed during withdrawal from chronic EtOH. It is possible that one or all of the glutamate transporter subtypes are altered during EtOH withdrawal. Therefore, it would be of interest to determine which transporter is responsible for the compensatory increase in glutamate uptake observed during withdrawal.

Glutamine Synthetase and Glial Fibrillary Acidic Protein Immunolabeling

Normal glutamatergic activity is dependent on glial cell function (Fig. 1). In addition to being responsible for the majority of uptake, astrocytes contain glutamine synthetase, an enzyme that metabolizes glutamate into glutamine. Glutamine synthetase is located in distal processes of astrocytes that are located in close proximity to glutamate-containing nerve terminals (Derouiche and Frotscher, 1991). When glutamate

is released from axon terminals, it is taken up into glial cells and metabolized. A direct association between uptake and metabolism has been suggested by Derouiche and Rauen (1995) who reported co-localization of glutamine synthetase and the glial glutamate transporter GLAST. In the present study, greater GLAST immunolabeling was observed in the CA1 region of the hippocampus of naive WSP-2 mice as compared to naive WSR-2 mice (Fig. 14). This may be indicative of greater glial uptake and therefore of greater glial metabolism of glutamate. Glutamine synthetase immunolabeling was measured in the stratum radiatum of the CA1 and CA3, the molecular layer of the dentate gyrus and layer II – VI of the somatosensory cortex. Analysis of variance indicated that there were no significant differences between the selected lines (Fig. 20). However, due to the similarity in the pattern of the results between GLAST immunolabeling and glutamine synthetase immunolabeling and the observation that GLAST immunoreactivity was only different between replicate line 2 mice, a post-hoc unpaired t-test that compared WSP-2 and WSR-2 mice was performed. This analysis revealed a trend towards significance in the stratum radiatum of the CA1 region of the hippocampus ($p = 0.091$) with glutamine synthetase labeling being higher in naive WSP-2 mice (142%) as compared to WSR-2 mice. Glutamine synthetase immunoreactivity in the somatosensory cortex of WSP-2 mice also was elevated (143%) as compared to WSR-2 mice, but again this approached, but did not achieve significance ($p = 0.087$). The trend toward a greater density of the glutamate-metabolizing enzyme may indicate that more glutamate is being released and taken up into glial cells. Taken together with the observed differences in glial glutamate transporter immunoreactivity, these data are consistent with the hypothesis that glutamatergic activity is increased in naive WSP mice, especially from replicate line 2, as compared to naive WSR mice (Table 4).

GFAP is a structural protein located in glial cell bodies and proximal glial processes. It is observed in most astrocytes, but protein levels are greatly increased following glial cell damage (Eng, 1985). Modest differences in glial transporters and

glutamine synthetase density between WSP and WSR mice (mostly from replicate line 2) raised the question of whether structural abnormalities in glial cells exist in one of the selected lines. A reactive gliosis is commonly observed following excessive excitatory activity (Steward et al., 1991) and is one of the most common observations in human temporal lobe epilepsy (Scheibel et al., 1974; Grisar, 1984). Therefore, since WSP mice, especially from replicate line 2, exhibit a heightened susceptibility to HICs (Buckman et al., *submitted*), it is possible that a gliotic reaction may have developed in WSP mice from exposure to drug-naïve, convulsion-inducing stimuli. We tested both replicate lines of WSP and WSR mice for the density of immunoperoxidase labeling of GFAP (in 50µm thick slices) within cell bodies and glial processes in regions of the hippocampus and cortex.

A significant difference in GFAP labeling between replicate lines was observed in the CA1 region of the hippocampus with replicate line 2 mice exhibiting significantly less GFAP (63 %) as compared to replicate line 1 mice (Fig. 23, Table 4). No significant selected line differences were observed in any region tested, but differences approached significance. WSR mice consistently showed greater GFAP labeling as compared to WSP mice [CA1: 129%, CA3: 137%, DG: 148%, SSC: 132%]. These observations were surprising because WSP mice had a tendency to express more GLAST, GLT-1 and glutamine synthetase immunolabeling as compared to WSR mice. Moreover, lower GFAP immunolabeling is the opposite of what would be expected if HIC activity in WSP mice had resulted in a reactive gliosis. Furthermore, since WSP-2 mice exhibit more consistent drug-naïve HIC activity as compared to WSP-1 mice (Buckman et al., *submitted*), greater GFAP immunolabeling would be expected in replicate line 2 mice as compared to replicate line 1 mice.

Analysis of glial cell body labeling in the CA1 also revealed significant replicate, but not line differences (Fig. 24). Again, replicate-2 mice exhibited significantly less GFAP labeling within glial cell bodies (71 %) as compared to replicate-1 mice. No

difference in the number or area of GFAP-immunopositive cell bodies was observed between the mouse lines. The immunolabeling data are suggestive of mild alterations in glial cell morphology between replicate lines and possibly between the selected lines. These structural differences do not appear to be associated with the number or size of glial cell bodies but rather may be related to the glial processes labeled by GFAP (Fig. 23).

Comparison of glutamine synthetase and GFAP immunolabeling in the hippocampus and cortex of naive WSP and WSR mice suggests that glial cells in WSP mice have a slightly greater density of the metabolizing enzyme, glutamine synthetase, but a somewhat lower density of the cytoskeletal protein, GFAP. These findings are difficult to interpret because glutamine synthetase and GFAP protein are differentially localized within glial cells (Norenberg and Martinez-Hernandez, 1979). Glutamine synthetase is found in the most distal astrocytic processes whereas GFAP is not typically found in these small diameter structures. WSP mice exhibit a trend toward a greater density of glutamine synthetase and a lower density of GFAP. No selected line differences in the number or area of GFAP-positive glial cells were detected. Therefore, glial cell arborization in WSP mice appears to be different than in WSR mice. Perhaps astrocytes in naive WSP mice have fewer large-diameter, proximal processes but have more small-diameter processes per proximal process. Alternatively, these data may indicate that glial cell activity is increased in WSP mice but is not associated with an increase in the number or size of GFAP-positive glial cells. The importance of this observation is unclear.

It is likely that the small group sizes are responsible for the numerous non-significant trends that were observed. In addition, as stated previously, very large differences in any one protein would not be expected due to the polygenic nature of ethanol withdrawal HICs. Thus analysis of glutamine synthetase and GFAP immunolabeling using a more specific immunochemical technique (i.e. immunogold or

immunofluorescence) or at the ultrastructural level may improve resolution sufficiently to detect subtle differences that exist between the selected lines.

Cytochrome Oxidase Activity

Glutamate receptors, glutamate transporters and glutamine synthetase are energy-dependent proteins. Receptor activation leads to postsynaptic membrane depolarization and active ion transport is required to rapidly return membrane potential to resting levels. The Na^+/K^+ ATPases are responsible for repolarization of excited cells and require a great deal of energy to perform properly (Erecinska and Silver, 1989). Glutamate transporters harness the Na^+ and K^+ ion gradients to bind and uptake glutamate in an expedient manner (Gegelashvili and Schousboe, 1998). Degradation of these ion gradients can result in failure or reversal of transporter activity (Szatkowski et al., 1990; Attwell et al., 1993). Reversal of glutamate transporter function has been implicated in the accumulation of extracellular glutamate observed during excitotoxic events, such as ischemia (Szatkowski et al., 1990; Attwell et al., 1993). Glutamine synthetase also requires ATP to metabolize glutamate into glutamine within glial cells. Therefore, normal glutamatergic neurotransmission is highly dependent on the availability of ATP.

Loss or depletion of ATP can lead to excessive glutamatergic activity, which has been associated with numerous disease states (Lipton and Rosenberg, 1994). Momentary loss of ATP can cause ion gradients to run down, leading to prolonged receptor activation and transporter failure which, in turn, acts in a feed-forward manner to excite the surrounding neurons further and lead to cell damage and death. ATP synthesis is typically coupled to its utilization. Thus, the more active a cell is, the more ATP it will generate. Rapid changes in energy requirements can result in an inability of the cell to synthesize sufficient concentrations of ATP.

Cytochrome oxidase is a mitochondrial enzyme associated with oxidative metabolism. Assessment of cytochrome oxidase activity can be used to measure energy

utilization in discrete brain regions. Cytochrome oxidase is regulated at the transcriptional level and therefore reflects the long-term energy requirements of a cell. Changes in cytochrome oxidase activity and protein density occur on the scale of days.

It was hypothesized that glutamatergic activity was greater in WSP mice as compared to WSR mice. Therefore, a greater demand for energy was expected in WSP mice. In the naive state, it was predicted that WSP mice would exhibit greater glutamate uptake and metabolism as compared to WSR mice. However, assessment of glutamate uptake using synaptosomal L-[³H]glutamate uptake assays revealed no differences in maximal uptake or affinity of the transporters for glutamate between naive WSP and WSR mice. Immunoperoxidase histochemistry of the CA1 region of the hippocampus revealed slightly greater levels of GLAST protein in naive WSP-2 mice as compared to WSR-2 mice. A trend towards greater GLT-1 immunolabeling density in the CA3 of the hippocampus of naive WSP mice was also observed. These data suggest that although the immunoperoxidase experiments are not a direct measure of activity, naive WSP mice, especially WSP-2 mice, may require more energy to maintain the function of more transporters. Additionally, a trend towards greater glutamine synthetase labeling in the CA1 region of the hippocampus of naive WSP mice was observed, further suggesting a greater energy requirement in naive WSP mice.

The activity of cytochrome oxidase in the stratum radiatum of the CA1 and CA3, the molecular layer of the dentate gyrus and the somatosensory cortex was determined in naive WSP and WSR mice. It was predicted that greater cytochrome oxidase activity would be seen in naive WSP mice as compared to naive WSR mice, but no differences in cytochrome oxidase activity were observed (Fig. 26). This indicates that cellular energy metabolism is similar in these selected lines.

WSP mice do not exhibit spontaneous convulsive activity in their naive state. In addition, Carter et al. (1995) reported that NMDA receptor activity, as measured by [³H]MK-801 binding, did not differ between naive WSP and WSR mice (but see

Valverius et al., 1990). Accordingly, it was predicted that naive WSP mice would show greater glutamatergic activity, but that this activity would be "balanced" (i.e. between release and uptake) such that no net accumulation of extracellular glutamate would occur. Therefore, glutamate receptor activation was not expected to differ between naive WSP and WSR mice. The similarities in the amount of cytochrome oxidase activity that were observed between naive WSP and WSR mice may be the consequence of similar excitatory receptor activity. Furthermore, cytochrome oxidase activity is thought to reflect neuronal activity more so than glial activity (Wong-Riley, 1989). Thus, because most glutamate transporters and glutamine synthetase are glial, mouse line differences in cytochrome oxidase activity may not exist.

Wong-Riley (1989) reported that variability in cytochrome oxidase activity within single cells exists. Cytochrome oxidase activity tends to be higher in dendrites that form excitatory synapses. Cytochrome oxidase activity is much lower in regions, such as the soma, that receives a greater number of inhibitory contacts. The present experiments assessed cytochrome oxidase activity at the light microscopic level. The histochemical stain was observed as a diffuse background label and cellular components could not be distinguished. Electron microscopic evaluation of cytochrome oxidase activity, specifically within cellular regions receiving glutamatergic innervations, may reveal subtle differences in energy utilization between naive WSP and WSR mice.

In conclusion, naive WSP and WSR mice do not exhibit differences in cytochrome oxidase activity in the hippocampus or cortex. This may indicate that no differences in neuronal activity or cellular energy demands exist between the selected lines in their naive state. This is in agreement with the present hypothesis as well as with Carter et al. (1995) who reported no naive mouse line differences in NMDA receptor binding. However, naive WSP mice have a significantly greater density of glutamate immunoreactivity within hippocampal nerve terminals (Buckman and Meshul, 1997) as well as somewhat greater GLAST, GLT-1 and glutamine synthetase immunolabeling in

hippocampal glial cells (Figs. 13, 15, 17; Table 4). These data, taken together, suggest that naive WSP mice may exhibit greater glutamatergic activity as compared to WSR mice. This was expected to result in increased energy utilization in WSP mice that would be observed using cytochrome oxidase histochemistry. Assessment of cytochrome oxidase activity at the ultrastructural level or following convulsions and/or withdrawal from chronic EtOH may offer insight into functional differences that exist in the excitatory transmitter systems in the brains of WSP and WSR mice.

SUMMARY AND CONCLUSIONS

Naive WSP and WSR mice exhibit a greater density of glutamate immunoreactivity within CA1 hippocampal nerve terminals (Buckman and Meshul, 1997). However, no differences in L-[³H]glutamate uptake were observed between the selected lines in their naive state. Naive WSP-2 mice exhibit a greater density of immunolabeling of the glutamate transporter subtype GLAST as compared to naive WSR-2 mice. A nonsignificant trend towards a greater density of the glutamate transporter subtype GLT-1 in naive WSP mice (versus WSR mice) was observed as well. However, no selected line differences were observed in the density of EAAC1 immunolabeling. These data suggest subtle differences in the density of glial glutamate transporters may exist between naive WSP and WSR mice. These differences could not be observed when tested in crude hippocampal and cortical synaptosomes, but were evident using light microscopic immunohistochemistry. Furthermore, WSP-2 mice exhibited a trend toward more glutamine synthetase as compared to WSR-2 mice, as measured using immunoperoxidase histochemistry. More glutamate metabolism by glutamine synthetase would be possible only if more glutamate were being taken up into glial cells (Derouiche and Rauen, 1995; Fig. 1).

Originally, it was proposed that naive WSP mice would exhibit greater glutamatergic activity as compared to naive WSR mice. It was hypothesized that this greater excitatory activity would be "balanced" such that greater glutamate metabolism and uptake, coinciding with the previously observed greater presynaptic glutamate availability (Buckman and Meshul, 1997), would be observed in naive WSP mice. The greater GLAST immunoreactivity in the CA1 region of the hippocampus of naive WSP-2 mice may be indicative of greater glutamatergic activity in this mouse line. The other, non-significant observations of more GLT-1 and glutamine synthetase immunolabeling in naive WSP mice also offer support, albeit weak, for the original hypothesis. It is interesting that, for all glutamatergic-related proteins, naive WSP mice, especially WSP-2 mice, exhibited a

greater density of immunolabeling as compared to naive WSR mice. The opposite trend was observed for GFAP labeling, which although associated with glial cells, is not involved in maintaining glutamatergic function. Cytochrome oxidase activity, which reflects neuronal activity, but is not specific for the glutamatergic system, revealed no selected line differences.

Theoretically, the WSP and WSR mouse lines should exhibit a large number of subtle genetic differences (Crabbe et al., 1985). The present results are consistent with this. However, due to the relatively small group sizes, the majority of differences reported were not statistically significant. It would be of interest to repeat these experiments using a greater number of animals per group. Alternatively, using techniques that offer higher resolution, the detection of very subtle neurochemical differences between the selected lines may be enhanced. To date, the most impressive differences in the glutamatergic system between the WSP and WSR mouse lines have been observed using electron microscopy (Buckman and Meshul, 1997; 1998).

To confound the interpretation of the near-significant differences between the selected lines further, in many of the immunohistochemical experiment presented, replicate differences were observed in hippocampal or cortical regions (Figs. 13, 19, 22, 23). There are a number of possible explanations for this. For example, these replicate differences may be due to inherent variance in the founding populations (see Falconer, 1996). Alternatively, the phenotypic similarities observed between replicate-1 and replicate-2 mice may be due to different genetic mechanisms. In other words, it is possible that the susceptibility to HICs observed in WSP-1 mice may be associated with insufficient GABAergic activity, whereas the susceptibility to HICs observed in WSP-2 mice may be associated with excess glutamatergic activity. It is unclear to what extent the same genes were influenced in the replicate lines. However, these explanations seem unlikely because previous data collected using the WSP and WSR mouse lines have rarely shown replicate differences and are typically collapsed across replicate (see Crabbe and Kosobud, 1986;

Crabbe et al., 1991a, 1991b, 1993). More recently, WSP-2 mice have been reported to be more sensitive to drug-naïve HICs than WSP-1 mice (Buckman et al., *submitted*). Thus, because replicate differences are relatively uncommon with this genetic model, it is plausible that the WSP-2 mouse line represents a more sensitive “HIC-prone” line as compared to the WSP-1 mouse line. Further experiments would be necessary to explore this hypothesis.

The present data offer preliminary evidence that differences in glutamatergic activity may exist between naïve WSP and WSR mice. These differences are most pronounced between WSP-2 and WSR-2 mice. The majority of differences observed approached, but did not attain significance due to the subtle nature of the selected differences as well as the small group sizes and/or low resolution of the techniques utilized. However, these experiments, taken together with the previous glutamate immunoreactivity data, suggest that the phenotypic differences that exist between the WSP and WSR mice are associated with underlying differences in hippocampal glutamatergic functioning.

REFERENCES

- Aas, JE, Berg-Johnsen, J, Hegstad, E, Laake, JH, Langmoen, IA, Ottersen, OP (1993) Redistribution of glutamate and glutamine in slices of human neocortex exposed to combined hypoxia and glucose deprivation *in vitro*. J Cereb Blood Flow Metab 13: 503-515.
- Abdul-Ghani, AS, Ghneim, H, El-Lati, S, Saca'an, A (1989) Changes in the activity of glutamate related enzymes in cerebral cortex, during insulin-induced seizures. Inter J Neurosci 44: 67-74.
- Akbar, MT, Torp, R, Danbolt, DC, Levy, LM, Meldrum, BS, Ottersen, OP (1997) Expression of glial glutamate transporters GLT-1 and GLAST is unchanged in the hippocampus in fully kindled rats. Neurosci 78(2): 351-359.
- Akbar, MT, Rattray, M, Williams, RJ, Chong, NWS, Meldrum, BS (1998) Reduction of GABA and glutamate transporter messenger RNAs in the severe-seizure Genetically Epilepsy-Prone Rat. Neurosci 85(4): 1235-1251.
- Aminoff, MJ, Simon, RP (1980) Status epilepticus: causes, consequences, and clinical features in 98 patients. Am J Med 69: 657-666.
- Arriza, JL, Fairman, WA, Wadiche, JI, Murdoch, GH, Kavanaugh, MP, Amara, SG (1994) Functional comparisons of three glutamate transporter subtypes cloned from human motor cortex. J Neurosci 14: 5559-5569.

- Arriza, JL, Eliasof, S, Kavanaugh, MP, Amara, SG (1997) Excitatory amino acid transporter 5, a retinal glutamate transporter coupled to a chloride conductance. *Proc Natl Acad Sci USA* 94: 4155-4160.
- Attwell, D, Barbour, B, Szatkowski, M (1993) Nonvesicular release of neurotransmitter. *Neuron* 11: 401-7.
- Ballenger, JC, Post, RM (1978) Kindling as a model for alcohol withdrawal syndromes. *Brit J Psychiat* 133: 1-14.
- Barres, BA (1991) New roles for glia. *J Neurosci* 11(12): 3685-3694.
- Becker, HC (1994) Positive relationship between the number of prior ethanol withdrawal episodes and the severity of subsequent withdrawal seizures. *Psychopharm* 116: 26-32.
- Belknap, JK, Laursen, SE, Crabbe, JC (1987) Ethanol and Nitrous Oxide Produce Withdrawal-Induced Convulsions by Similar Mechanisms in Mice. *Life Sci* 41: 2033-2040.
- Belknap, JK, Danielson, PW, Lane, M, Crabbe, JC (1988) Ethanol and Barbiturate Withdrawal Convulsions are Extensively Codetermined in Mice. *Alcohol* 5(2): 161-171.
- Belknap, JK, Crabbe, JC, Laursen, SE (1989) Ethanol and Diazepam Withdrawal Convulsions are Extensively Codetermined in WSP and WSR Mice. *Life Sci* 44: 2075-2080.

- Bondy, SC, Guo, SX (1994) Effect of ethanol treatment on indices of cumulative oxidative stress. *Eur J Pharmacol* 270: 349-355.
- Bradford, HF, Ward, HK, Thomas, AJ (1978) Glutamine - a major substrate for nerve endings. *J Neurochem* 30: 1453-1459.
- Brigande, JV, Wieraszko, A, Albert, MD, Balkema, GW, Seyfried, TN (1992) Biochemical correlates of epilepsy in the El mouse: analysis of glial fibrillary acidic protein and gangliosides. *J Neurochem* 58: 752-760.
- Brines, ML, Tabuteau, H, Sundaresan, S, Kim, J, Spencer, DD, de Lanerolle, N (1995) Regional distributions of hippocampal Na⁺, K⁺-ATPase, cytochrome oxidase, and total protein in temporal lobe epilepsy. *Epilepsia* 36(4): 371-383.
- Buckman, JF, Meshul, CK (1997) Immunocytochemical analysis of glutamate and GABA in selectively bred mice. *Brain Res* 760(1-2):193-203.
- Buckman, JF, Meshul, CK (1998) Changes in presynaptic glutamate immunoreactivity following handling-induced convulsions. *Society for Neuroscience abstracts: in press.*
- Buckman, JF, Meshul, CK, Finn, DA, Janowsky, A (*submitted*) Glutamate uptake in mice bred for ethanol withdrawal severity.
- Carl, GF, Thompson, LA, Williams, JT, Wallace, VC, Gallagher, BB (1992) Comparison of glutamine synthetase from brains of Genetically Epilepsy Prone and Genetically Epilepsy Resistant Rats. *Neurochem Res* 17(10): 1015-1019.

- Carl, GF, Blackwell, LK, Barnett, FC, Thompson, LA, Rissinger, CJ, Olin, KJ, Critchfield, JW, Keen, CL, Gallagher, BB (1993) Manganese and epilepsy: brain glutamine synthetase and liver arginase activities in Genetically Epilepsy Prone and chronically seized rats. *Epilepsia* 34(3): 441-446.
- Carroll, EW, Wong-Riley, MTT (1984) Quantitative light and electron microscopic analysis of cytochrome oxidase-rich zones in the striate cortex of the squirrel monkey. *J Comp Neurol* 222:1-17.
- Carroll, EW, Wong-Riley, MTT (1985) Correlation between cytochrome oxidase staining and the uptake and laminar distribution of tritiated aspartate, glutamate, γ -aminobutyrate and glycine in the striate cortex of the squirrel monkey. *Neurosci* 15(4): 959-976.
- Carter, LA, Belknap, JK, Crabbe, JC, Janowsky, A (1995) Allosteric regulation of the N-methyl-D-aspartate receptor-linked ion channel complex and effects of ethanol in ethanol-Withdrawal Seizure-Prone and -Resistant mice. *J Neurochem* 64: 213-219.
- Chaudhry, FA, Lehre, KP, van Lookeren Campagne, M, Ottersen, OP, Danbolt, NC, Storm-Mathisen, J (1995) Glutamate transporters in glial plasma membranes: highly differentiated localizations revealed by quantitative ultrastructural immunocytochemistry. *Neuron* 15: 711-720.
- Choi, DW (1988) Glutamate neurotoxicity and diseases of the nervous system. *Neuron* 1:623-34.

- Coco, S, Verderio, C, Trotti, D, Rothstein, JD, Volterra, A, Matteoli, M (1997) Non-synaptic localization of the glutamate transporter EAAC1 in cultured hippocampal neurons. *Eur J Neurosci* 9: 1902-1910.
- Conti, F, DeBiasi, S, Minelli, A, Rothstein, JD, Melone, M (1998) EAAC1, a high-affinity glutamate transporter, is localized to astrocytes and GABAergic neurons besides pyramidal cells in the rat cerebral cortex. *Cerebral Cortex* 8: 108-116.
- Cordero, ML, Ortiz, JG, Santiago, G (1994) High affinity [^3H]glutamate uptake systems in normal and audiogenic seizure-susceptible mice. *Dev Brain Res* 78:44-48.
- Crabbe, JC, Kosobud, A, Young, ER (1983) Genetic selection for ethanol withdrawal severity: differences in replicate lines. *Life Sci* 33: 955-962.
- Crabbe, JC, Kosobud, A, Young, ER, Tam, BR, McSwigan, JD (1985) Bidirectional selection for susceptibility to ethanol withdrawal seizures in *Mus musculus*. *Behav Genet* 15(6): 521-536.
- Crabbe, JC, Kosobud, A (1986) Sensitivity and Tolerance to Ethanol in Mice Bred to be Genetically Prone or -Resistant to Ethanol Withdrawal Seizures. *J Pharmacol Exp Ther* 239(2): 327-333.
- Crabbe, JC, Phillips, TJ, Kosobud, A, Belknap, JK (1990) Estimation of Genetic Correlation: Interpretation of Experiments Using Selectively Bred and Inbred Animals. *Alcohol: Clin Exp Res* 14(2): 141-51.

- Crabbe, JC, Merrill, CD, Belknap, JK (1991a) Effects of convulsants on handling-induced convulsions in mice selected for ethanol withdrawal severity. *Brain Res* 550: 1-6.
- Crabbe, JC, Merrill, CM and Belknap, JK (1991b) Acute dependence on depressant drugs is determined by common genes in mice. *J Pharmacol Exp Ther* 257(2): 663-667.
- Crabbe, JC, Merrill, CD, Belknap (1993) Effects of acute alcohol withdrawal on sensitivity to pro- and anticonvulsant treatments in WSP mice. *Alcohol: Clin Exp Res* 17(6): 1233-1239.
- Crabbe, JC, Phillips, TJ (1993) Selective breeding for alcohol withdrawal severity. *Behav Genetics* 23(2): 171-177.
- Crabbe, JC, Young, ER, Dorow, J (1994a) Effects of Dizocilpine in Withdrawal Seizure-Prone (WSP) and Withdrawal Seizure-Resistant (WSR) Mice. *Pharmacol, Biochem, Behav* 47(3): 443-450.
- Crabbe JC, Belknap, JK, Buck, KJ (1994b) Genetic animal models of alcohol and drug abuse. *Science* 264(5166): 1715-1723.
- Crews, FT, Morrow, L, Criswell, J, Breese, G (1996) Effects of ethanol on ion channels. *Int Rev Neurobiol* 39: 283- 367.

- Danbolt, NC, Storm-Mathisen, J, Kanner, BI (1992) An $[Na^+ + K^+]$ coupled L-glutamate transporter purified from rat brain is located in glial cell processes. *Neurosci* 51(2): 295-310.
- Davies, DL, Vernadakis, A (1984) Effects of ethanol on cultured glial cells: proliferation and glutamine synthetase activity. *Dev Brain Res* 16: 27-35.
- Dehnes, Y, Chaudhry, FA, Ullensvang, K, Lehre, KP, Storm-Mathisen, J, Danbolt, NC (1998) The glutamate transporter EAAT4 in rat cerebellar purkinje cells: a glutamate-gated chloride channel concentrated near the synapse in parts of the dendritic membrane facing astroglia. *J Neurosci* 18(10): 3606-3619.
- Derouiche, A, Frotscher, M (1991) Astroglial processes around identified glutamatergic synapses contain glutamine synthetase: evidence for transmitter degradation. *Brain Res* 552: 346-350.
- Derouiche, A, Heimrich, B, Frotscher, M (1993) Loss of layer specific astrocytic GS immunoreactivity in slice cultures of hippocampus. *Eur J Neurosci* 5(2): 122-127.
- Derouiche, A, Rauen, T (1995) Coincidence of L-glutamate/L-aspartate transporter (GLAST) and glutamine synthetase (GS) immunoreactions in retinal glia: evidence for coupling of GLAST and GS in transmitter clearance. *J Neurosci Res* 42: 131-143.
- Dingledine, R, McBain, CJ, McNamara, JO (1990) Excitatory amino acid receptors in epilepsy. *Trends in Pharmacol Sci* 11: 334-338.

- Dowd, LA, Coyle, AJ, Rothstein, JD, Pritchett, DB, Robinson, MB (1996) Comparison of Na⁺-dependent glutamate transporter activity in synaptosomes, C6 glioma, and *Xenopus* oocytes expressing excitatory amino acid carrier 1 (EAAC1). *Mol Pharmacol* 49 465-473.
- Earnest, MP, Yarnell, PR (1976) Seizure admissions to a city hospital: the role of alcohol. *Epilepsia* 17: 387-393.
- Eckhardt, MJ, Campbell, GA, Marietta, CA, Majchrowicz, E, Weight, FF (1988) Acute ethanol administration selectively alters localized cerebral glucose metabolism. *Brain Res* 444: 53-58.
- Eng, LF, Vanderhaeghen, JJ, Bignami, A, Gerstl, B (1971) An acidic protein isolated from fibrous astrocytes. *Brain Res* 28: 351-354.
- Eng, LF (1985) Glial fibrillary acidic protein (GFAP) : the major protein of glial intermediate filaments in differentiated astrocytes. *J Immunol* 8: 203-214.
- Engel, J Jr. (1989) *Seizures and Epilepsy*. FA Davis Co., Philadelphia, p.34.
- Erecinska, M, Silver, IA (1989) ATP and brain function. *J Cereb Blood Flow Metab* 9: 2-19.
- Fairman, WA, Vandenberg, RJ, Arriza, JL, Kavanaugh, MP, Amara, SG (1995) An excitatory amino-acid transporter with properties of a ligand-gated chloride channel. *Nature* 375: 599-603.

- Falconer, DS, Mackay, TFC (1996) *Introduction to Quantitative Genetics*. 4th Ed. Longman Group Ltd, Essex, pp. 184-245.
- Feller, DJ, Harris, RA, Crabbe, JC (1988) Differences in GABA Activity Between Ethanol Withdrawal Seizure-Prone and Resistant Mice. *Eur J Pharmacol* 157: 147-154.
- Feller, DJ, Bassir, JM, Crabbe, JC, LeFevre, CA (1994) Audiogenic Seizure Susceptibility in WSP and WSR Mice. *Epilepsia* 35(4): 861-867.
- Fonnum, F (1984) Glutamate: a neurotransmitter in mammalian brain. *J Neurochem* 42(1): 1-11.
- Franklin, KBJ, Paxinos, G (1997) *The Mouse Brain in Stereotaxic Coordinates*. Academic Press, San Diego, CA.
- Furuta, A, Martin, LJ, Lin, CLG, Dykes-Hoberg, M, Rothstein, JD (1997) Cellular and synaptic localization of the neuronal glutamate transporters excitatory amino acid transporter 3 and 4. *Neurosci* 81(4): 1031-1042.
- Gegelashvili, G, Schousboe, A (1998) Cellular distribution and kinetic properties of high-affinity glutamate transporters. *Brain Res Bull* 45(3): 232-238.
- Glass, M, Dragunow, M (1995) Neurochemical and morphological changes associated with human epilepsy. *Brain Res Rev* 21: 29-41.

- Goldstein, DB (1972) Relationship of alcohol dose to intensity of withdrawal signs in mice. *J Pharmacol Exp Ther* 180: 203-213.
- Goldstein, DB (1983) *Pharmacology of Alcohol*, Oxford University Press, New York Oxford, pp 7.
- Gray, EG (1959) Axo-somatic and axo-dendritic synapses of the cerebral cortex: an electron microscopic study. *J Anat* 93: 420-433.
- Green, RC, Rees, HD, Feller, DJ (1993) Olfactory Bulb Kindling in Mice Susceptible and Resistant to Ethanol Withdrawal. *Epilepsia* 34(3): 416-419.
- Grisar, T, (1984) Glial and neuronal $\text{Na}^+\text{-K}^+$ pump in epilepsy. *Ann Neurol* 16 (Suppl): S128-S134.
- Grunwald, F, Schrock, H, Biersack, HJ, Kuschinsky, W (1993) Changes in local cerebral glucose utilization in the awake rat during acute and chronic administration of ethanol. *J Nucl Med* 34: 793-798.
- Gulya, K, Grant, KA, Valverius, P, Hoffman, PL, Tabakoff, B (1991) Brain regional specificity and time-course of changes in the NMDA receptor-ionophore complex during ethanol withdrawal. *Brain Res* 547: 129-134.
- Gumnit, RJ (1995) *The epilepsy handbook: the practical management of seizures*, 2nd ed. Raven Press, New York, p. 51.

- Gundersen, V, Danbolt, NC, Ottersen, OP, Storm-Mathisen, J (1993) Demonstration of glutamate/aspartate uptake activity in nerve endings recognizing exogenous D-aspartate. *Neurosci* 57:97-111.
- Gundersen, V, Shupliakov, O, Brodin, L, Ottersen, OP, Storm-Mathisen, J (1995) Quantification of excitatory amino acid uptake at intact glutamatergic synapses by immunocytochemistry of exogenous D-aspartate. *J Neurosci* 15(6):4417-4428.
- Hamberger, A, Han Chiang, G, Nylen, ES, Scheff, SW, Cotman, CW (1979a) Glutamate as a CNS transmitter. I. Evaluation of glucose and glutamine as precursors for the synthesis of preferentially released glutamate. *Brain Res* 168: 513-530.
- Hamberger, A, Han Chiang, Sandoval, E, SW, Cotman, CW (1979b) Glutamate as a CNS transmitter. II. Regulation of synthesis in the releaseable pool. *Brain Res* 168: 531-541.
- Hesdorffer, DC, Verity, CM (1997) Risk Factors. In: Engels, J Jr., Pedley, TA, eds. *Epilepsy: A Comprehensive Textbook*. Lipincott-Raven, Philadelphia, p. 59-67.
- Hevner, RF, Wong-Riley, MTT (1989) Brain cytochrome oxidase: purification, antibody production, and immunohistochemical/histochemical correlations in the CNS. *J Neurosci* 9(11): 3884-3898.
- Hevner, RF, Wong-Riley, MTT (1990) Regulation of cytochrome oxidase protein levels by functional activity in the Macaque monkey visual system. *J Neurosci* 10(4): 1331-1340.

- Hevner, RF, Duff, RS, Wong-Riley, MTT (1992) Coordination of ATP production and consumption in brain: parallel regulation of cytochrome oxidase and Na⁺, K⁺-ATPase. *Neurosci Letters* 138: 188-192.
- Horton, RW (1991) GABA dysfunction in animal models of epilepsy. In: *GABA Mechanisms in Epilepsy*. Wiley-Liss Inc. p.121-147.
- Kageyama, GH, Wong-Riley, MTT (1982) Histochemical localization of cytochrome oxidase in the hippocampus: correlation with specific neuronal types and afferent pathways. *Neurosci* 7(10): 2337-2361.
- Kanai, Y, Hediger, MA (1992) Primary structure and functional characterization of a high-affinity glutamate transporter. *Nature* 360: 467-471.
- Keller, E, Cummins, JT, von Hungen, K (1983) Regional effects of ethanol on glutamate levels, uptake and release in slice and synaptosome preparations from rat brain. *Substance Alcohol Actions/Misuse* 4:383-392.
- Kosobud, A, Crabbe, JC (1986) Ethanol withdrawal in mice bred to be genetically prone or resistant to ethanol withdrawal seizures. *JPET* 238(1): 170-177.
- Kosobud, A, Crabbe, JC (1993) Sensitivity to N-Methyl-D-Aspartic Acid-Induced Convulsions is Genetically Associated with Resistance to Ethanol Withdrawal Seizures. *Brain Res* 610: 176-179.
- Laake, JH, Slyngstad, A, Haug, FMS, Ottersen, OP (1995) Glutamine from glial cells is essential for the maintenance of the nerve terminal pool of glutamate:

immunogold evidence from hippocampal slice cultures. *J Neurochem* 65: 871-881.

Lallement, G, Carpentier, P, Collet, A, Pernot-Marino, I, Baubichon, D, Blanchet, G (1991) Effects of soman-induced seizures on different extracellular amino acid levels and on glutamate uptake in rat hippocampus. *Brain Res* 563: 234-240.

Laming, PR, Cosby, SL, O'Neill, JK (1989) Seizures in the Mongolian gerbil are related to a deficiency in cerebral glutamine synthetase. *Comp Biochem Physiol* 94C(2): 399-404.

Ledig, M, Tholey, G, Megias-Megias, L, Kopp, P, Wedler, F (1991) Combined effects of ethanol and manganese on cultured neurons and glia. *Neurochem Res* 16(5): 591-596.

Lehre, KP, Levy, LM, Ottersen, OP, Storm-Mathisen, J, Danbolt, NC (1995) Differential expression of two glial glutamate transporters in the rat brain: quantitative and immunocytochemical observations. *J Neurosci* 15(3): 1835-1853.

Levy, LM, Lehre, KP, Rolstad, B, Danbolt, NC (1993) A monoclonal antibody raised against an $[Na^+ + K^+]$ -coupled L-glutamate transporter purified from rat brain confirms glial cell localization. *FEBS Letters* 317(1,2): 79-84.

Levy, LM, Lehre, KP, Walaas, SI, Storm-Mathisen, J, Danbolt, NC (1995) Down-regulation of glial glutamate transporters after glutamatergic denervation in the rat brain. *Eur J Neurosci* 7: 2036-2041.

- Lin, CLG, Bristol, LA, Jin, L, Dykes-Hoberg, M, Crawford, T, Clawson, L, Rothstein, JD (1998) Aberrant RNA processing in a neurodegenerative disease: the cause for absent EAAT2, a glutamate transporter, in amyotrophic lateral sclerosis. *Neuron* 20: 589-602.
- Lipton, SA, Rosenberg, PA (1994) Mechanisms of disease: Excitatory amino acids as a final common pathway for neurologic disorders. *New Engl J Med* 330(9): 613-622.
- Lovinger, DM, White, G, Weight, FF (1989) Ethanol inhibits NMDA-activated ion current in hippocampal neurons. *Sci* 243: 1721-1724.
- Lovinger, DM (1993) Excitotoxicity and alcohol-related brain damage. *Alcoholism: Clin Exp Res* 17(1): 19-27.
- Lowry, OH, Rosebrough, NJ, Farr, AL, Randall, RJ (1951) Protein measurement with the folin phenol reagent. *J Biol Chem* 193: 265-275.
- Madl, JE, Burgesser, K (1993) Adenosine triphosphate depletion reverses sodium-dependent, neuronal uptake of glutamate in rat hippocampal slices. *J Neurosci* 13(10): 4429-4444.
- Mathern, GW, Babb, TL, Armstrong, DL (1997) Hippocampal Sclerosis. In: Engels, J Jr., Pedley, TA, eds. *Epilepsy: A Comprehensive Textbook*. Lipincott-Raven, Philadelphia, p. 133-155.

- Martinez-Hernandez, A, Bell, KP, Norenberg, MD (1977) Glutamine synthetase: glial localization in the brain. *Science* 195: 1356-1358.
- Meldrum, BS (1994) The role of glutamate in epilepsy and other CNS disorders. *Neurol* 44(Suppl 8): S14-S23.
- Meldrum, BS (1995) Neurotransmission in epilepsy. *Epilepsia* 36 (Suppl 1): S30-S35.
- Mennerick, Zorumski (1994) Glial contributions to excitatory neurotransmission in cultured hippocampal cells. *Nature* 368: 59-62.
- Mennerick, S, Dhond, RP, Benz, A, Xu, W, Rothstein, JD, Danbolt, NC, Isenberg, KE, Zorumski, CF (1998) Neuronal expression of the glutamate transporter GLT-1 in hippocampal microcultures. *J Neurosci* 18(12): 4490-4499.
- Mennini, T, Bastone, A, Crespi, D, Comoletti, D, Manzoni, C (1998) Spinal cord GLT-1 glutamate transporter and blood glutamic acid alterations in motor neuron degeneration (Mnd) mice. *J Neurol Sci* 157: 31-36.
- Michaelis, EK, Michaelis, ML, Freed, WJ (1980) Chronic ethanol intake and synaptosomal glutamate binding activity. *Adv Exp Med Biol* 126: 43-56.
- Mjaatvedt, AE, Wong-Riley, MTT (1988) Relationship between synaptogenesis and cytochrome oxidase activity in purkinje cells of the developing rat cerebellum. *J Comp Neurol* 277: 155-182.

- Nie, F, Wong-Riley, MTT (1995) Double labeling of GABA and cytochrome oxidase in the Macaque visual cortex: quantitative EM analysis. *J Comp Neurol* 356: 115-131.
- Nie, F, Wong-Riley, MTT (1996) Differential glutamatergic innervation in cytochrome oxidase-rich and -poor regions of the Macaque striate cortex: quantitative EM analysis of neurons and neuropil. *J Comp Neurol* 369: 571-590.
- Nobrega, JN, Raymond, R, DiStefano, L, Burnham, WM (1993a) Long-term changes in regional brain cytochrome oxidase activity induced by electroconvulsive treatment in rats. *Brain Res* 605: 1-8.
- Nobrega, JN, Petrasek, JS, Raymond, R, Dixon, LM, Burnham, WM (1993b) Brain cytochrome oxidase activity after kindled seizures: a quantitative histochemical mapping study. *Brain Res* 622: 113-118.
- Nobrega, JN, Richter, A, Jiwa, D, Raymond, R, Loscher, W (1998) Regional alterations in neuronal activity in dystonic hamster brain determined by quantitative cytochrome oxidase histochemistry. *Neurosci* 83(4): 1215-1223.
- Nonaka, M, Kohmura, E, Yamashita, T, Shimada, S, Tanaka, K, Yoshimine, T, Tohyama, M, Hayakawa, T (1998) Increased transcription of glutamate-aspartate transporter (GLAST/GLuT-1) mRNA following kainic acid-induced limbic seizure. *Mol Brain Res* 55: 54-60.
- Norenberg, MD (1979) The distribution of glutamine synthetase in the rat central nervous system. *J Histochem Cytochem* 27(3): 756-762.

- Norenberg, MD, Martinez-Hernandez (1979) Fine structural localization of glutamine synthetase in astrocytes of rat brain. *Brain Res* 161: 303-310.
- Oda, M, Ikeda, K, Yamamoto, T (1983) Immunohistochemistry of glutamine synthetase of the mouse and human brain. *Neuropathol* 4:19-30.
- Peghini, P, Janzen, J, Stoffel, W (1997) Glutamate transporter EAAC-1-deficient mice develop dicarboxylic aminoaciduria and behavioral abnormalities but no neurodegeneration. *EMBO J* 16(13): 3822-3832.
- Pellerin, L, Magistretti, PJ (1997) Glutamate uptake stimulates Na^+ , K^+ -ATPase activity in astrocytes via activation of a distinct subunit highly sensitive to ouabain. *J Neurochem* 69: 2131-2137.
- Pines, G, Danbolt, NC, Bjoras, M, Zhang, Y, Bendahan, A, Eide, L, Koepsell, H, Storm-Mathisen, J, Seeberg, E, Kanner, BI (1992) Cloning and expression of a rat brain L-glutamate transporter. *Nature* 360: 464-467.
- Prince Miller, H, Levy, AI, Rothstein, JD, Tzingounis, AV, Conn, PJ (1997) Alterations in glutamate transporter protein levels in kindling-induced epilepsy. *J Neurochem* 68: 1564-1570.
- Raghavendra Rao, VL, Baskaya, MK, Dogan, A, Rothstein, JD, Dempsey, RJ (1998) Traumatic brain injury down-regulates glial glutamate transporter (GLT-1 and GLAST) proteins in rat brain. *J Neurochem* 70: 2020-2027.

- Rangaraj, N, Kalant, H (1978) Effects of ethanol withdrawal, stress and amphetamine on rat brain ($\text{Na}^+ + \text{K}^+$)-ATPase. *Biochem Pharmacol* 27: 1139-1144.
- Roach, MK and Creaven, PJ (1968) A micro-method for the determination of acetylaldehyde and ethanol in blood. *Clin Chim Acta* 21(2): 275-278.
- Roach, MK, Kahn, MM, Coffman, R, Pennington, W, Davis, DL (1973a) Brain ($\text{Na}^+ + \text{K}^+$)-activated adenosine triphosphatase activity and neurotransmitter uptake in alcohol-dependent rats. *Brain Res* 63: 323-329.
- Roach, MK, Pennington, W, Nordyke, E (1973b) Effect of ethanol on the uptake by rat synaptosomes of [^3H]DL-Norepinephrine, [^3H]5-hydroxytryptamine, [^3H]GABA and [^3H]glutamate. *Life Sci* 12(1): 433-441.
- Rosenberg, PA, Amin, S, Leitner, M (1992) Glutamate uptake disguises neurotoxic potency of glutamate agonists in cerebral cortex in dissociated cell culture. *J Neurosci* 12(1): 56-61.
- Rothman, SM, Olney, JW (1987) Excitotoxicity and the NMDA receptor. *Trends in Neurosci* 10: 299-302.
- Rothstein, JD, Tabakoff, B (1984) Alteration of striatal glutamate release after glutamine synthetase inhibition. *J Neurochem* 43: 1438-1446.
- Rothstein, JD, Martin, LJ, Kuncel, RW (1992) Decreased glutamate transport by the brain and spinal cord in amyotrophic lateral sclerosis. *N Engl J Med* 326: 1464-1468.

- Rothstein, JD, Martin, L, Levey, AI, Dykes-Hoberg, M, Jin, L, Wu, D, Nash, N, Kuncel, RW (1994) Localization of neuronal and glial glutamate transporters. *Neuron* 13: 713-725.
- Rothstein, JD, Van Kammen, M, Levey, AI, Martin, LJ, Kuncel, RW (1995) Selective loss of glial glutamate transporter GLT-1 in amyotrophic lateral sclerosis. *Ann Neurol* 38: 73-84.
- Rothstein, JD, Dykes-Hoberg, M, Pardo, CA, Bristol, LA, Jin, L, Kuncel, RW, Kanai, Y, Hediger, MA, Wang, Y, Schielke, JP, Welty, DF (1996) Knockout of glutamate transporters reveals a major role for astroglial transport in excitotoxicity and clearance of glutamate. *Neuron* 16: 675-686.
- Rubio, S, Begega, A, Santin, LJ, Arias, L (1996) Ethanol- and diazepam-induced cytochrome oxidase activity in mammillary bodies. *Pharmacol Biochem Behav* 55(2): 309-314.
- Sakellaridis N, Mangoura, D, Masserrano, JM, Detsis, V, Leoni, CJ, Deitrich, R, Vernadakis, A (1989) Developmental profile of glutamine synthetase in lines of mice bred for ethanol sensitivity. *J Neurosci Res* 24: 391-397.
- Scheibel, ME, Crandall, PH, Scheibel, AB (1974) The hippocampal-dentate complex in temporal lobe epilepsy. *Epilepsia* 15: 55-80.
- Schunzel, G, Wolf, G, Pomrenke, U, Pomrenke, C, Schmidt, W (1992) Pentylentetrazol kindling and factors of glutamate transmitter metabolism in rat hippocampus. *Neurosci* 49(2): 365-371.

- Schwartz, WJ, Smith, CB, Davidsen, L, Mata, M, Fink, DJ, Gainer, H (1979) Metabolic mapping of functional activity in the hypothalamo-neurohypophysial system of the rat. *Science* 205: 723-725.
- Sherwin, A, Quesney, F, Gauthier, S, Olivier, A, Robitaille, Y, McQuaid, P, Harvey, C, van Gelder, N (1984) Enzyme changes in actively spiking areas of human epileptic cerebral cortex. *Neurol* 34: 927-933.
- Singh, SP, Ehmann, S, Snyder, AK (1994) Ethanol and glucose-deprivation neurotoxicity in cortical cell cultures. *Metab* 43(9): 1108-1113.
- Smith, TL, Zsigo, A (1996) Increased Na^+ -dependent high affinity uptake of glutamate in astrocytes chronically exposed to ethanol. *Neurosci Letters* 218: 142-144.
- Sokoloff, L, Reivich, M, Kennedy, C, DesRosiers, H, Patlack, CS, Pettigrew, KD, Sakurada, O, Shinohara, M (1977) The [^{14}C]deoxyglucose method for the measurement of local cerebral glucose utilization: theory, procedure, and normal values in the conscious and anesthetized albino rat. *J Neurochem* 28: 897-916.
- Steward, O, Torre, ER, Tomasulo, R, Lothman, E (1991) Neuronal activity up-regulates astroglial gene expression. *Proc Natl Acad Sci* 88: 6819-6823.
- Storck, T, Schulte, S, Hofmann, K, Stoffel, W (1992) Structure, expression, and functional analysis of a Na^+ -dependent glutamate/aspartate transporter from rat brain. *Proc Natl Acad Sci USA* 89: 10955-9.

- Svenneby, G, Torgner, IA (1987) Localization and function of glutamine synthetase and glutaminase. *Biochem Soc Trans* 15: 213-215.
- Swann, AC (1990) Ethanol and (Na⁺,K⁺)-ATPase: Alteration of Na⁺-K⁺ Selectivity. *Alcohol: Clin Exp Res* 14(6): 922-927.
- Szatkowski, M, Barbour, B, Attwell, D (1990) Non-vesicular release of glutamate from glial cells by reversed electrogenic glutamate uptake. *Nature* 348: 443-446.
- Tabakoff, B, Hoffman, PL, Liljequist, S (1987) Effects of ethanol on the activity of brain enzymes. *Enzyme* 37: 70-86.
- Tanaka, K, Watase, K, Manabe, T, Yamada, K, Watanabe, M, Takahashi, K, Iwama, H, Nishikawa, T, Ichihara, N, Kikuchi, T, Okuyama, S, Kawashima, N, Hori, S, Takimoto, M, Wada, K (1997) Epilepsy and exacerbation of brain injury in mice lacking the glutamate transporter GLT-1. *Science* 276: 1699-1702.
- Thayer, WS, Rottenberg, H (1992) Comparative effects of chronic ethanol consumption on the properties of mitochondria from rat brain and liver. *Alcohol: Clin Exp Res* 16(1): 1-4.
- Torp, R, Danbolt, NC, Babaie, E, Bjoras, M, Seeberg, E, Storm-Mathisen, J, Ottersen, OP (1994) Differential expression of two glial glutamate transporters in the rat brain: an *in situ* hybridization study. *Eur J Neurosci* 6: 936-942.

- Torre, ER, Lothman, E, Steward, O (1993) Glial response to neuronal activity: GFAP-mRNA and protein levels are transiently increased in the hippocampus after seizures. *Brain Res* 631: 256-264.
- Ulrichsen, J, Clemmesen, L, Hemmingsen, R (1992) Convulsive behaviour during alcohol dependence: discrimination between the role of intoxication and withdrawal. *Psychopharmacol* 107: 97-102.
- Valverius, P, Crabbe, JC, Hoffman, PL, Tabakoff, B (1990) NMDA receptors in mice bred to be prone or resistant to ethanol withdrawal seizures. *Eur J Pharmacol* 184: 185-189.
- Wadiche, JI, Amara, SG, Kavanaugh, MP (1995) Ion fluxes associated with excitatory amino acid transport. *Neuron* 15(3):721-8.
- Ward HK, Thanki, CM, Bradford, HF (1983) Glutamine and glucose as precursors of transmitter amino acids: *ex vivo* studies. *J Neurochem* 40: 855-860.
- Williams-Hemby, L, Porrino, LJ (1994) Low and moderate doses of ethanol produce distinct patterns of cerebral metabolic changes in rats. *Alcohol: Clin Exp Res* 18(4): 982-988.
- Wong-Riley, MTT (1989) Cytochrome oxidase: an endogenous metabolic marker for neuronal activity. *TINS* 12(3): 94-101.
- Wong-Riley, MTT, Anderson, B, Liebl, W, Huang, Z (1998) Neurochemical organization of the Macaque striate cortex: correlation of cytochrome oxidase

with Na⁺K⁺ATPase, NADPH-diaphorase, nitric oxide synthetase, and N-methyl-D-aspartate receptor subunit 1. *Neurosci* 83(4): 1025-1045.

Zerangue, N, Arriza, JL, Amara, SG, Kavanaugh, MP (1995) Differential modulation of human glutamate transporter subtypes by arachidonic acid. *J Biol Chem* 270(12): 6433-5.

Zhang, C, Wong-Riley, MTT (1996) Do nitric oxide synthetase, NMDA receptor subunit R1 and cytochrome oxidase co-localize in the rat central nervous system? *Brain Res* 729: 205-215.

Figure 1

Cartoon of glutamatergic neurotransmission: neuronal and glial roles in synthesis and metabolism.

In the presynaptic nerve terminal, glutamate (yellow) is synthesized from glutamine (orange) by the mitochondrial enzyme, glutaminase. This glutamate is sequestered into synaptic vesicles and made ready for release. Upon stimulation, vesicular glutamate is released where it activates pre- and postsynaptic glutamate receptors (i.e. metabotropic (mGluR), NMDA, non-NMDA). Extracellular glutamate is taken up into postsynaptic structures (i.e. dendritic spines) by the neuronal transporter EAAC1 or into glial cells via the glutamate transporters GLAST and GLT-1. Glutamate taken up into glial cells is converted into glutamine via glutamine synthetase. This glutamine can then be released from the glial processes and taken up into presynaptic terminals via glutamine transporters. This represents the 'glutamate-glutamine' cycle.

Cytochrome oxidase is a mitochondrial enzyme that catalyzes the terminal oxidative reaction for the conversion of glucose to ATP. Most ATP in the brain is derived from oxidative metabolism, thus neuronal functioning is highly dependent on the activity of this enzyme. The greatest activity of cytochrome oxidase is seen in mitochondria located in postsynaptic structures near excitatory synapses (Wong-Riley, 1989). An association between cytochrome oxidase activity and excitatory activity in the brain has been reported (Mjaatvedt and Wong-Riley, 1988)

Glia

glutamine synthetase

GLUTAMATE

GLAST

GLT-1

mGluR

GLUTAMINE

glutaminase

GLUTAMATE

cytochrome oxidase

Postsynaptic

Presynaptic

EAAC1

NMDA

non-NMDA

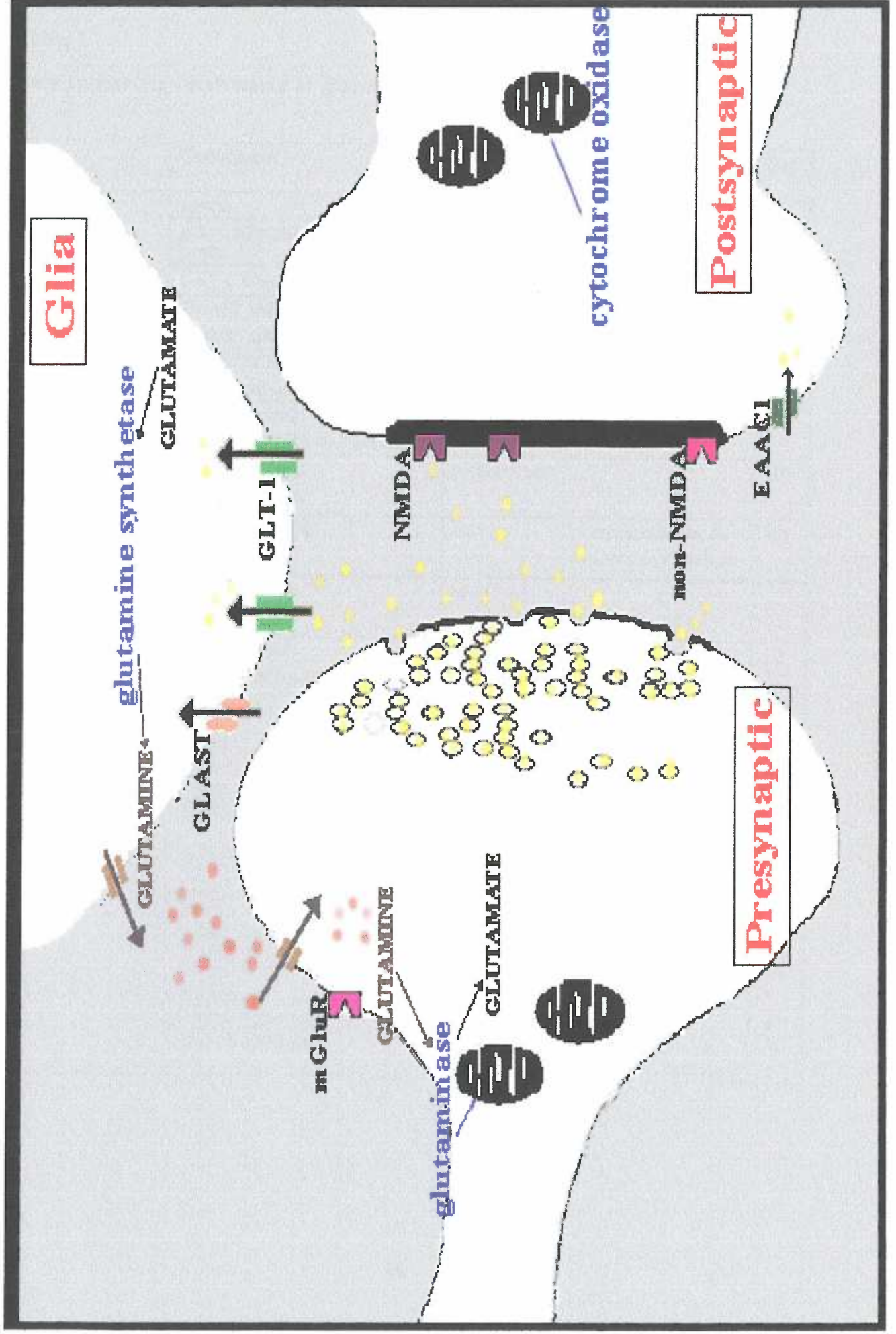


Table 1 (continued)

Glutamine Synthetase	GEPR	whole brain	↓	4
	seizure-prone gerbils	cerebrum	↓	7
	MES seizures	whole brain	n.c.	4
	insulin-induced seizures	ctx	n.c.	1
	= GS activity -picROTOXIN-induced seizures, cortex	ctx	n.c.	1
	human epilepsy	epileptic focus	n.c.	12
	GS inhibitor, L-methionine sulfoximine		seizures	13

Data implicating glutamate uptake and metabolism in seizure activity from previous experiments is summarized above. References (REF) are listed to the right.

hpc = hippocampus, ctx = cortex, MES = maximal electroshock, n.c. = no change.

-
- 1 Abdul-Ghani et al., 1989
 - 2 Akbar et al., 1997
 - 3 Akbar et al., 1998
 - 4 Carl et al., 1993
 - 5 Cordero et al., 1994
 - 6 Lallement et al., 1991
 - 7 Laming et al., 1989

-
- 8 Nonaka et al., 1998
 - 9 Peghini et al., 1997
 - 10 Prince Miller et al., 1997
 - 11 Rothstein et al., 1996
 - 12 Sherwin et al., 1984
 - 13 Svenneby and Torgner, 1987
 - 14 Tanaka et al., 1997

Table 2**Evidence for a role of glutamate uptake and metabolism in EtOH-related behaviors**

	EtOH treatment	Tissue preparation	Effect	Ref
Glutamate Uptake & <i>in vitro</i> EtOH	5-30 mg/ml, 10 minute	rat whole brain	↓	6
	50 or 100 mM, 6 hours	cortical astrocytes	↓	8
	100 mM, 15 minutes	cortical astrocytes	↑	9
	100 mM, 4 days	cortical astrocyte	↑↑	9
	56 mM, 2 hours	rat ctx, hpc & str	n.c.	3
Glutamate Uptake & <i>in vivo</i> EtOH	acute intoxication (4 g/kg i.p.)	rat ctx, hpc & str	n.c.	3
	liquid diet (21-25 days)	rat ctx	n.c.	3
	liquid diet (21-25 days)	rat hpc	↑	3
	liquid diet (21-25 days) withdrawal (36 hours)	rat ctx, hpc & str	n.c.	3
	EtOH vapor (7 days) withdrawal, (12 hours)	rat whole brain * convulsions	↓	5
Glutamine Synthetase	<i>in vitro</i> , 4-15 days (0.1 – 2.0%)	cerebral cultures	↓	2
	<i>in vitro</i> , 6-15 days (30 mM)	cortical cultures	↓	4
	<i>in vivo</i> , acute EtOH (4.5 g/kg)	rat ctx	↑	1
	<i>in vivo</i> , chronic EtOH (4.5 g/kg)	rat ctx	↓	1
	mice that differ in sensitivity to EtOH's hypnotic effects	throughout brain early development	LS > SS	7
	mice bred for differences in EtOH withdrawal severity	forebrain late development	MEW < SEW	7

This table summarizes previously reported data assessing the effect of EtOH on glutamate uptake and metabolism. Thus far, the role of the individual glutamate transporter subtypes is unknown. hpc = hippocampus, ctx = cortex, str = striatum, LS = Long Sleep mice, SS = Short Sleep mice, MEW = Mild EtOH withdrawal, SEW = Severe EtOH withdrawal, n.c. = no change

1 Bondy & Guo, 1994

2 Davies & Vernadakis, 1984

3 Keller et al., 1983

4 Ledig et al., 1991

5 Roach et al., 1973a

6 Roach et al., 1973b

7 Sakalleridis et al., 1989

8 Singh et al., 1994

9 Smith & Zsigo, 1996

Table 3

Scale for measuring severity of handling-induced convulsions*

Score	Characteristics of convulsions
0	No convulsion
1	Facial grimace when lifted and spun
2	Tonic convulsion when lifted and spun
3	Tonic-clonic convulsion when lifted and spun
4	Tonic convulsion when lifted
5	Tonic-clonic convulsion when lifted
6	Severe tonic-clonic convulsion when lifted
7	Spontaneous tonic-clonic convulsion (no lifting required)

*This scale, modified from Crabbe et al. (1991b), was used to rate the severity of HICs elicited in drug-naive WSP-1 and WSP-2 mice. Scores are based on the type of handling necessary to induce a convulsion (i.e., convulsions elicited by lifting alone versus convulsions resulting from lifting and spinning the mouse by the tail) and the type of convulsion observed (tonic versus clonic).

Figure 2

Regional analysis of the density of immunoperoxidase labeling

A cartoon of a coronal slice of the hippocampus is depicted, with colored regions representing the areas analyzed in the GLAST, GLT-1, glutamine synthetase, GFAP and cytochrome oxidase experiments. The stratum radiatum (SR) of the CA1 and CA3 subfields of the hippocampus was assessed for the mean optical density of immunolabeling. The molecular layer (ML) (including the inner, middle and outer molecular layers) of the dentate gyrus (DG) was analyzed as well. Layers II – VI of the somatosensory cortex (SSC) also was tested for immunoreactivity. For the EAAC1 experiment, the immunoreactivity within cells in the stratum pyramidale (SP) was assessed.

CA1 – CA3 = the subfields of the hippocampus, SO = stratum oriens of the hippocampus, SP = stratum pyramidale of the hippocampus, SR = stratum radiatum of the hippocampus, DG = dentate gyrus, ML = molecular layer of the dentate gyrus, GL = granule cell layer of the dentate gyrus, HIL = hilar region of the dentate gyrus, CTX = cortex, SSC = somatosensory cortex, HF = hippocampal fissure

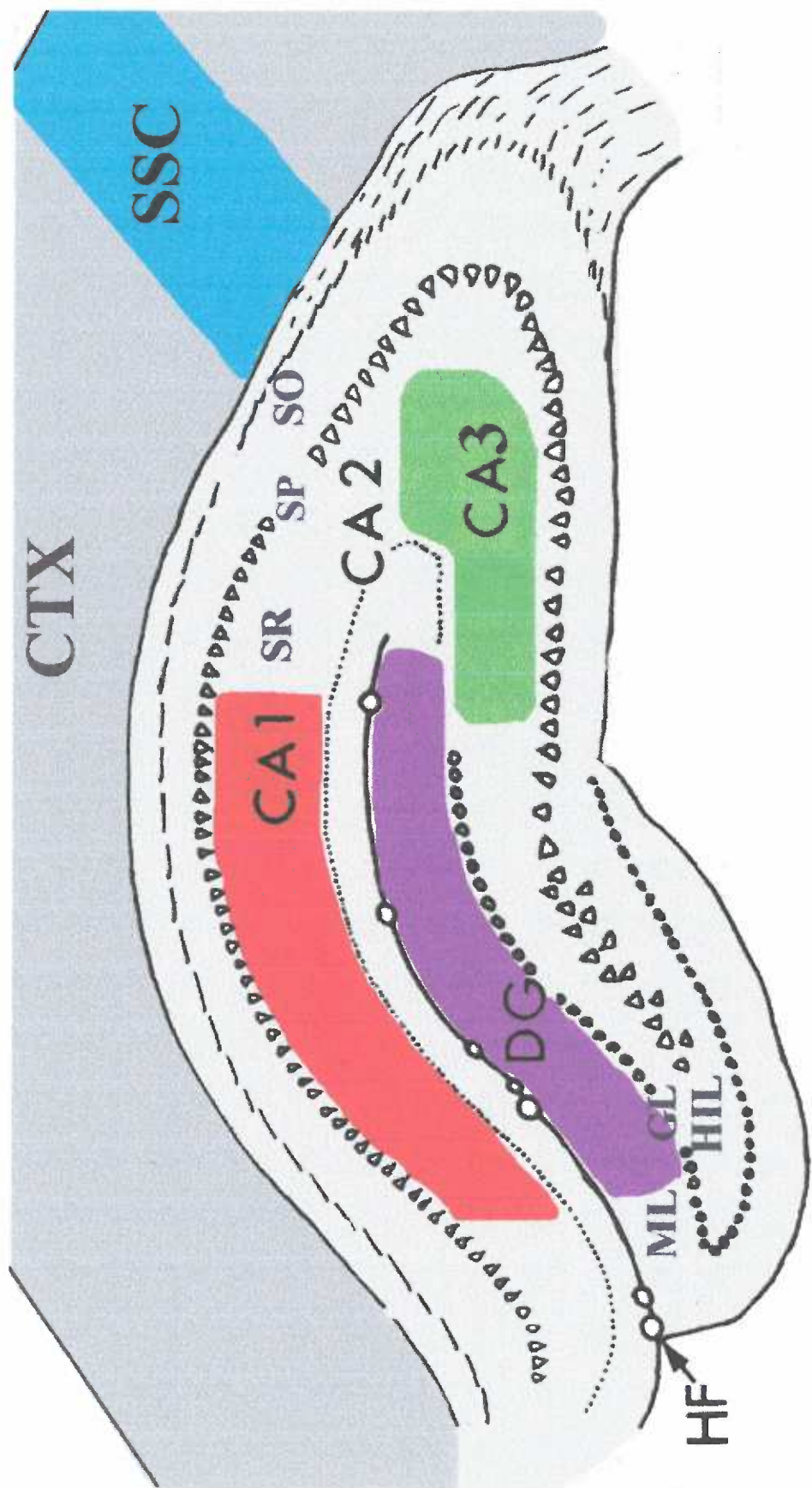


Figure 3

L-[³H]glutamate uptake into hippocampal synaptosomes from colony raised (CR) and specially raised (SR) WSP and WSR mice. (A) maximal uptake (V_{\max} in nmol uptake/mg protein/2 minutes); (B) affinity of the transporter for glutamate (K_m in μM).

Depicted is the mean glutamate uptake (\pm SEM) of hippocampal synaptosomes prepared from both replicate lines of WSP and WSR mice. Colony raised (CR) mice were raised using standard animal care procedures. This may result in HIC activity in WSP mice during cage cleaning. Specially raised (SR) mice were raised separately, but within the same colony room. These mice were handled in a manner that avoided elicitation of HIC activity. No replicate line differences in V_{\max} were observed using t-tests, therefore data were collapsed (WSP-1 vs. WSP-2 SR: $t=0.8$, NS; WSP-1 vs. WSP-2 CR: $t=-0.3$, NS; WSR-1 versus WSR-2 SR: $t=0.8$, NS; WSR-1 versus WSR-2 CR: $t=0.9$, NS). No replicate line differences were observed in K_m , therefore these data were collapsed (WSP-1 vs. WSP-2 SR: $t=1.5$, NS; WSP-1 vs. WSP-2 CR: $t=-0.5$, NS; WSR-1 versus WSR-2 SR: $t=0.8$, NS; WSR-1 versus WSR-2 CR: $t=0.9$, NS). The number of synaptosomal preparations used per group is presented in (A). Statistical analysis revealed no significant differences between any groups. V_{\max} values, mouse line: ($F_{(1,32)}=2.41$, NS); treatment group: ($F_{(1,32)}=1.38$, NS); line x treatment interaction: ($F_{(1,32)}=0.05$, NS). K_m values, line: ($F_{(1,32)}=1.0$, NS), treatment group: ($F_{(1,32)}=0.4$, NS); interaction: ($F_{(1,32)}=0.3$, NS).

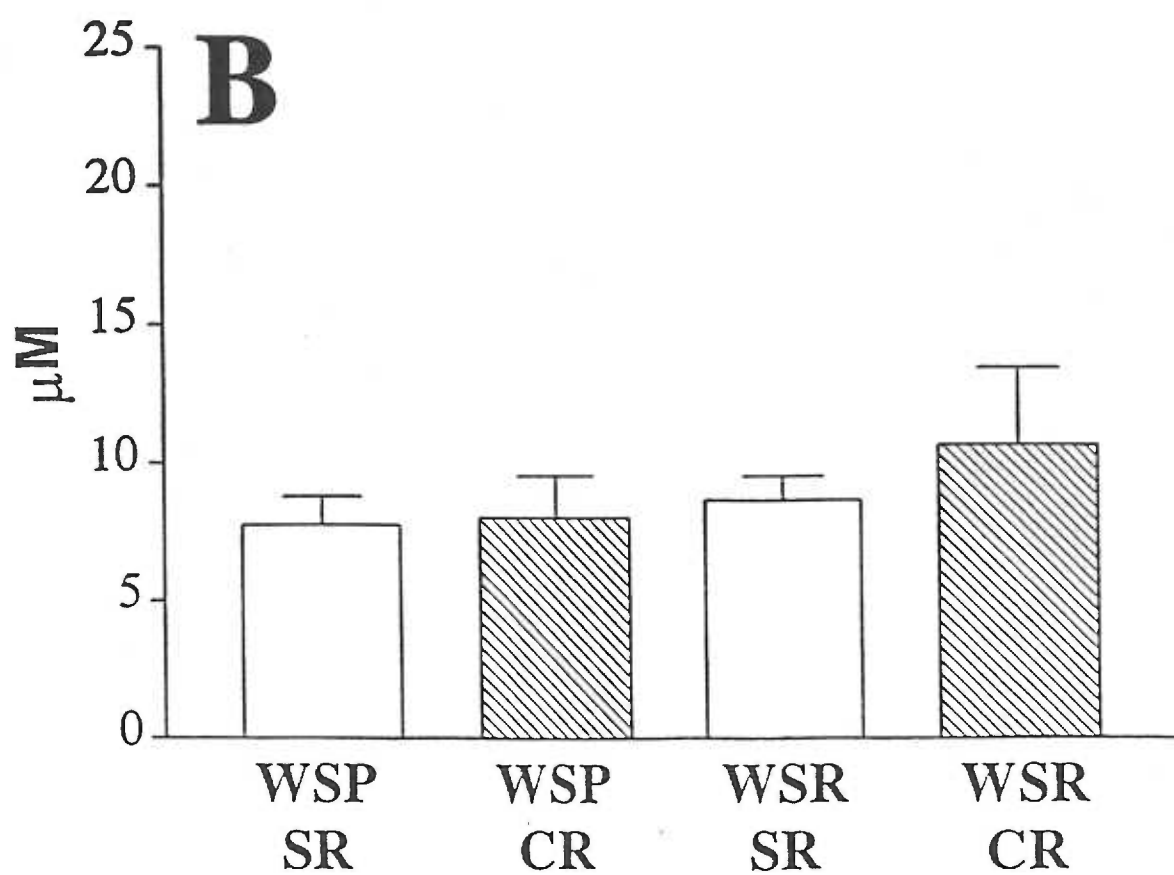
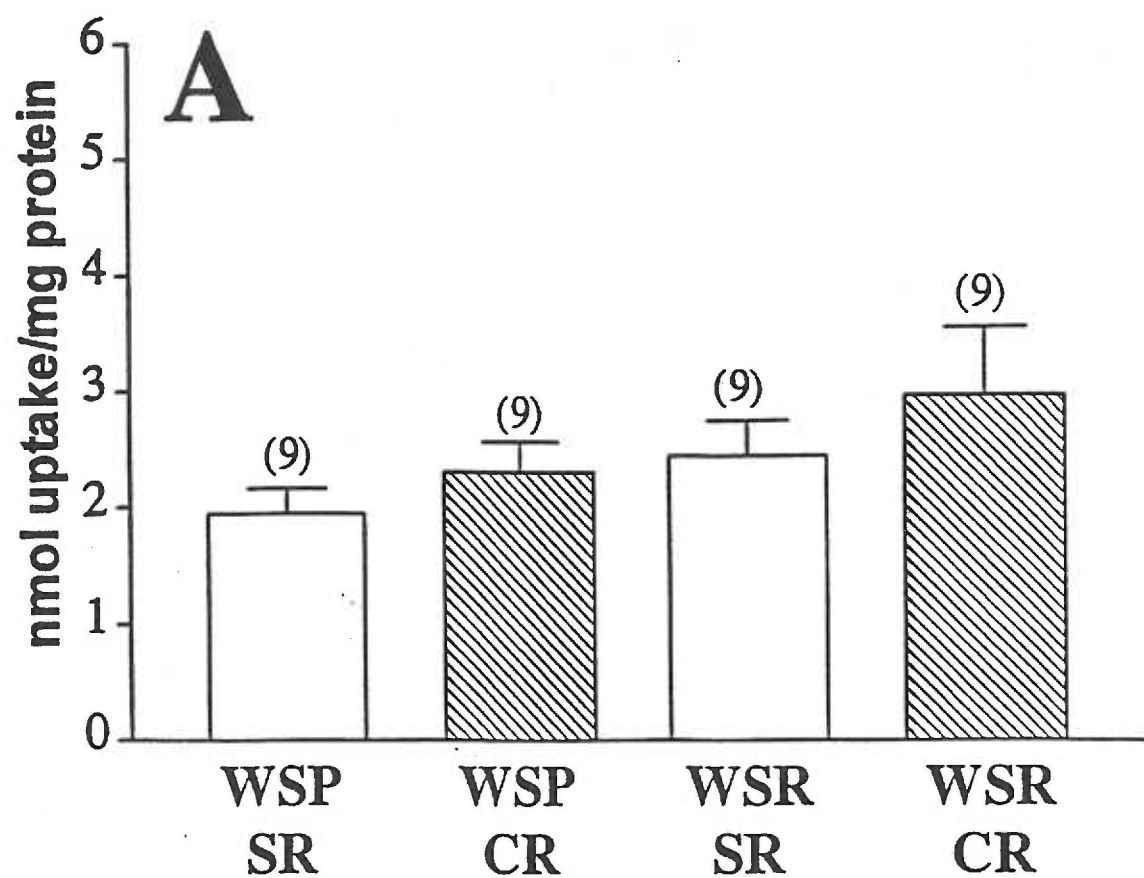


Figure 4

L-[³H]glutamate uptake into cortical synaptosomes from colony raised (CR) and specially raised (SR) WSP and WSR mice. (A) maximal uptake (V_{max} in nmol uptake/mg protein/2 minutes); (B) affinity of the transporter for glutamate (K_m in μ M).

Depicted is the mean glutamate uptake (\pm SEM) of cortical synaptosomes prepared from WSP and WSR mice (Fig. 3). No replicate line differences in V_{max} were observed using t-tests and therefore data were collapsed (WSP-1 versus WSP-2 SR: $t=1.0$, NS; WSP-1 versus WSP-2 CR: $t=-0.6$, NS; WSR-1 versus WSR-2 SR: $t=1.3$, NS; WSR-1 versus WSR-2 CR: $t=1.8$, NS). No replicate line differences were observed in K_m , therefore these data were collapsed (WSP-1 versus WSP-2 SR: $t=0.3$, NS; WSP-1 versus WSP-2 CR: $t=1.1$, NS; WSR-1 versus WSR-2 SR: $t=0.9$, NS; WSR-1 versus WSR-2 CR: $t=2.1$, NS). The number of synaptosomal preparations analyzed for each group is presented in (A). Statistical analysis revealed no significant differences between any groups. V_{max} values, mouse line: ($F_{(1,31)}=0.5$, NS); treatment group: ($F_{(1,31)}=0.3$, NS); line x treatment interaction: ($F_{(1,31)}=0.2$, NS). K_m values, line: ($F_{(1,31)}=0.01$, NS), treatment group: ($F_{(1,31)}=0.01$, NS); interaction: ($F_{(1,31)}=0.4$, NS).

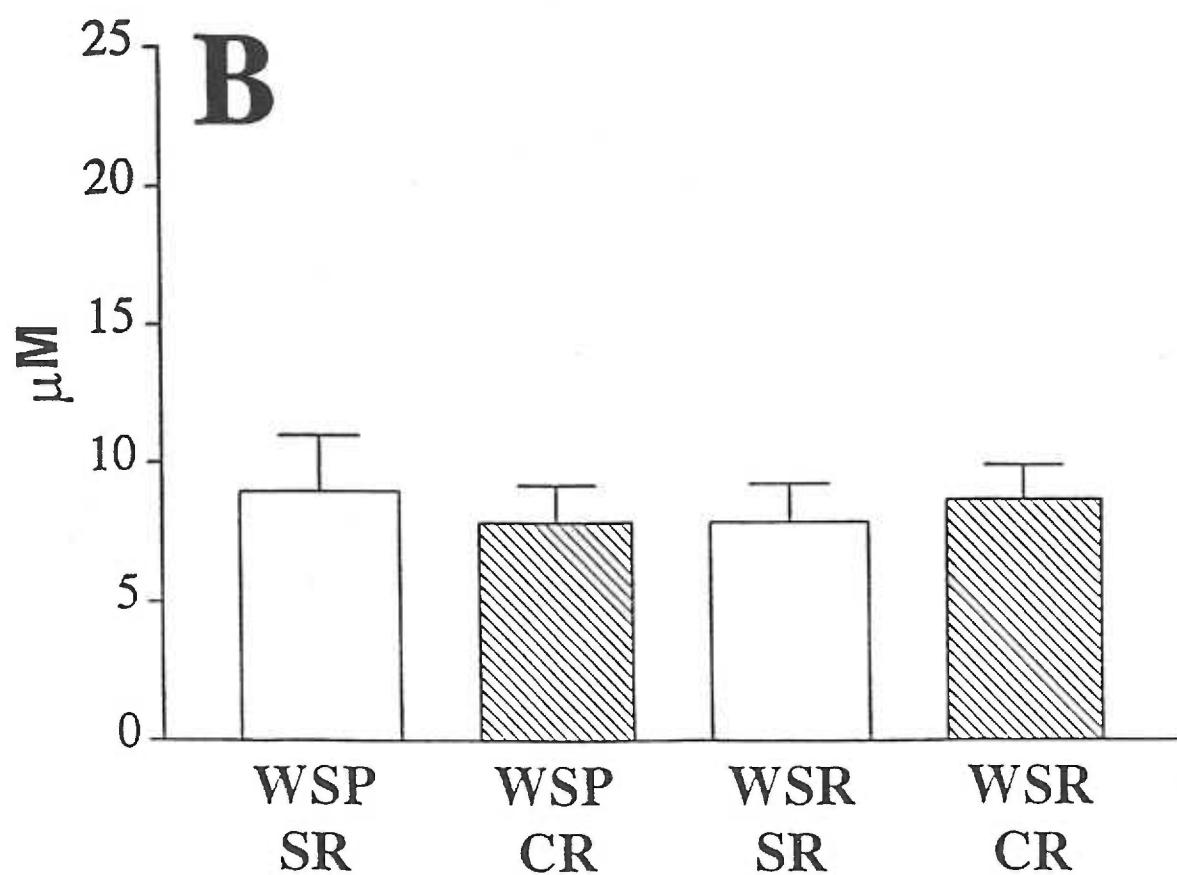
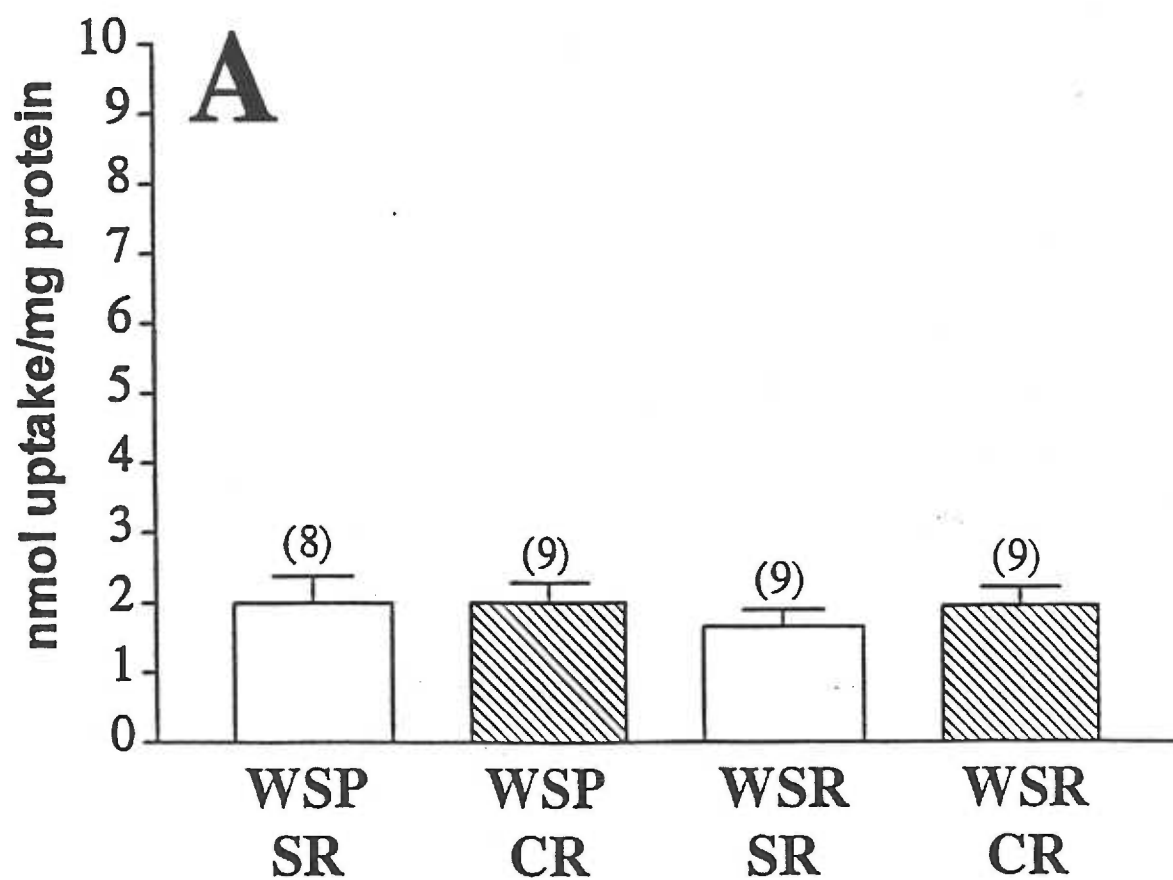


Figure 5

L-[³H]glutamate uptake into hippocampal synaptosomes from naive and handled WSP and WSR mice(A) maximal uptake (V_{max} in nmol uptake/mg protein/2 minutes); (B) affinity of the transporter for glutamate (K_m in μM). Depicted is the mean glutamate uptake (\pm SEM) of hippocampal synaptosomes prepared from WSP-2 and WSR-2 mice. This experiment was repeated 4 times. "Naive" mice did not experience HICs, whereas "handled" WSP mice exhibited drug-naive HICs during at least 8 of ten trials. "Handled" WSR mice did not show any HIC activity. The number of synaptosomal preparations used for each group is depicted in (A). Statistical analysis revealed no significant differences between any groups. V_{max} values, mouse line: ($F_{(1,13)}=0.6$, NS); treatment group: ($F_{(1,13)}=2.0$, NS); line x treatment interaction: ($F_{(1,13)}=0.006$, NS). K_m values, line: ($F_{(1,13)}=0.2$, NS), treatment group: ($F_{(1,13)}=0.03$, NS); interaction: ($F_{(1,13)}=0.7$, NS).

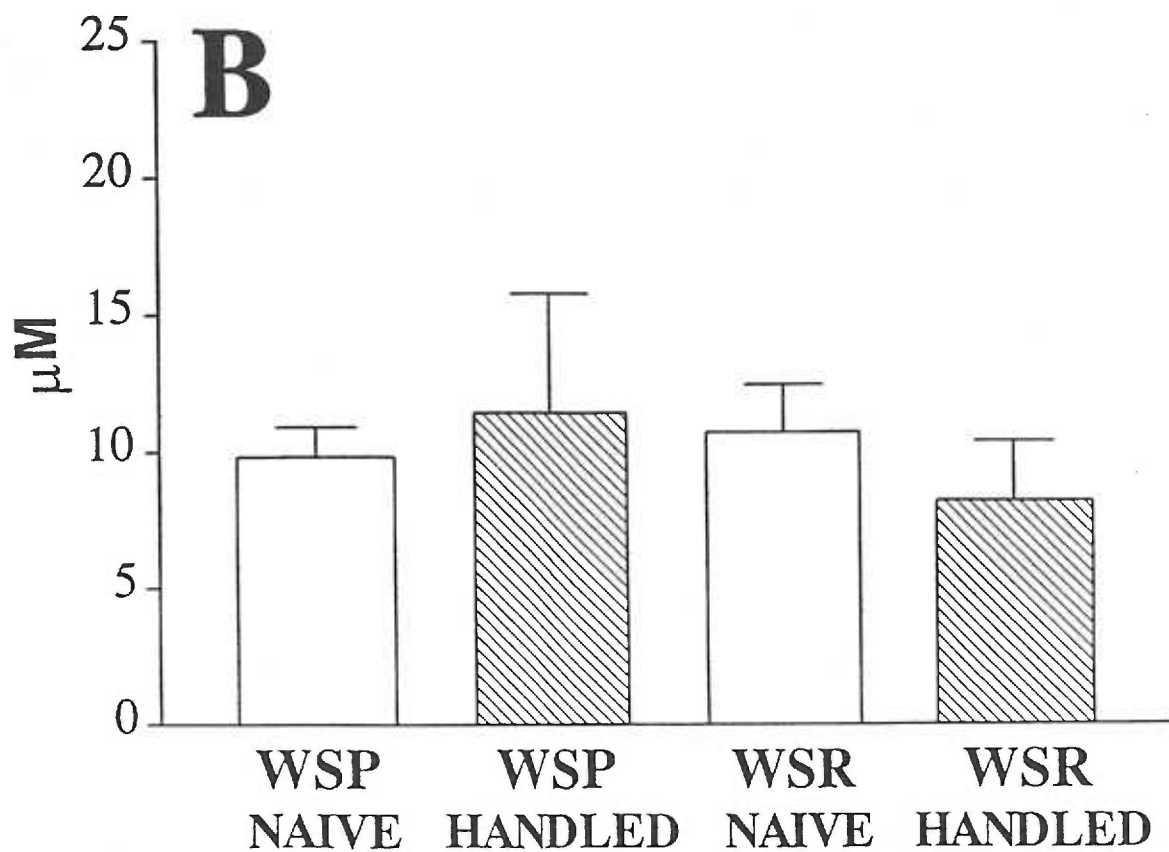
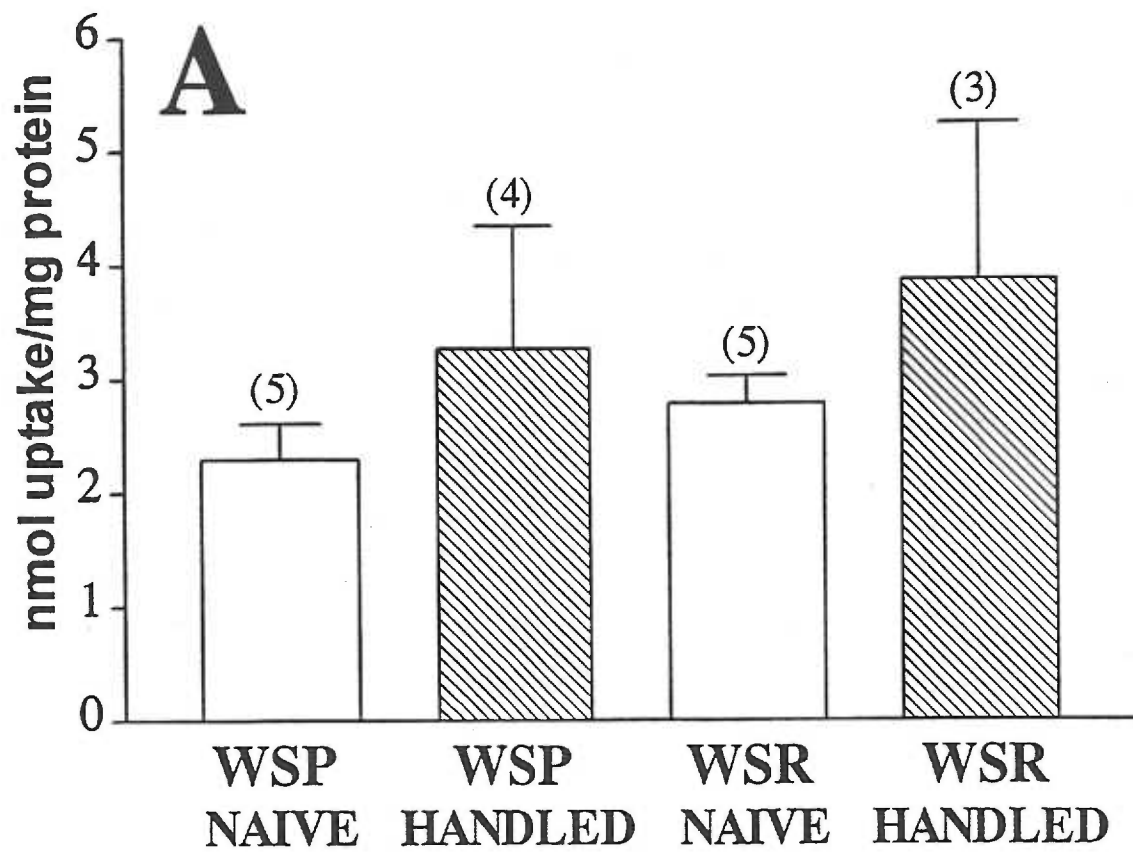


Figure 6

L-[³H]glutamate uptake into cortical synaptosomes from naive and handled WSP and WSR mice. (A) maximal uptake (V_{\max} in nmol uptake/mg protein/2 minutes); (B) affinity of the transporter for glutamate (K_m in μM). Illustrated is the mean glutamate uptake (\pm SEM) of cortical synaptosomes prepared from WSP-2 and WSR-2 mice (Fig. 5). The number of synaptosomal preparations used per group is presented in (A). Statistical analysis revealed no significant differences between any groups. V_{\max} values, mouse line: ($F_{(1,13)}=0.3$, NS); treatment group: ($F_{(1,13)}=1.0$, NS); line x treatment interaction: ($F_{(1,13)}=0.02$, NS). K_m values, line: ($F_{(1,13)}=2.9$, NS), treatment group: ($F_{(1,13)}=0.9$, NS); interaction: ($F_{(1,13)}=3.3$, $p=0.09$).

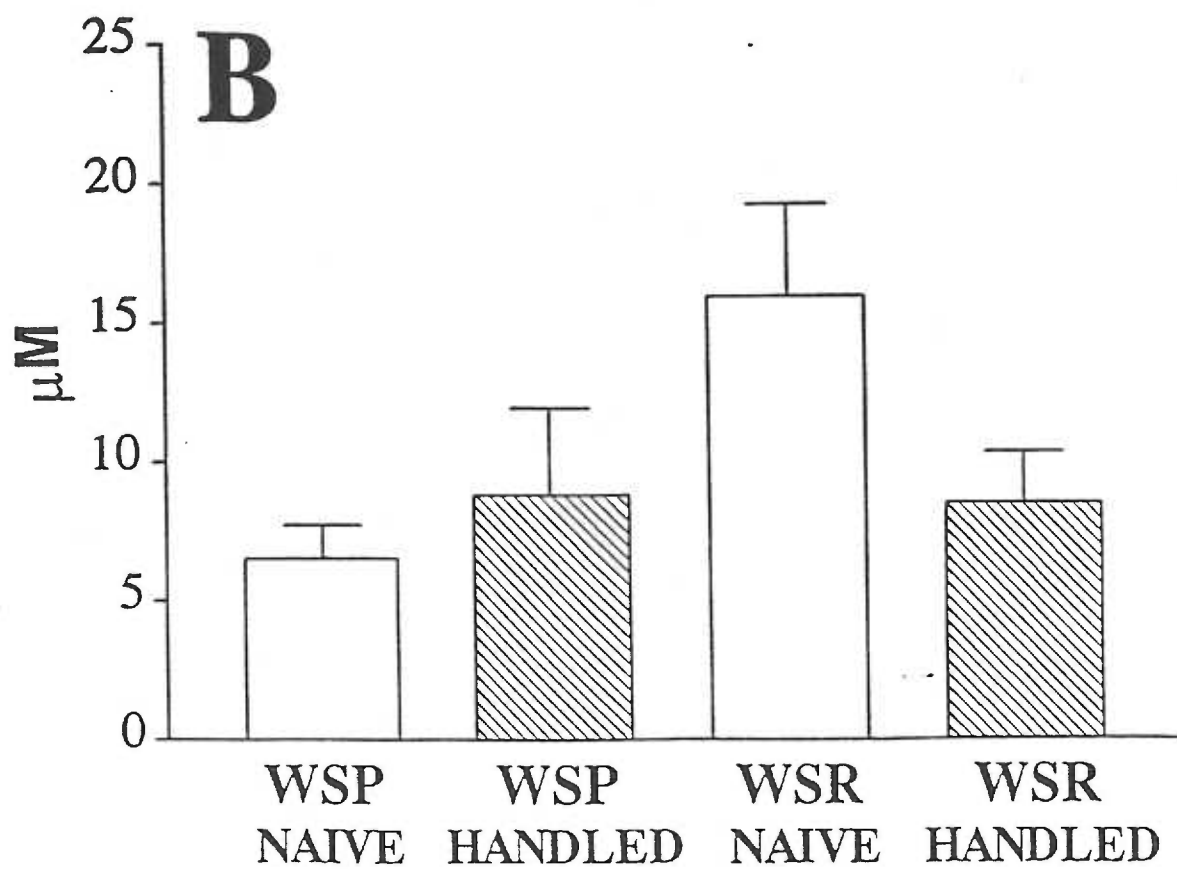
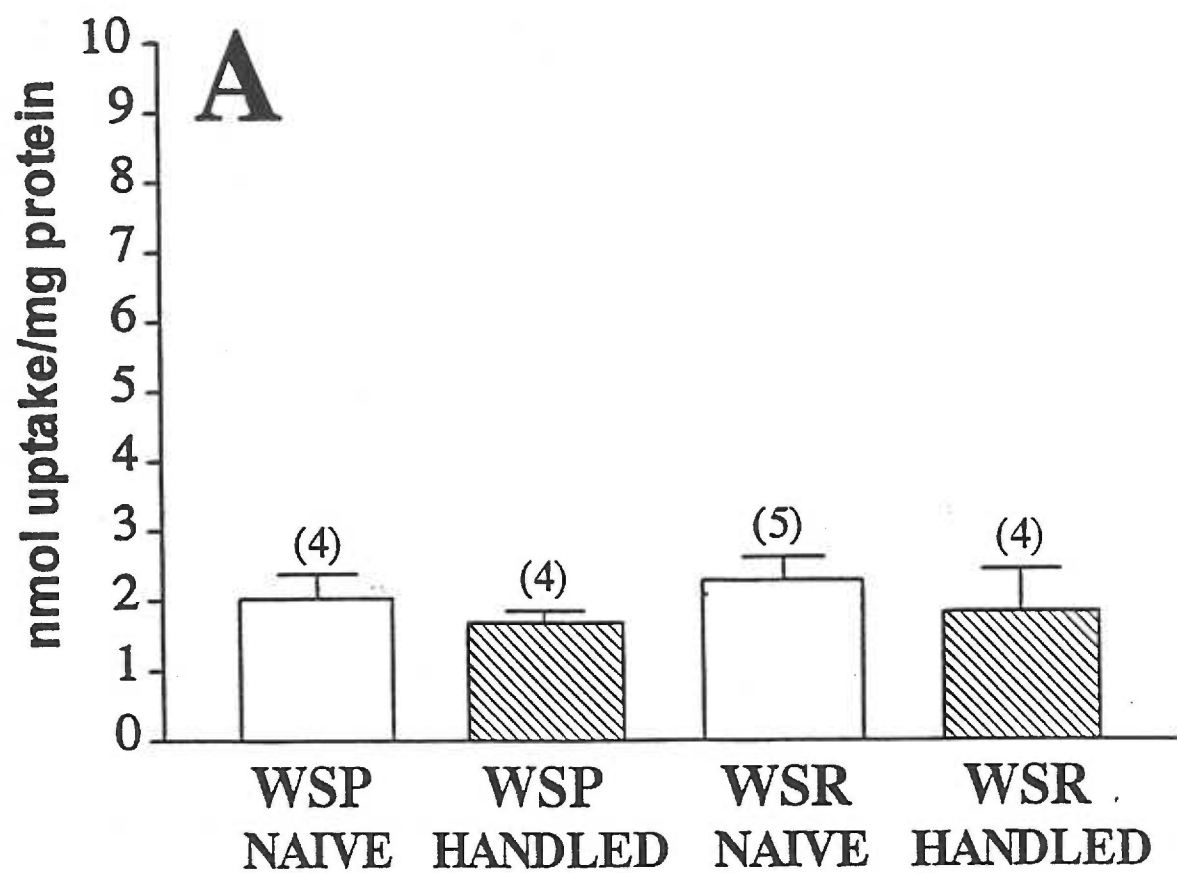


Figure 7

L-[³H]glutamate uptake into hippocampal synaptosomes following injection of saline or a hypnotic dose of EtOH in WSP and WSR mice(A) maximal uptake (V_{max} in nmol uptake/mg protein/2 minutes); (B) affinity of the transporter for glutamate (K_m in μ M). Depicted is the mean glutamate uptake (\pm SEM) of hippocampal synaptosomes prepared from WSP-2 and WSR-2 mice. This experiment was done 3 times. Mice were injected i.p. with 4 g/kg EtOH (20% v/v) or equal volume of saline. Uptake was measured during peak intoxication (5 minutes post-injection). The number of synaptosomal preparations analyzed per group is presented in (A). No significant differences between any groups were observed. V_{max} values, line: ($F_{(1,8)}=0.008$, NS); treatment group: ($F_{(1,8)}=0.6$, NS); line x treatment interaction: ($F_{(1,8)}=2.6$, NS). K_m values, line: ($F_{(1,8)}=0.08$, NS); treatment: ($F_{(1,8)}=0.2$, NS); line x treatment: ($F_{(1,8)}=1.7$, NS).

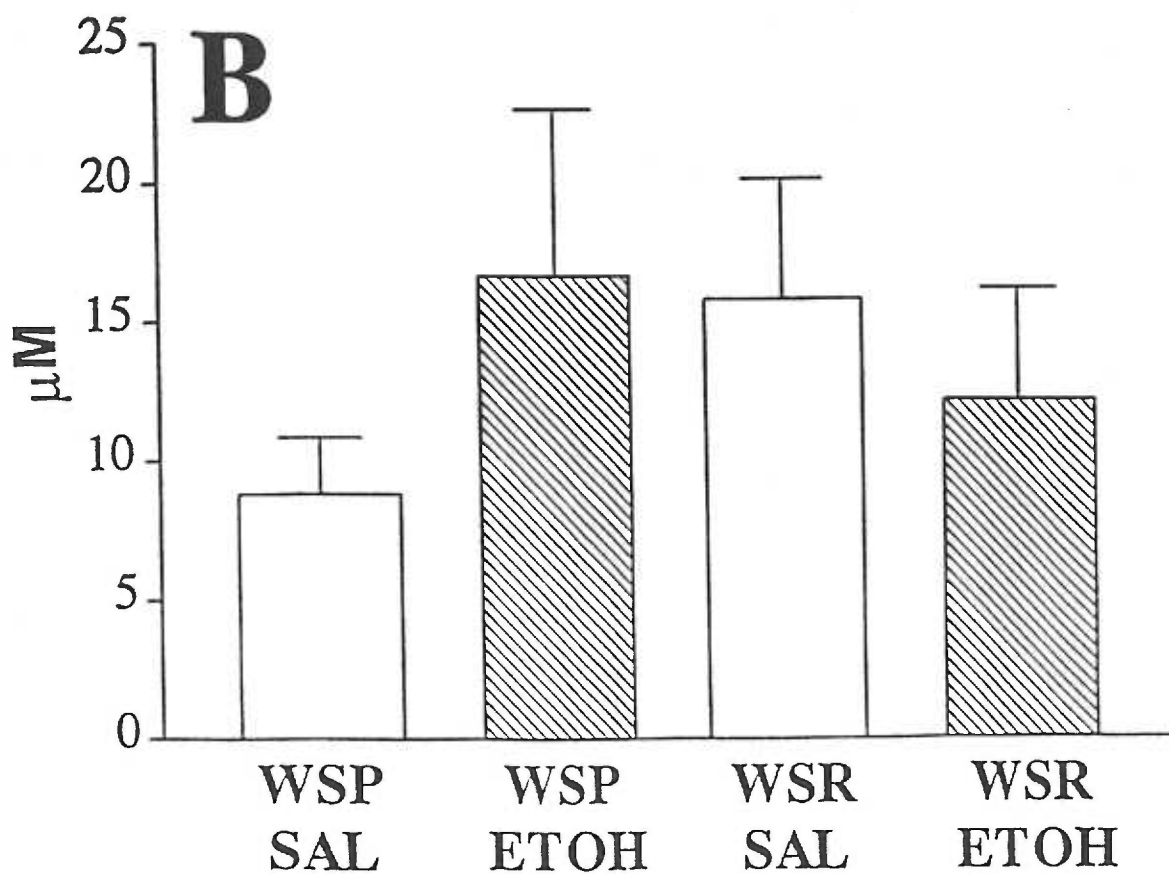
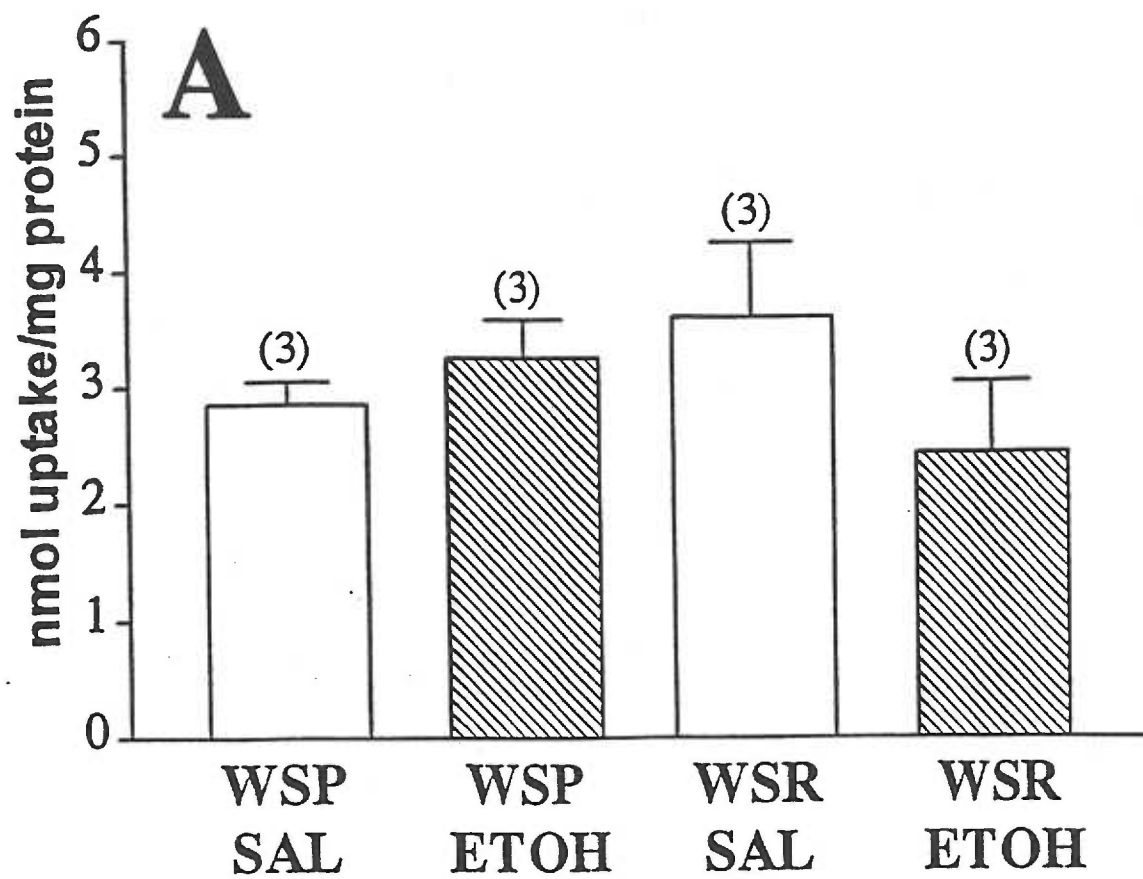


Figure 8

L-[³H]glutamate uptake into cortical synaptosomes following injection of saline or a hypnotic dose of EtOH in WSP and WSR mice. (A) maximal uptake (V_{\max} in nmol uptake/mg protein/2 minutes); (B) affinity of the transporter for glutamate (K_m in μM). Depicted is the mean glutamate uptake (\pm SEM) of cortical synaptosomes prepared from WSP-2 and WSR-2 mice (Fig. 7). The number of synaptosomal preparations analyzed is presented in (A). No significant differences between any groups were observed. V_{\max} values, line: ($F_{(1,8)}=1.8$, NS); treatment group: ($F_{(1,8)}=0.3$, NS); line x treatment interaction: ($F_{(1,8)}=0.2$, NS). K_m values, line: ($F_{(1,8)}=0.1$, NS); treatment: ($F_{(1,8)}=2.1$, NS); line x treatment: ($F_{(1,8)}=0.02$, NS).

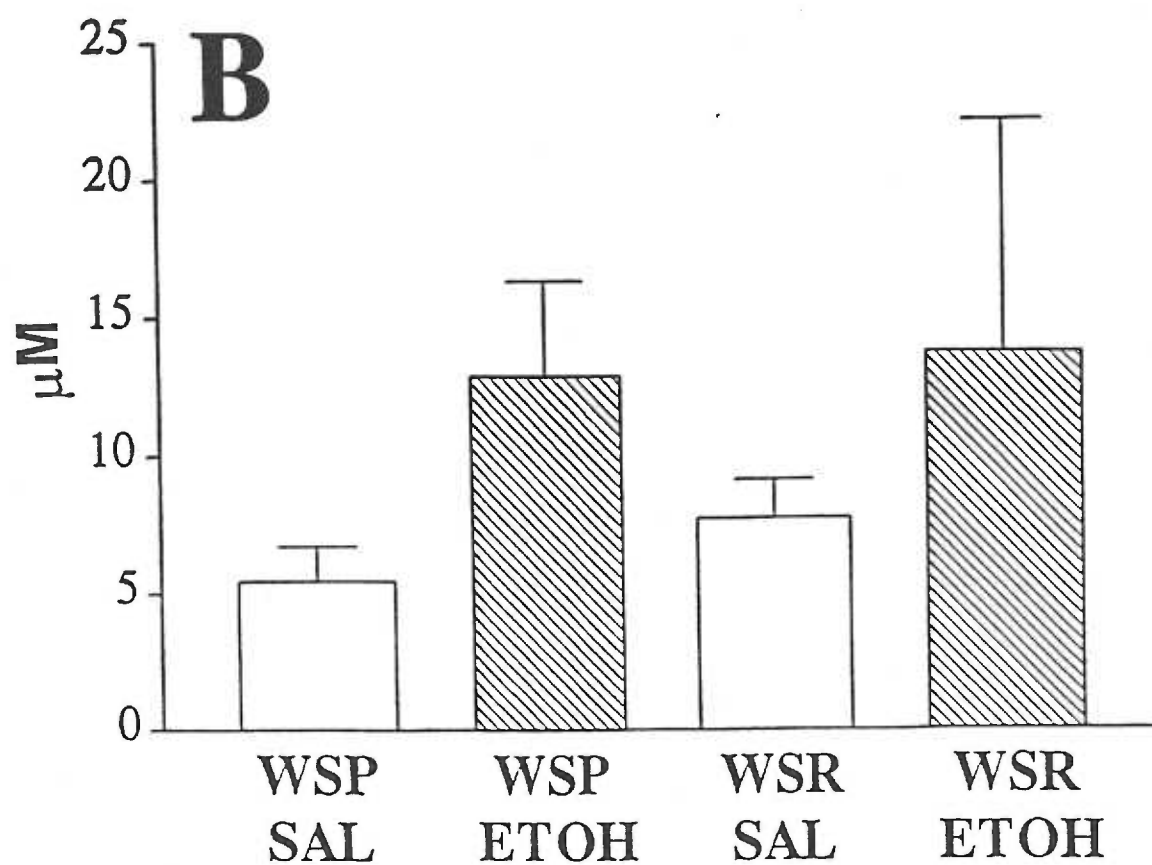
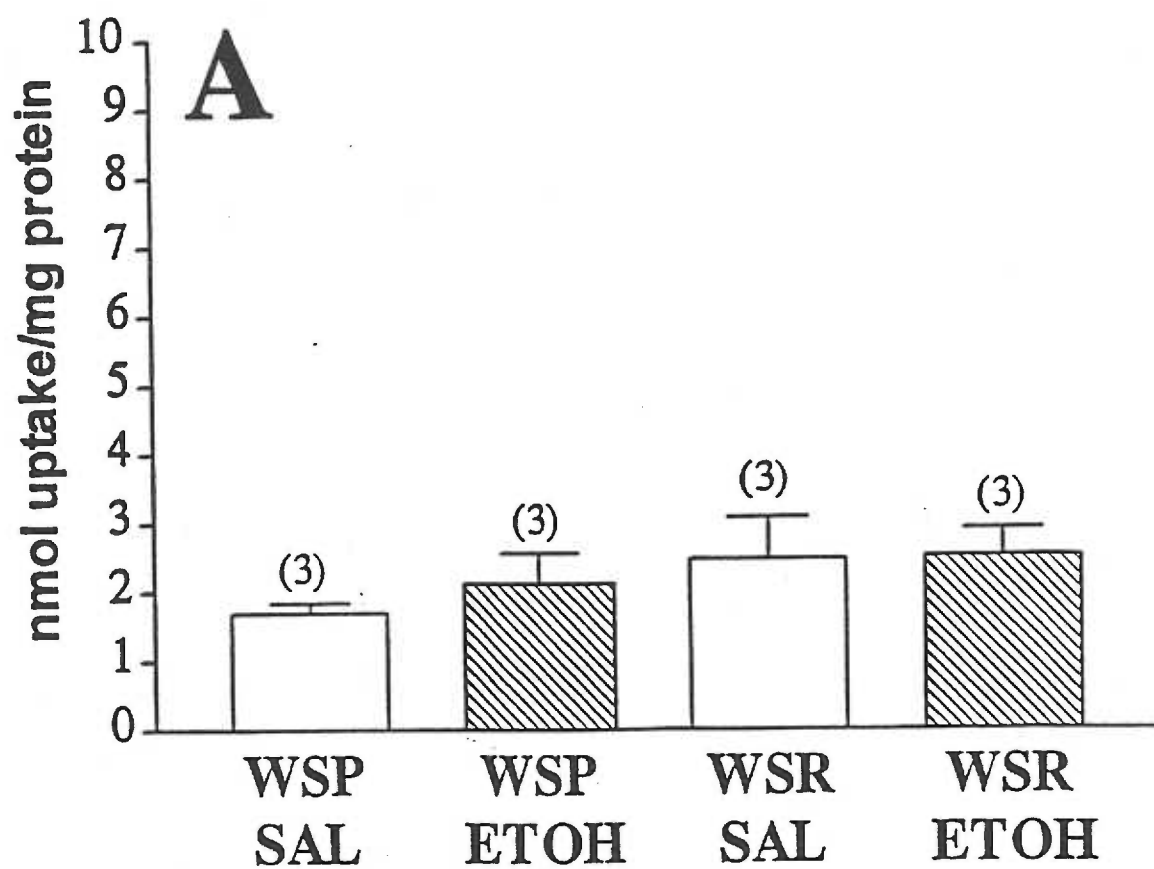


Figure 9

Dose-dependent inhibition of L-[³H]glutamate uptake by *in vitro* exposure to EtOH, PDC or kainic acid.

Hippocampal synaptosomes were prepared from naive WSP-1 mice and exposed to various concentrations of (A) EtOH, (B) PDC (a nonspecific uptake inhibitor) and (C) kainic acid (an uptake inhibitor somewhat specific for GLT-1). Data are presented as percent of control (uptake in the presence of no inhibitor). Inhibition by PDC and kainic acid were dose-dependent. No dose response curve was observed with EtOH. Data in (A) are presented as the mean \pm SEM (n=5). Data in (B) and (C) are representative curves from single experiments that were repeated two or three times, respectively, with similar results.

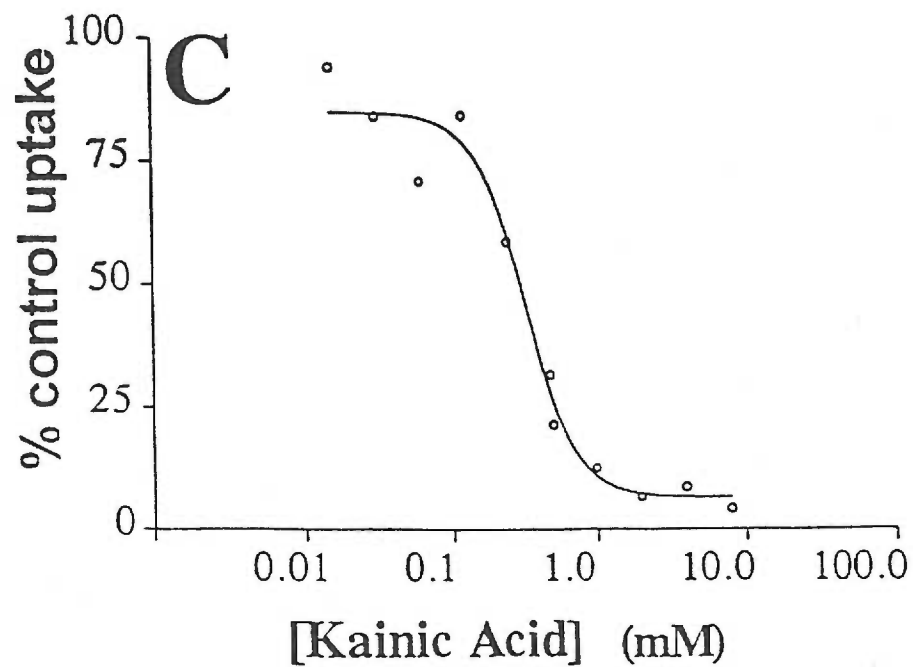
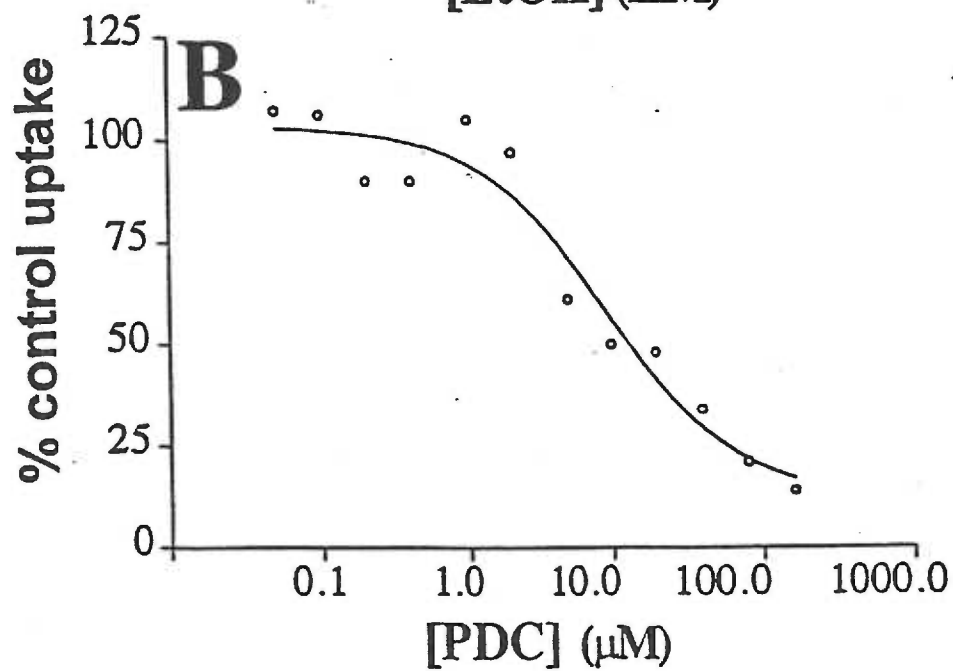
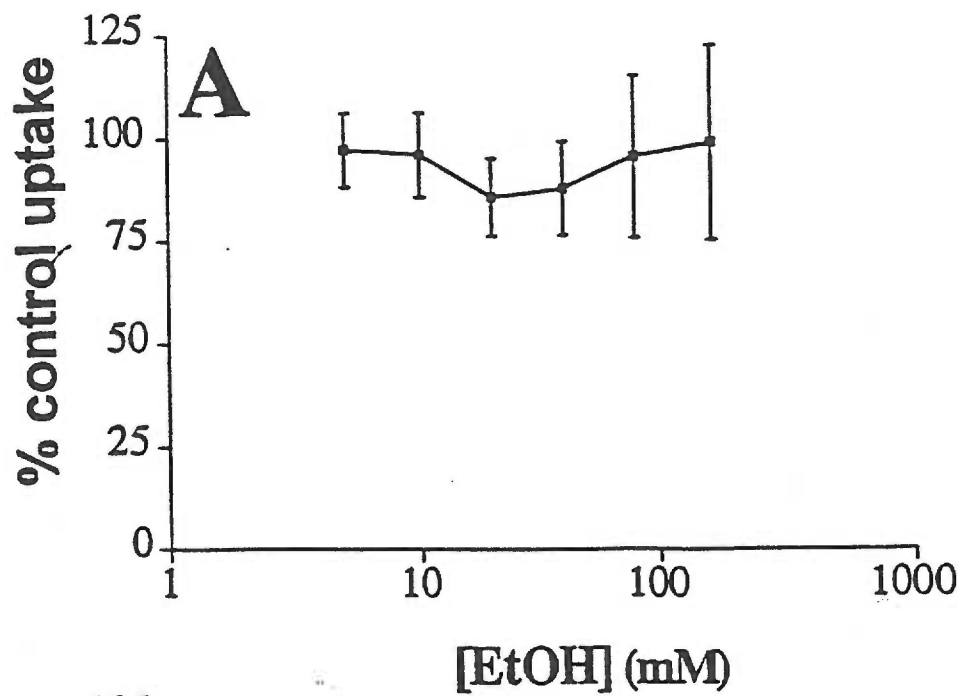


Figure 10

Effect of withdrawal from exposure to 72 hour EtOH vapor on L-[³H]glutamate uptake in hippocampal synaptosomes. Depicted are representative dose-response curves showing glutamate uptake in WSP-2 and WSR-2 mice. This figure shows data from air exposed animals treated with saline or pyrazole separately. These groups were combined into a single control group for statistical analysis (Fig. 11).

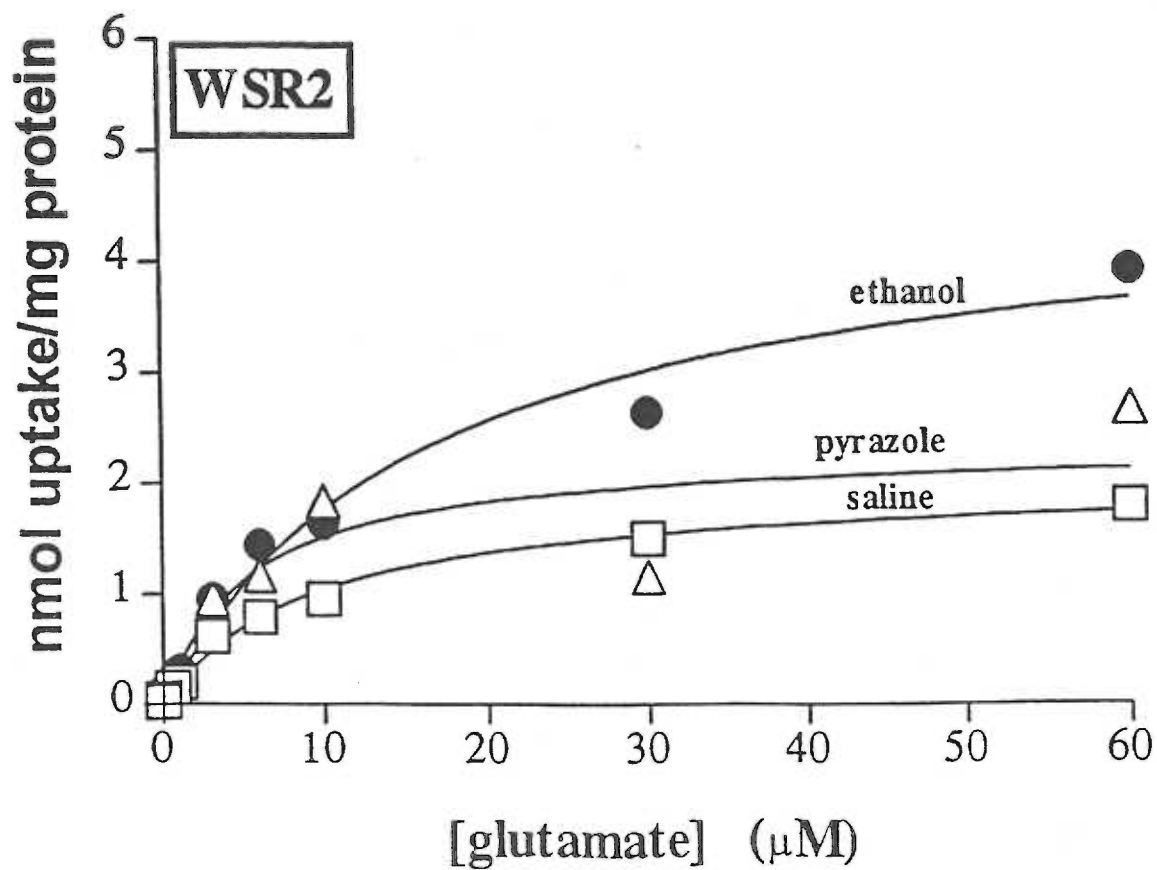
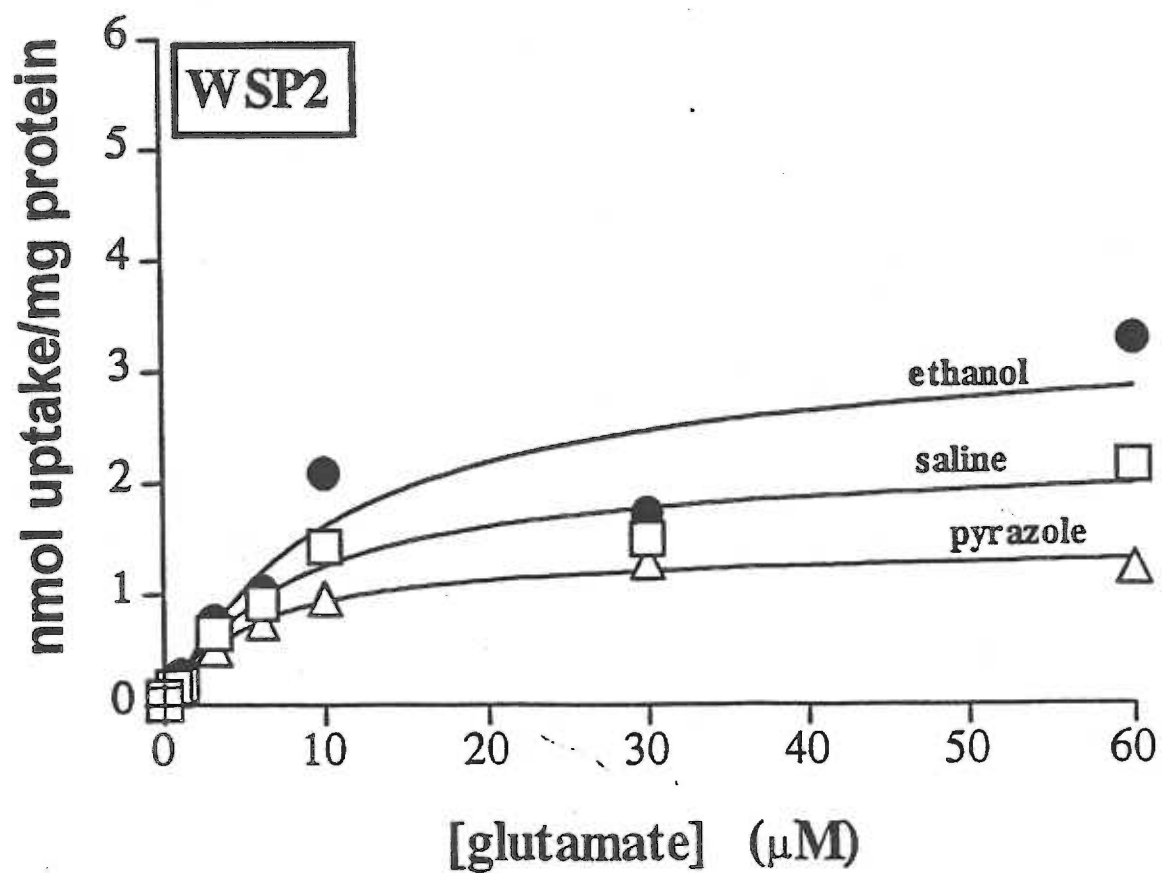


Figure 11

L-[³H]glutamate uptake into hippocampal synaptosomes from WSP and WSR mice during peak withdrawal from chronic EtOH inhalation. (A) maximal uptake (V_{\max} in nmol uptake/mg protein/2 minutes); (B) affinity of the transporter for glutamate (K_m in μ M). Data are pooled across replicate lines because no differences between WSP-1 and WSP-2 lines in any of three treatment groups (SAL: $F_{(1,6)}=3.0$; NS; PYR: $F_{(1,5)}=0.0003$; NS; ETOH: $F_{(1,10)}=0.6$; NS) or between WSR-1 and WSR-2 lines were observed (SAL: $F_{(1,5)}=0.5$; NS; PYR: $F_{(1,6)}=0.2$; NS; ETOH: $F_{(1,9)}=0.1$; NS). Open bars represent uptake in mice that were exposed to air in the inhalation chambers (control, CONT). Because no significant differences were observed between air exposed mice that were given saline injections versus those given pyrazole injections, the data were collapsed across treatments [V_{\max} values, lines: ($F_{(1,26)}=0.2$, NS); SAL and PYR treatments: ($F_{(1,26)}=1.7$, NS); line x treatment interaction: ($F_{(1,26)}=1.5$, NS)]. K_m values, lines: ($F_{(1,26)}=0.1$, NS); treatment groups: ($F_{(1,26)}=0.2$, NS); interaction: ($F_{(1,26)}=1.5$, NS)]. The striped bars represent uptake in mice that were exposed to EtOH vapor and pyrazole injections (ETOH). Each bar represents the mean \pm standard error [group size is presented above each bar in (A)]. Hippocampal V_{\max} was not different between the lines: ($F_{(1,48)}=1.7$, NS), but a significant difference was detected between the CONT (SAL + PYR) and ETOH treatment groups ($F_{(1,48)}=18.6$, $p < 0.0001$). No interaction between line and treatment was observed ($F_{(1,48)}=0.6$, NS). No differences in K_m were observed between lines ($F_{(1,48)}=1.3$, NS), between treatments ($F_{(1,48)}=0.4$, NS), nor was there a significant interaction between these factors ($F_{(1,48)}=1.9$, NS). [$* p < 0.01$ vs. control groups]

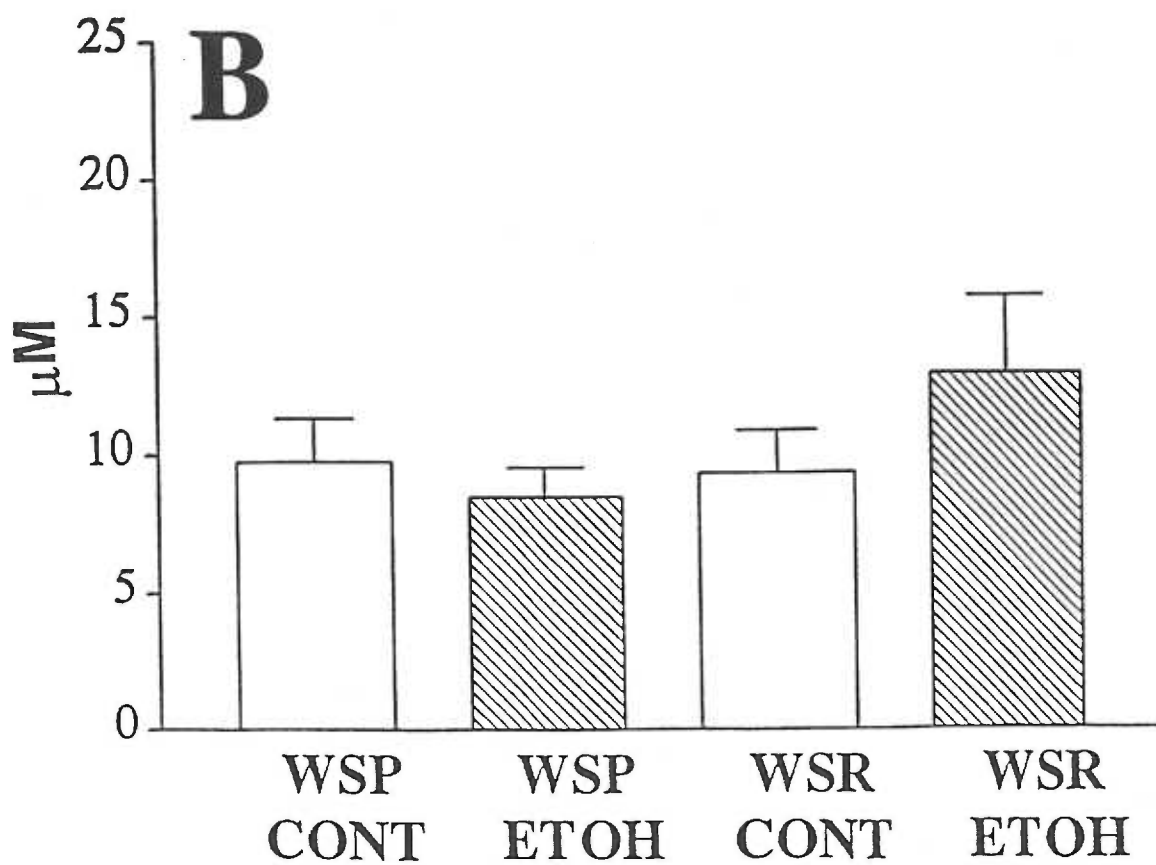
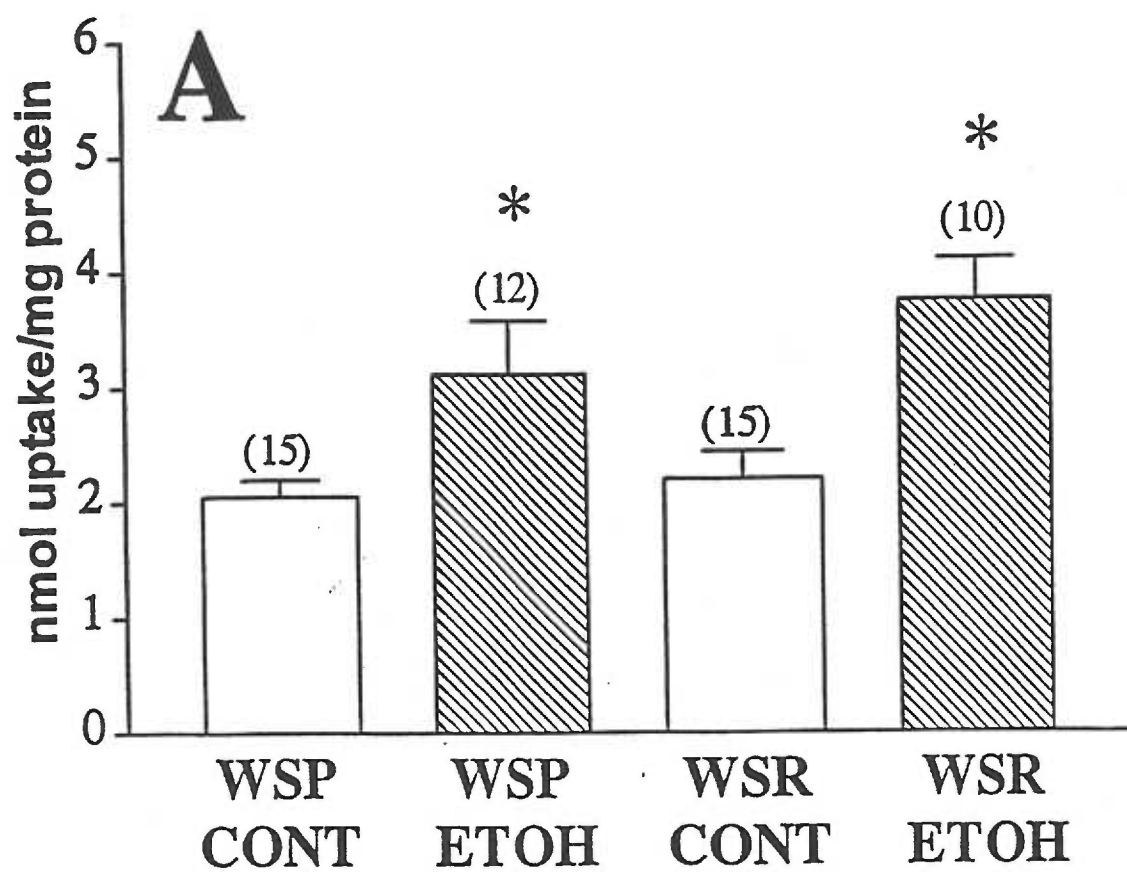


Figure 12

Correlation of uptake parameters and blood-ethanol concentration (BEC)

BEC (mg/ml) was determined following 72 hours of EtOH vapor exposure, immediately upon removal from the inhalation chambers. Mean BECs (from 3-4 mice used in each synaptosomal preparation) from each experiment were compared to withdrawal V_{\max} and K_m from that same experiment using linear regression. (A) correlation between V_{\max} and BEC; $r=0.15$, $p = \text{NS}$ (B) correlation between K_m and BEC; $r=0.15$, $p = \text{NS}$.

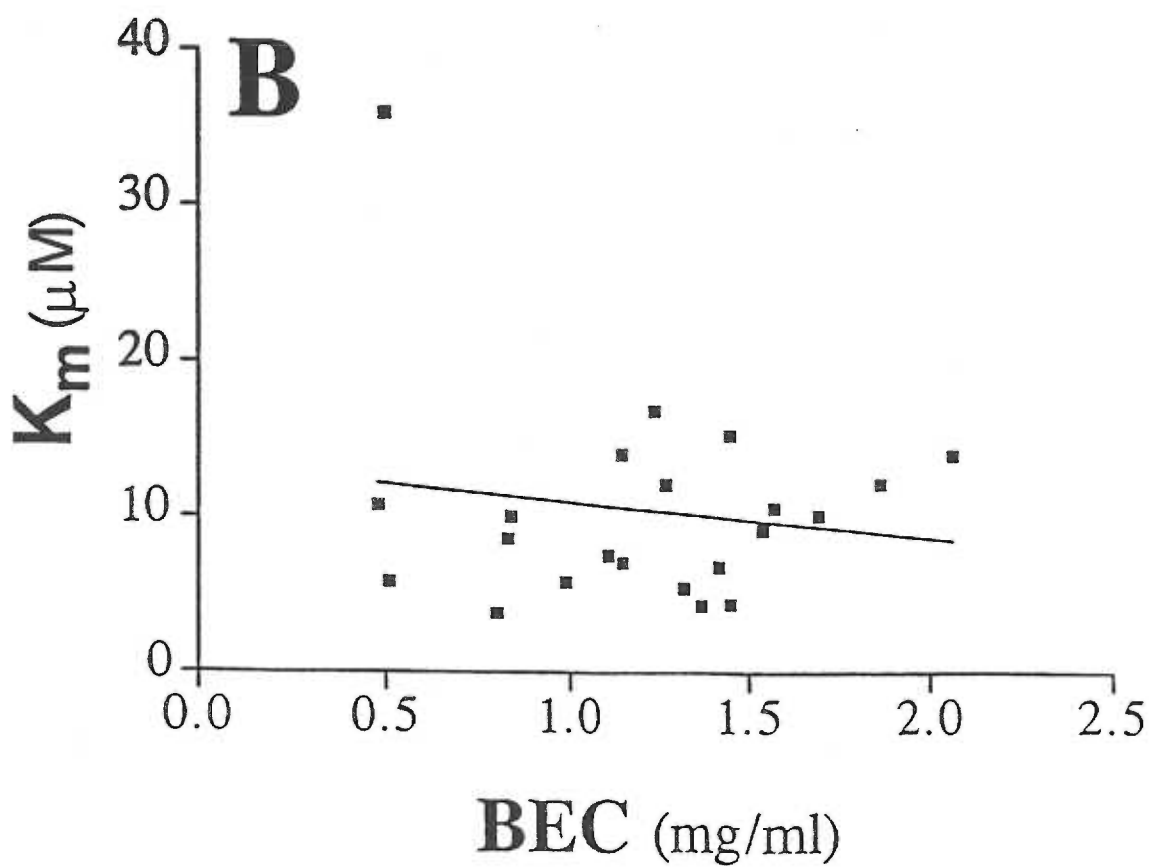
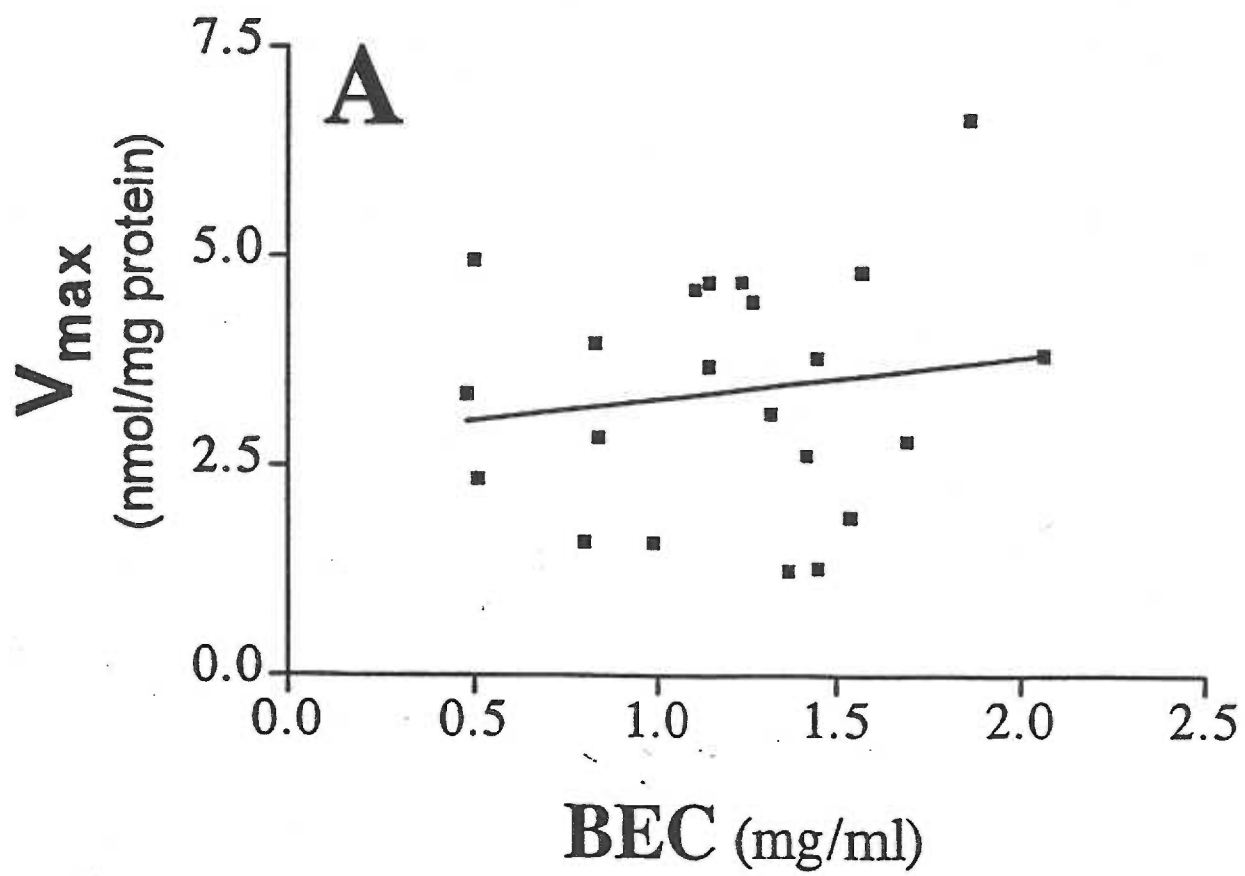
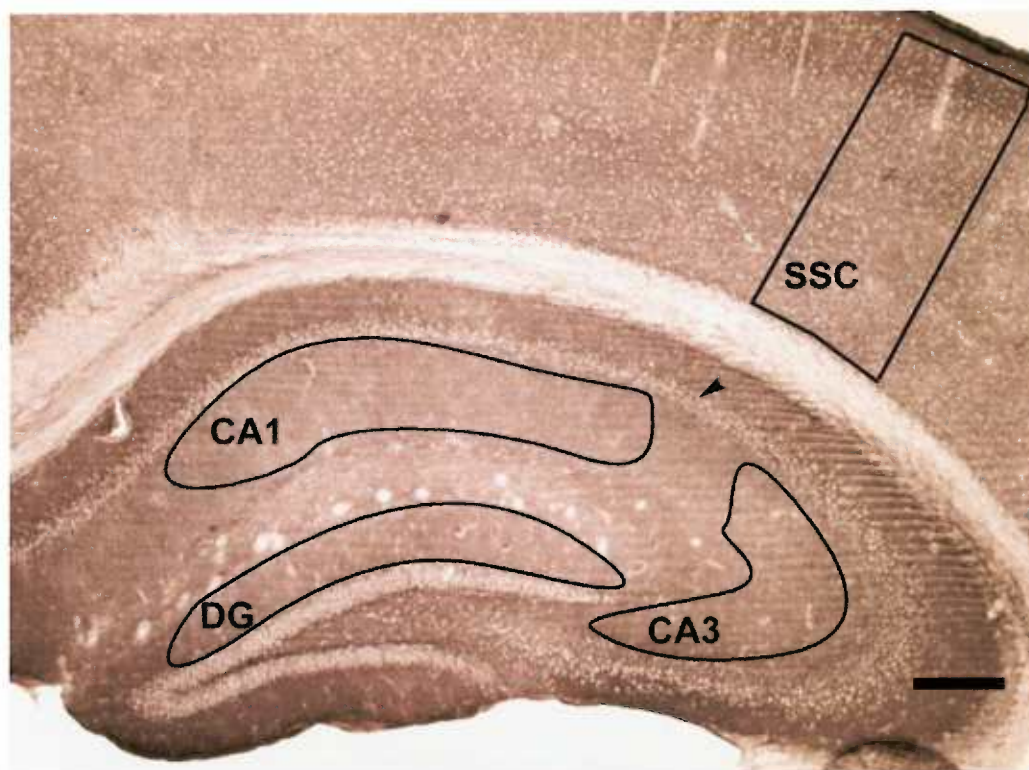


Figure 13

Immunoperoxidase staining for GLAST in naive WSP and WSR mice

Depicted is a representative 50 μm slice from one (A) WSP-2 and (B) WSR-2 mouse following overnight incubation in a primary antibody against GLAST, a glial glutamate transporter. The DAB/nickel reaction results in a diffuse purple stain seen throughout the hippocampus and cortex but is absent from white matter and neuronal cell bodies (*arrowhead*). The regions analyzed are outlined and include the stratum radiatum (located directly below pyramidal cell layer in the hippocampus, *arrowhead*) of the CA1 and CA3, the molecular layer of the dentate gyrus (DG) and the region of the somatosensory cortex (SSC) present in this slice. Scale bar, 200 μm .

A



B

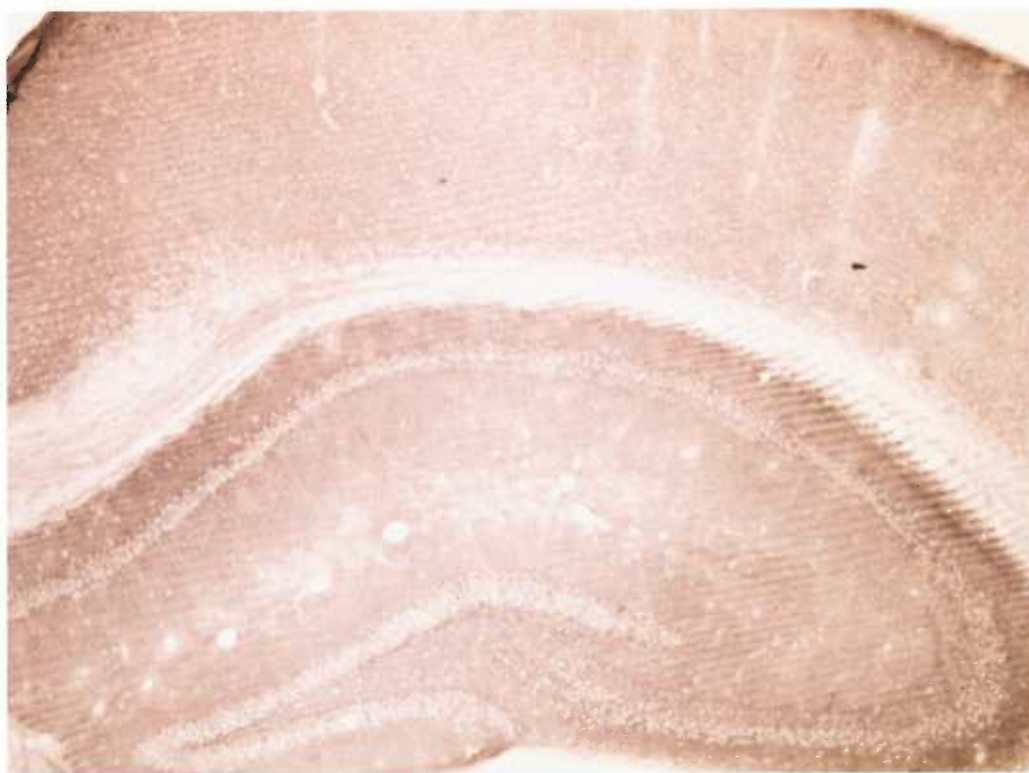


Figure 14

Density of the glial transporter GLAST immunolabeling in hippocampus and cortex

(A) stratum radiatum of the CA1 (CA1), (B) stratum radiatum of the CA3 (CA3), (C) molecular layer of the dentate gyrus (DG), (D) somatosensory cortex (SSC). Depicted is the mean optical density (\pm SEM), in arbitrary units, of GLAST immunolabeling in naive WSP and WSR mice from both replicate lines. The number of tissue slices analyzed per group is presented above each bar. A significant interaction between selected and replicate lines was observed in the CA1. CA1: selected line: ($F_{(1,18)}=0.6$, NS); replicate line: ($F_{(1,18)}=2.3$, NS); selected x replicate line interaction: ($F_{(1,18)}=5.1$, $p = 0.037$). Post-hoc analysis of simple effects revealed that significant differences existed between replicate line 2 mice (i.e. WSP-2 vs. WSR-2). Replicate line 1: $F_{(1,18)}=3.5$, $p =$ NS, replicate line 2: $F_{(1,18)}=10.2$, $p < 0.01$). CA3: selected line: ($F_{(1,18)}=0.4$, NS); replicate line: ($F_{(1,18)}=2.0$, NS); selected x replicate line interaction: ($F_{(1,18)}=1.5$, $p =$ NS). DG: selected line: ($F_{(1,17)}=0.1$, NS); replicate line: ($F_{(1,17)}=1.3$, NS); selected x replicate line interaction: ($F_{(1,17)}=0.2$, $p =$ NS). SSC: selected line: ($F_{(1,16)}=0.1$, NS); replicate line: ($F_{(1,16)}=0.5$, NS); selected x replicate line interaction: ($F_{(1,16)}=0.7$, $p =$ NS). [+ $p < 0.01$, WSP-2 vs. WSR-2 mice]

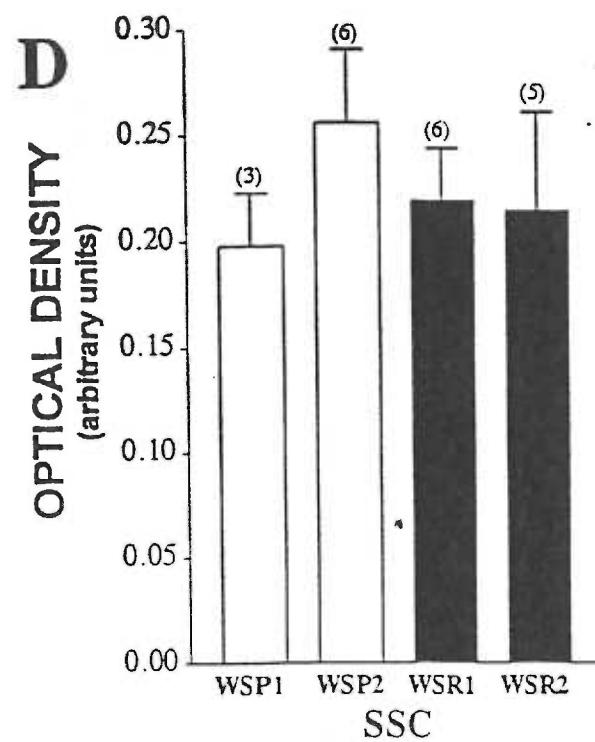
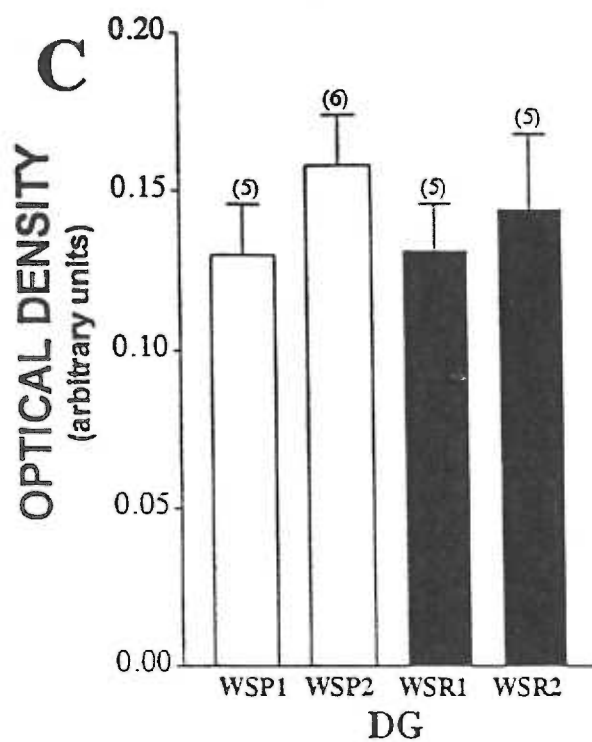
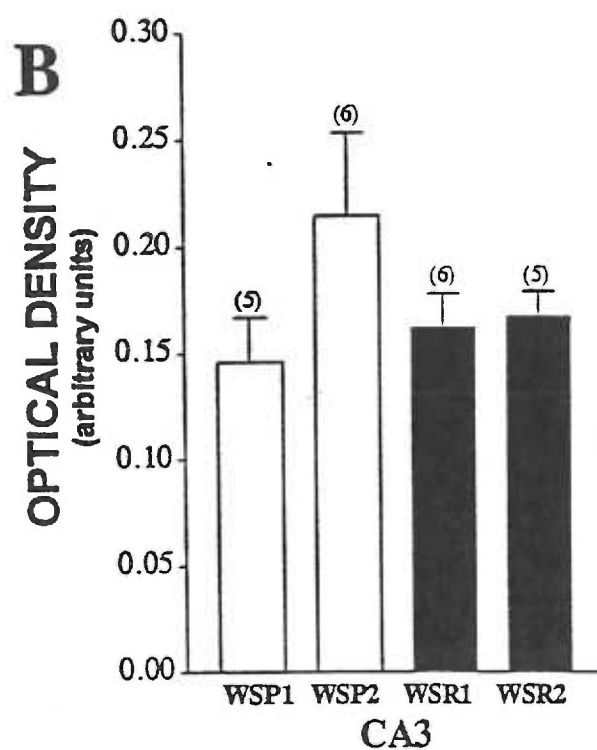
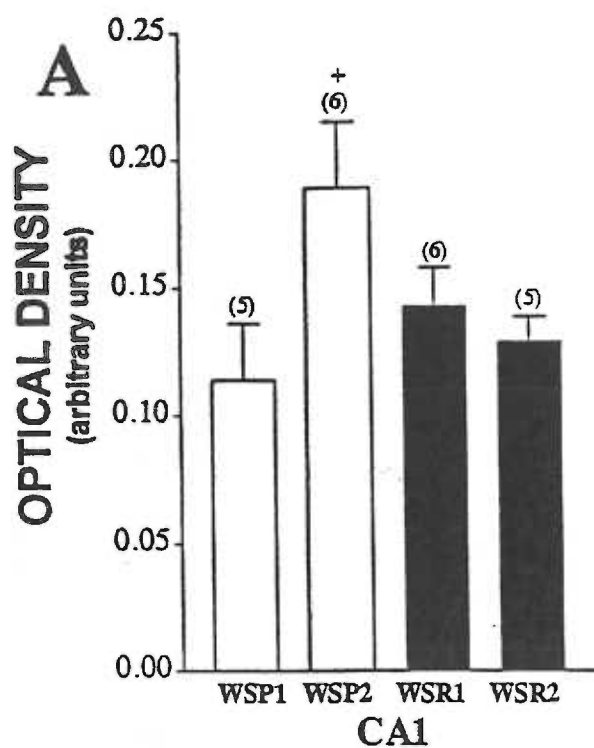


Figure 15

Immunoperoxidase staining for GLT-1 in naive WSP and WSR mice

Depicted is a representative 50 μm slice from one (A) WSP-2 and (B) WSR-2 mouse following overnight incubation in a primary antibody against GLT-1, the most abundant glial glutamate transporter. The regions analyzed include the stratum radiatum (located directly below pyramidal cell layer in the hippocampus, *arrowhead*) of the CA1 and CA3, the molecular layer of the dentate gyrus and the somatosensory cortex (Figs. 2 and 13). Scale bar, 200 μm .

A



B



Figure 16

Density of the glial transporter GLT-1 immunolabeling in hippocampus and cortex

(A) stratum radiatum of the CA1 (CA1), (B) stratum radiatum of the CA3 (CA3), (C) molecular layer of the dentate gyrus (DG), (D) somatosensory cortex (SSC). Depicted is the mean optical density (\pm SEM), in arbitrary units, of GLT-1 immunolabeling in naive WSP and WSR mice from both replicate lines. The number of tissue slices analyzed per group is presented above each bar. No significant differences between any groups were observed in any region tested. CA1: selected line ($F_{(1,26)}=1.2$, NS); replicate line ($F_{(1,26)}=1.5$, NS); selected x replicate line interaction: ($F_{(1,26)}=0.3$, NS). CA3: selected line ($F_{(1,25)}=3.4$, $p=0.076$); replicate line ($F_{(1,25)}=0.8$, NS); selected x replicate line interaction: ($F_{(1,25)}=1.0$, NS). DG: selected line ($F_{(1,27)}=0.3$, NS); replicate line ($F_{(1,27)}=0.001$, NS); selected x replicate line interaction: ($F_{(1,27)}=0.5$, NS). SSC: selected line ($F_{(1,25)}=1.3$, NS); replicate line ($F_{(1,25)}=0.001$, NS); selected x replicate line interaction: ($F_{(1,25)}=0.6$, NS). Because no differences between replicate lines were observed, data were collapsed. A one-way ANOVA comparing pooled WSP and WSR data revealed no significant differences, although a trend towards significance was observed in the CA3: $F_{(1,27)}=3.8$, $p=0.0625$.

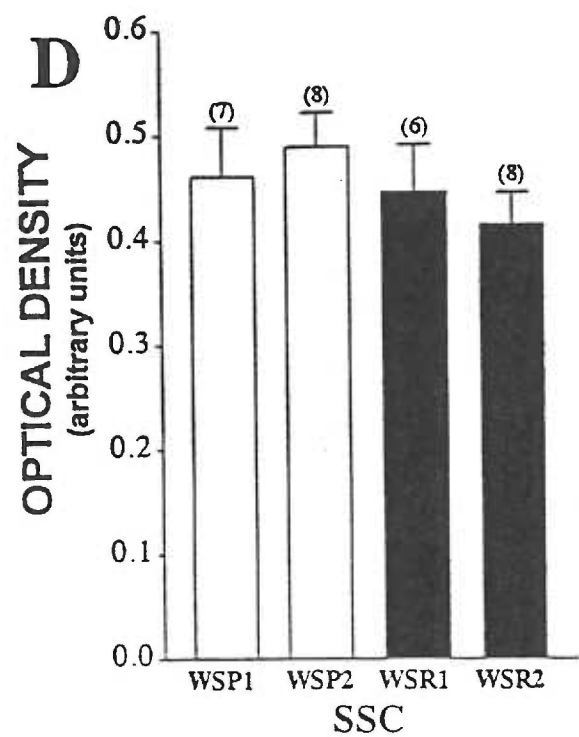
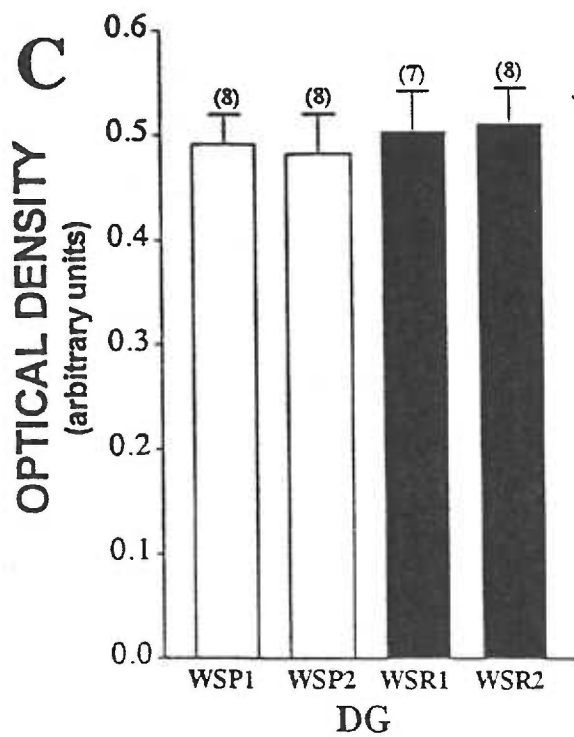
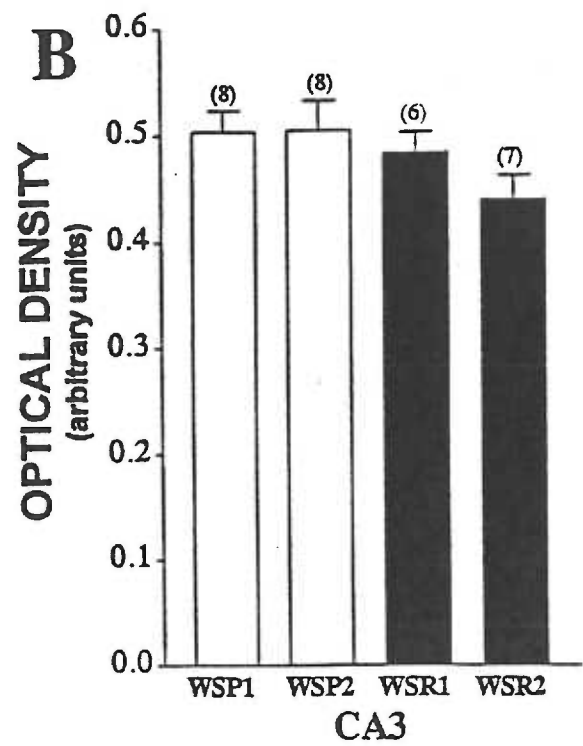
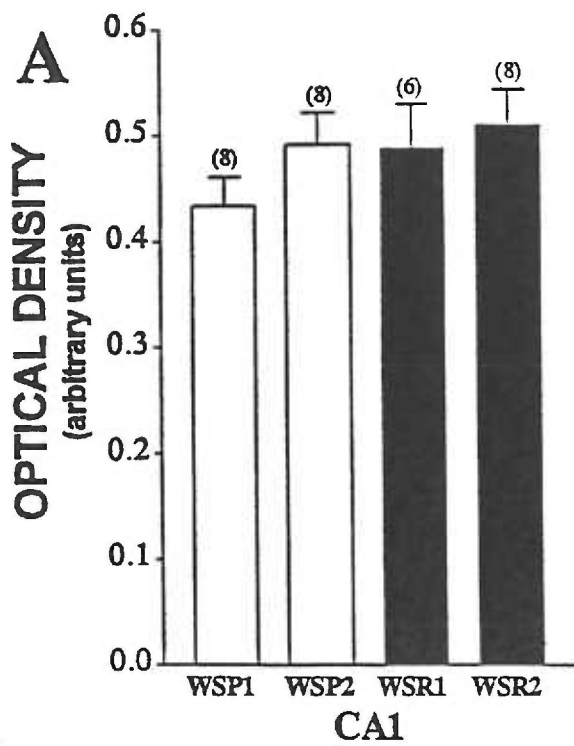
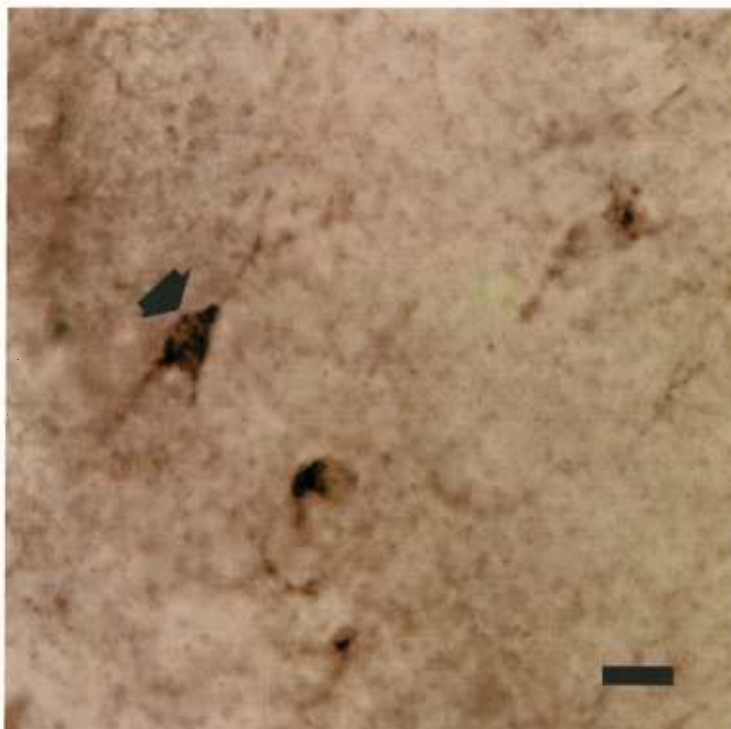


Figure 17

Immunoperoxidase staining for EAAC1 in naive WSP and WSR mice

Presented is the CA1 pyramidal cell layer from a representative 50 μm slice from one (A) WSP-2 and (B) WSR-2 mouse following overnight incubation in a primary antibody against EAAC1, a neuronal glutamate transporter. The density of immunolabeling within individual pyramidal cell bodies (*solid arrow*) in the CA1 was analyzed. Note the labeled proximal process (*dotted arrow*) and the unlabeled nucleus (*open arrow*) in (B). Scale bar, 20 μm .

A



B

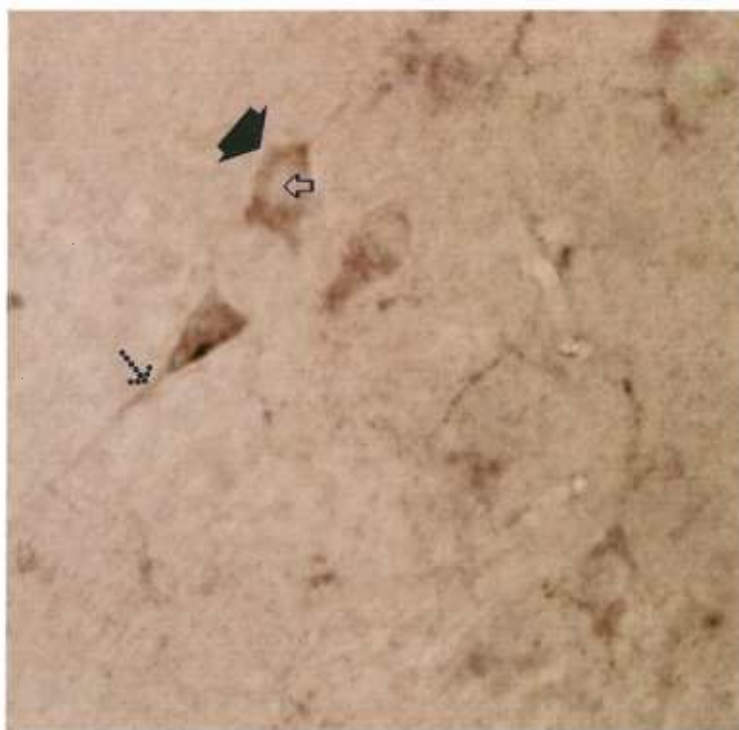


Figure 18

Density of the neuronal transporter EAAC1 immunolabeling in hippocampus

The mean optical density of immunolabeling from pyramidal cells in the CA1 (CA1).

Depicted is the mean optical density (\pm SEM), in arbitrary units, of individual pyramidal cell EAAC1 immunolabeling from naive WSP and WSR mice from both replicate lines.

The number of tissue slices analyzed per group is presented above each bar. A total of

47 cells from WSP-1, 56 cells from WSP-2, 16 cells from WSR-1 and 44 cells from

WSR-2 slices were used in the analysis. Data from all cells from each animal were

combined and averaged and data from all animals from each mouse line were combined

and averaged. No significant differences between any groups were observed. CA1:

selected line ($F_{(1,16)}=0.56$, NS); replicate line ($F_{(1,16)}=0.16$, NS); selected x replicate line

($F_{(1,16)}=2.7$, $p = 0.12$).

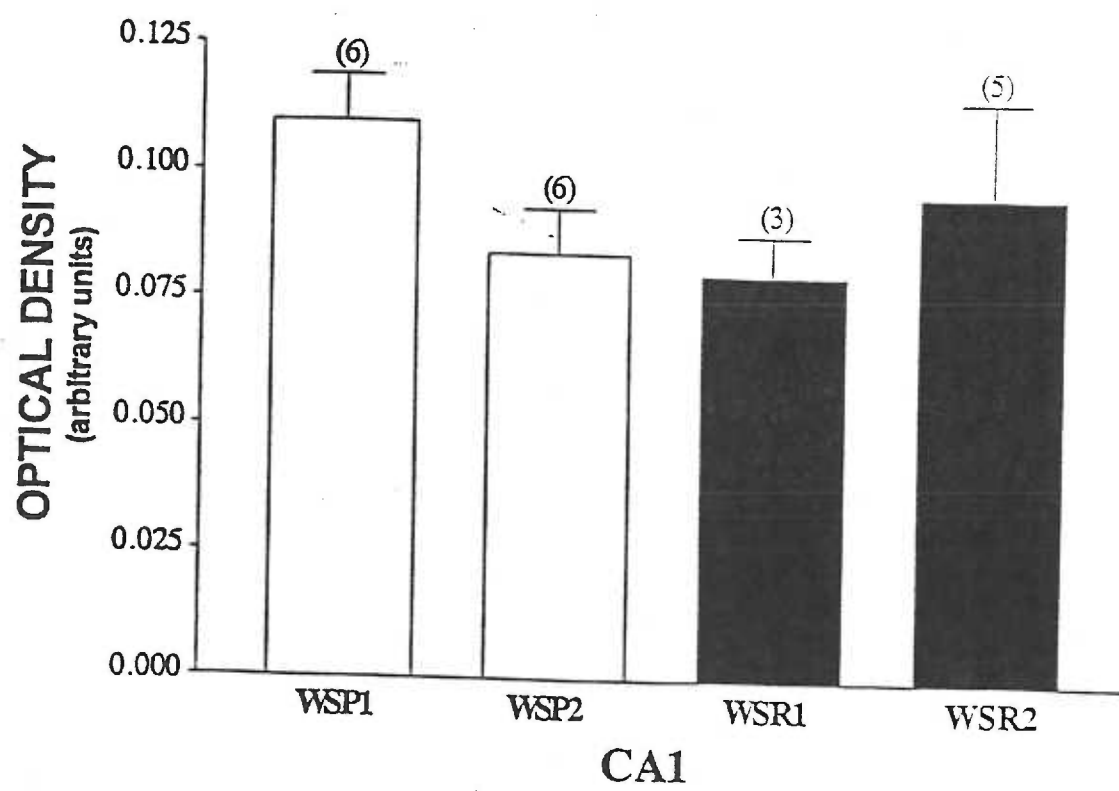
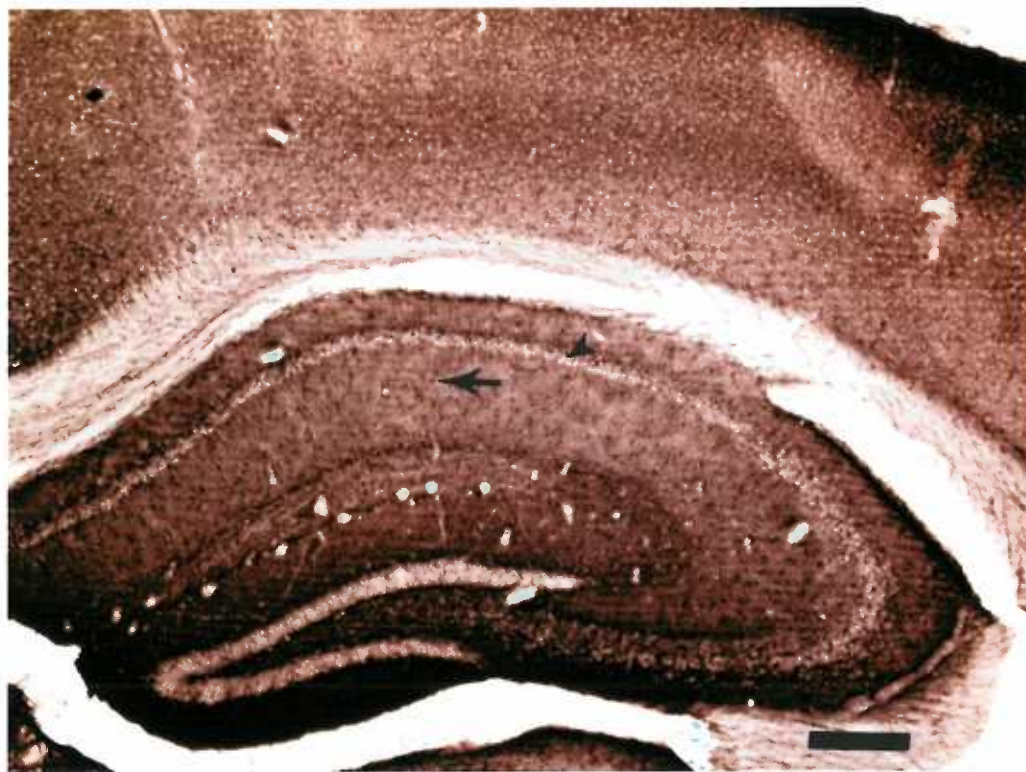


Figure 19

Immunoperoxidase staining for glutamine synthetase in naive WSP and WSR mice

Depicted is a representative 50 μm slice from one (A) WSP-2 and (B) WSR-2 mouse following overnight incubation in a primary antibody against glial metabolic enzyme, glutamine synthetase (GS). The stratum radiatum of the CA1 and CA3 was analyzed, as was the molecular layer of the dentate gyrus and the somatosensory cortex (Figs. 2 and 13). Examples of a labeled glial cell (*arrow*) and an unlabeled pyramidal cell (*arrowhead*) are shown in (A). Scale bar, 200 μm .

A



B



Figure 20

Density of glutamine synthetase (GS) immunolabeling in hippocampus and cortex

(A) stratum radiatum of the CA1 (CA1), (B) stratum radiatum of the CA3 (CA3), (C) molecular layer of the dentate gyrus (DG), (D) somatosensory cortex (SSC). Depicted is the mean optical density (\pm SEM), in arbitrary units, of GS immunolabeling from naive WSP and WSR mice from both replicate lines. The number of tissue slices per group used in each analysis is presented above each bar. No significant differences between any groups were observed in any region tested. CA1: selected line ($F_{(1,20)}=1.3$, NS); replicate line ($F_{(1,20)}=0.3$, NS); selected x replicate line interaction: ($F_{(1,20)}=1.6$, NS). CA3: selected line ($F_{(1,21)}=0.1$, NS); replicate line ($F_{(1,21)}=0.2$, NS); selected x replicate line interaction: ($F_{(1,21)}=1.1$, NS). DG: selected line ($F_{(1,19)}=0.4$, NS); replicate line ($F_{(1,19)}=1.0$, NS); selected x replicate line interaction: ($F_{(1,19)}=0.4$, NS). SSC: selected line ($F_{(1,21)}=1.6$, NS); replicate line ($F_{(1,21)}=0.1$, NS); selected x replicate line interaction: ($F_{(1,21)}=0.4$, NS). However, when the mean optical density data from replicate line 2 mice was analyzed separately using an unpaired t-test, a trend suggested that naive WSP-2 had more GS labeling as compared to naive WSR-2 mice in the CA1 ($t=1.87$; $p = 0.091$) and the somatosensory cortex ($t=1.88$, $p=0.087$).

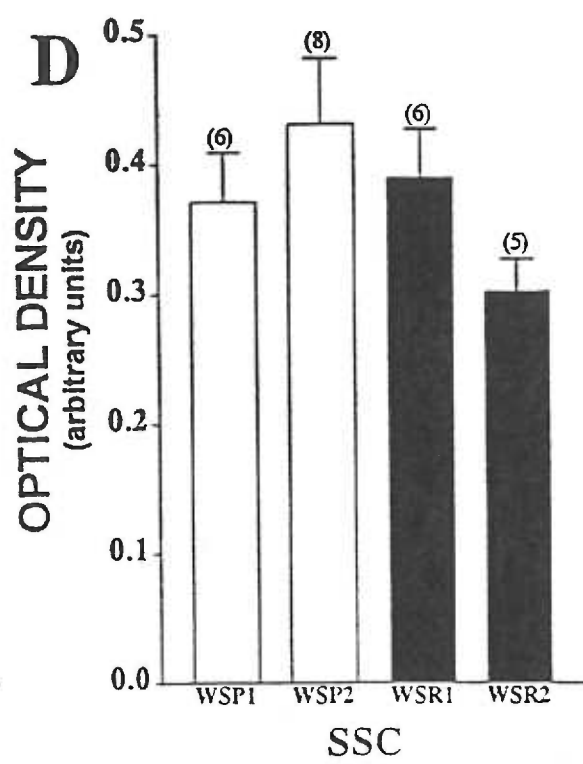
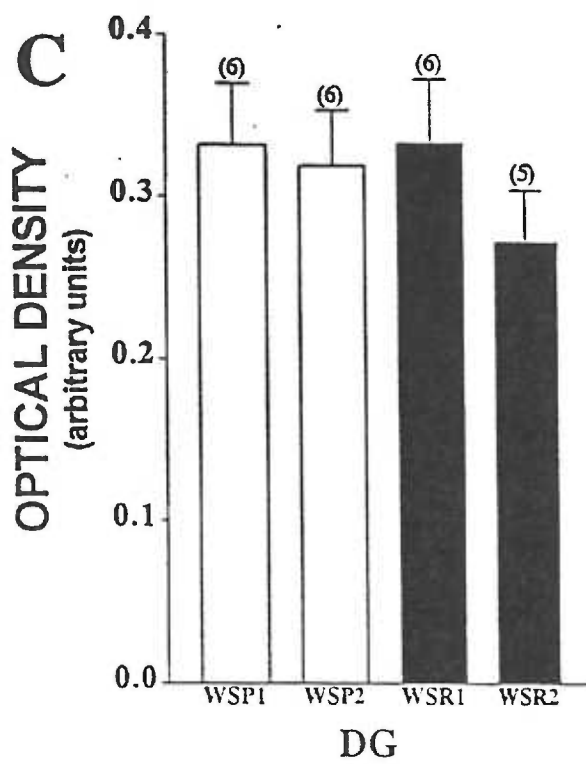
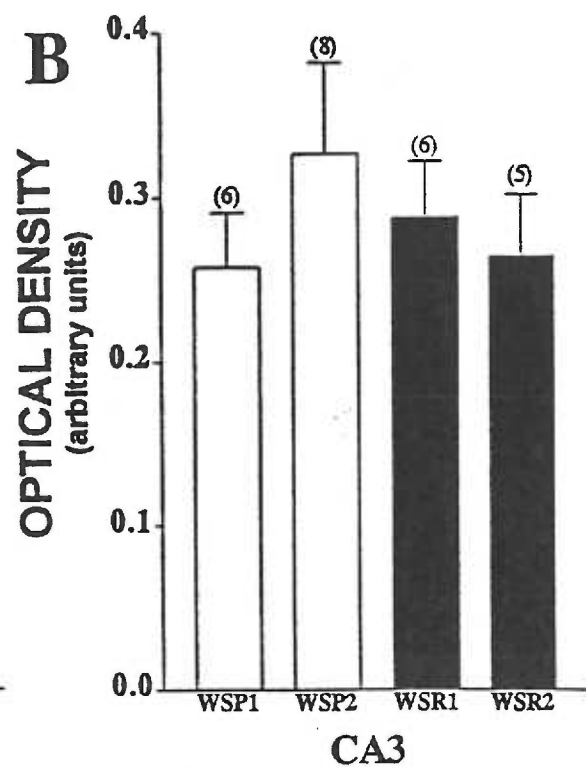
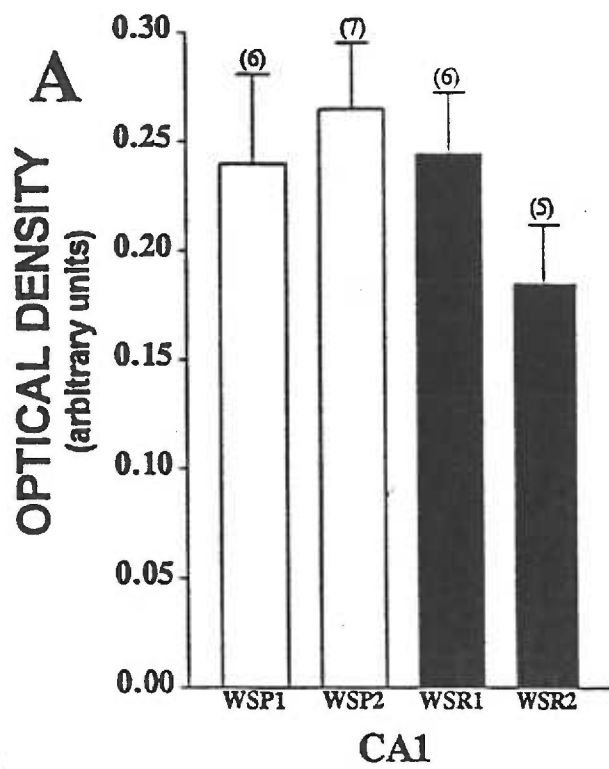
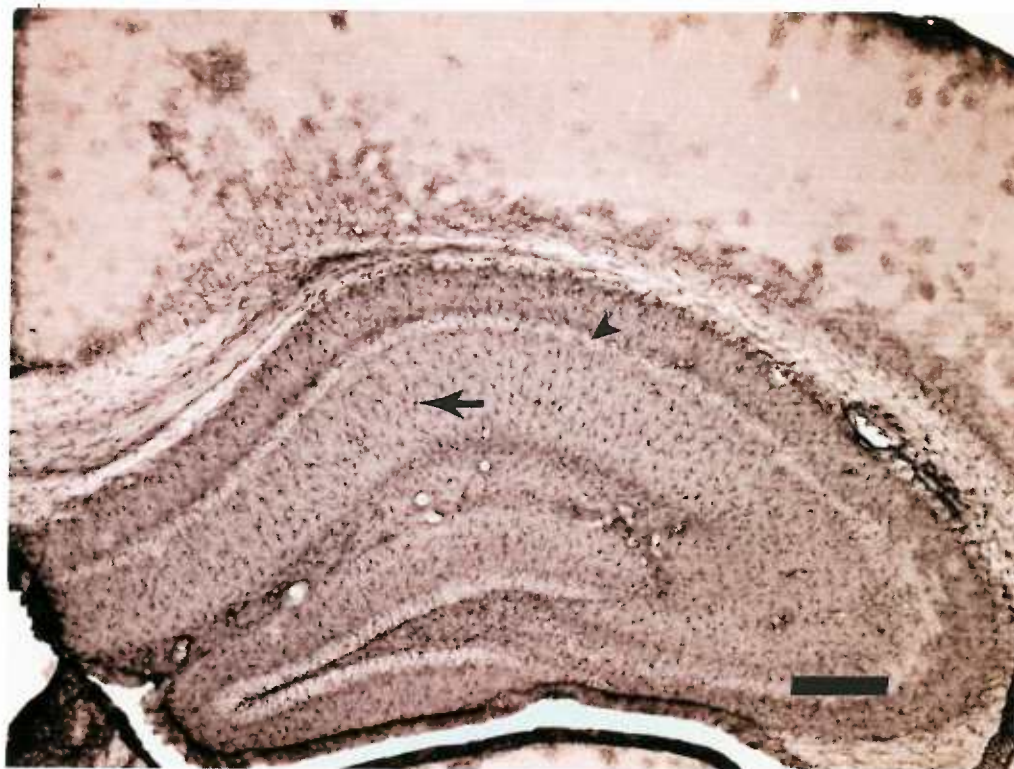


Figure 21

Immunoperoxidase staining for GFAP in naive WSP and WSR mice

Represented are 50 μm slices from a (A) WSP-2 mouse; (B) WSR-2 mouse following overnight incubation in a primary antibody against glial fibrillary acidic protein (GFAP). Individual labeled glial cells (*arrow*) can be seen throughout the hippocampus. Note the unlabeled pyramidal cell layer (*arrowhead*). Labeling in the cortex varied between layers, with the most apparent staining seen in the superficial and deep layers. The density of immunolabeling in the stratum radiatum of the CA1 and CA3, the molecular layer of the dentate gyrus and the somatosensory cortex were analyzed (Figs. 2 and 13). Scale bar, 200 μm .

A



B

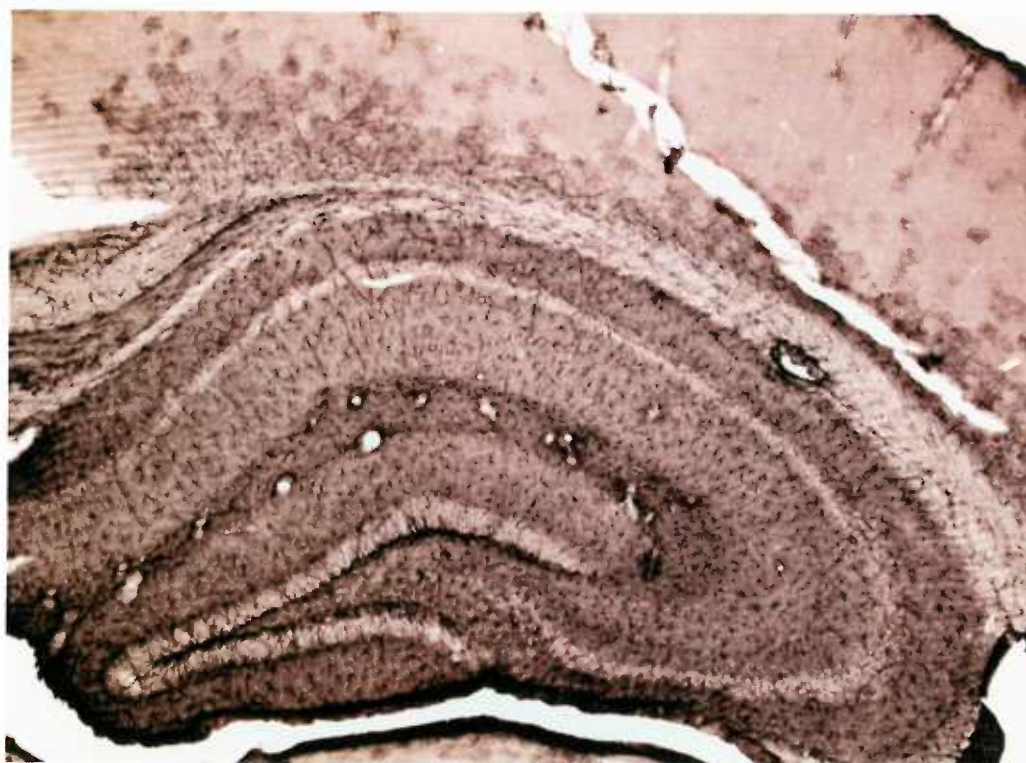
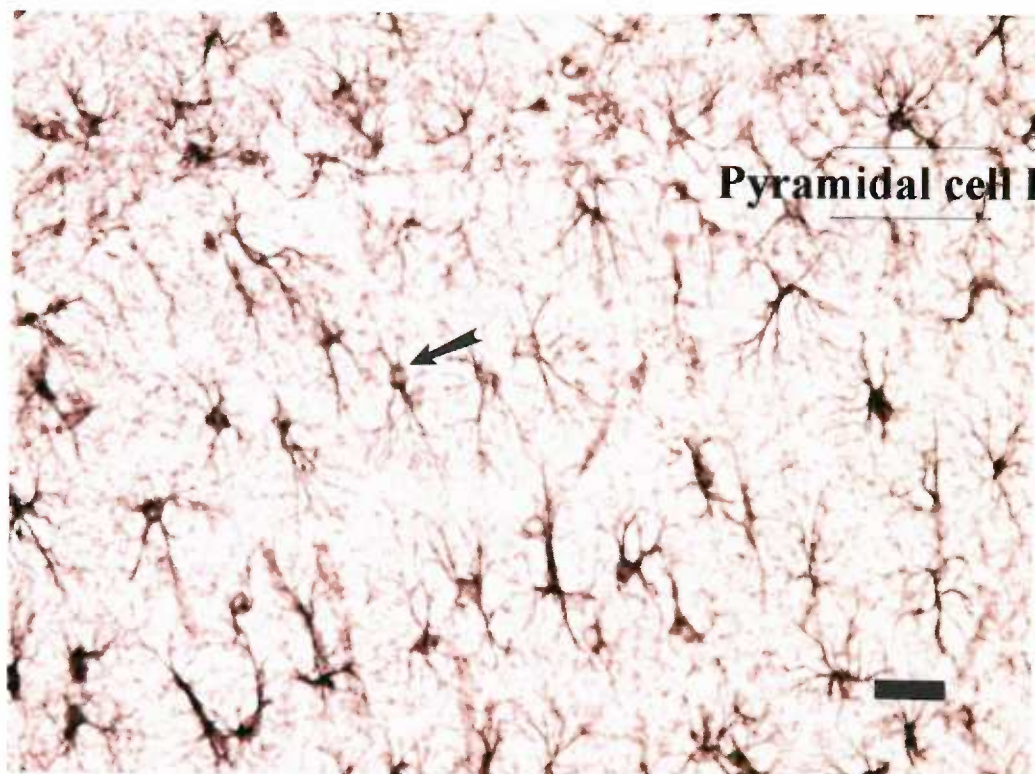


Figure 22

Immunoperoxidase staining for GFAP in glial cell bodies of naive WSP and WSR mice

Representative 50 μm slices that were visualized at high magnification from a (A) WSP-2 mouse; (B) WSR-2 mouse following overnight incubation in a primary antibody against glial structural protein, glial fibrillary acidic protein (GFAP) are presented. Individual glial cell bodies display intense staining (*arrow*). The neurons within the pyramidal cell layer, however, do not appear labeled. The number of cells, the area of cell bodies and the density of labeling within the cell bodies were analyzed in the stratum radiatum (directly below the pyramidal cell layer) of the CA1 region of the hippocampus. Scale bar, 20 μm .

A



B

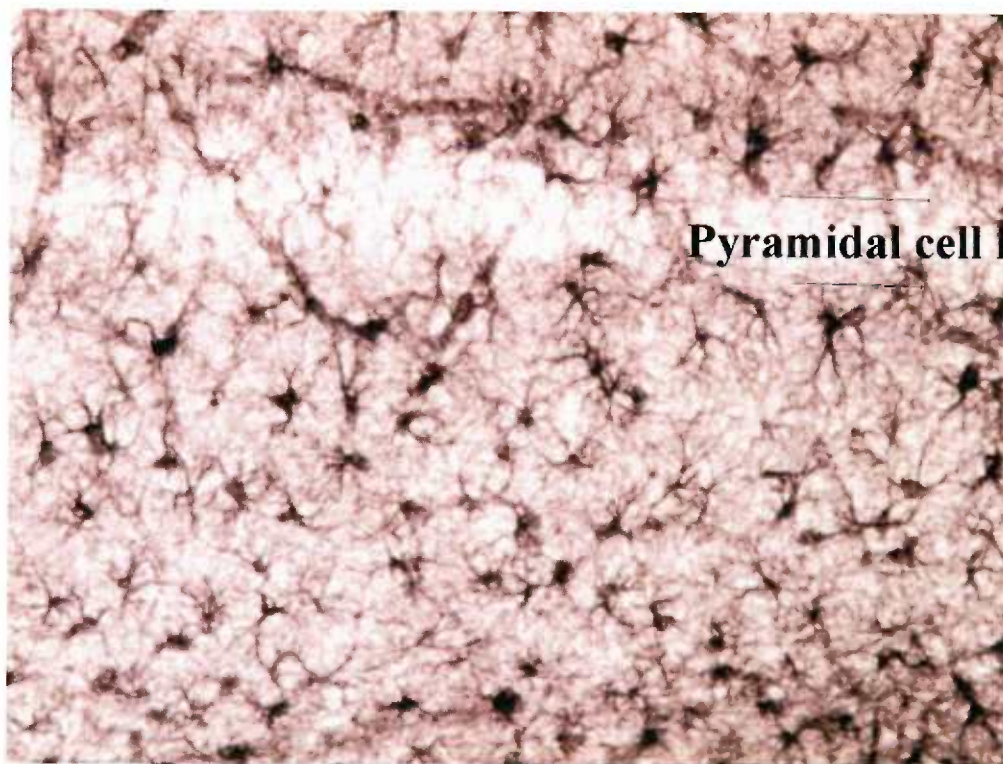


Figure 23

Density of GFAP immunolabeling in hippocampus and cortex

(A) stratum radiatum of the CA1 (CA1), (B) stratum radiatum of the CA3 (CA3), (C) molecular layer of the dentate gyrus (DG), (D) somatosensory cortex (SSC). Depicted is the mean optical density (\pm SEM), in arbitrary units, of GFAP immunolabeling from naive WSP and WSR mice from both replicate lines. The number of tissue slices per group used in each analysis is presented above each bar. A significant difference between the replicate lines was observed in the CA1 but no other significant differences were detected. Differences between the selected lines, though, did approach significance in all brain regions. The lack of significance between selected lines is most likely due to the small number of subjects used in this analysis. CA1: selected line ($F_{(1,8)}=3.2$, $p=0.11$); replicate line ($F_{(1,8)}=10.8$, $p=0.011$); selected x replicate line interaction: ($F_{(1,8)}=0.18$, NS). CA3: selected line ($F_{(1,8)}=3.8$, $p=0.087$); replicate line ($F_{(1,8)}=3.2$, $p=0.11$); selected x replicate line interaction: ($F_{(1,8)}=0.02$, NS). DG: selected line ($F_{(1,8)}=5.1$, $p=0.0538$); replicate line ($F_{(1,8)}=1.9$, NS); selected x replicate line interaction: ($F_{(1,8)}=1.0$, NS). SSC: selected line ($F_{(1,8)}=4.0$, $p=0.08$); replicate line ($F_{(1,8)}=2.5$, NS); selected x replicate line interaction: ($F_{(1,8)}=1.9$, NS).

[* $p < 0.05$, WSP-1 vs. WSP-2 and WSR-1 vs. WSR-2].

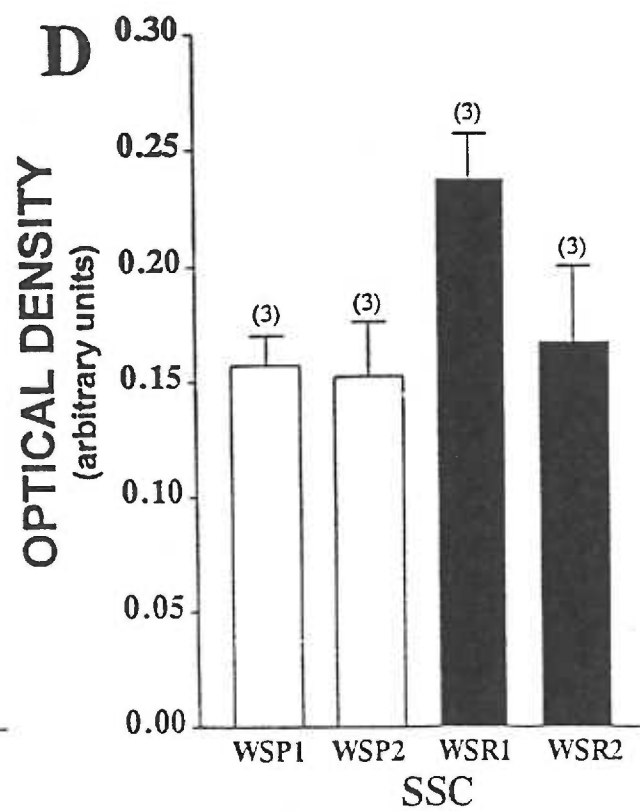
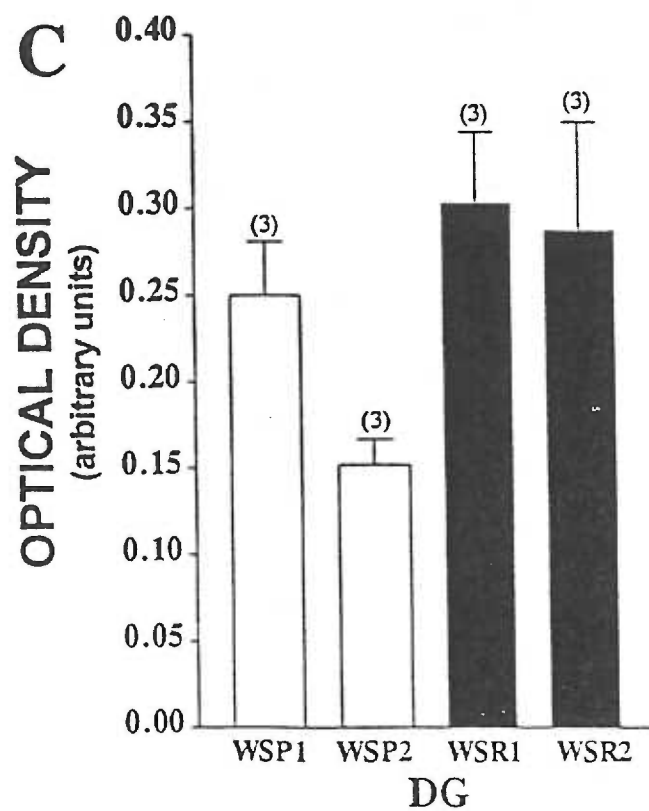
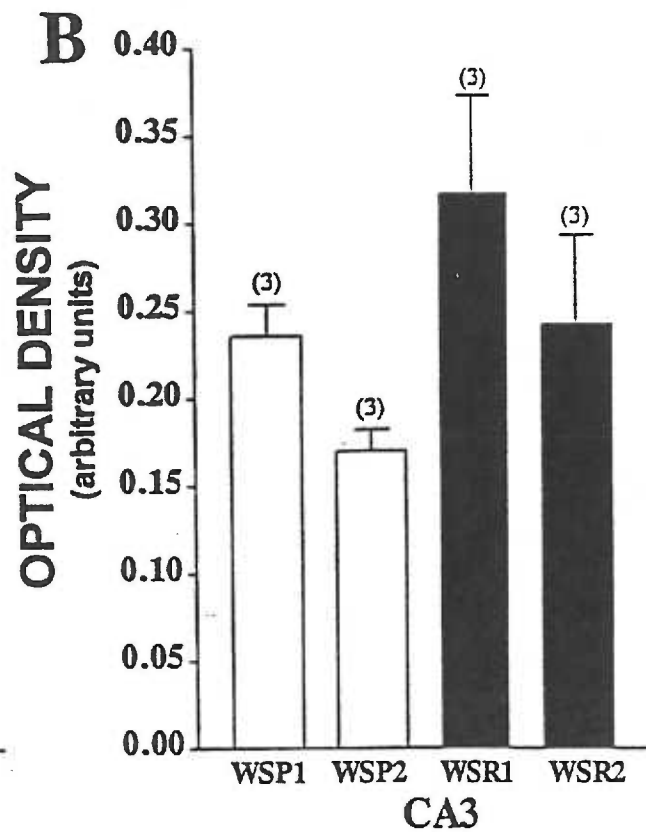
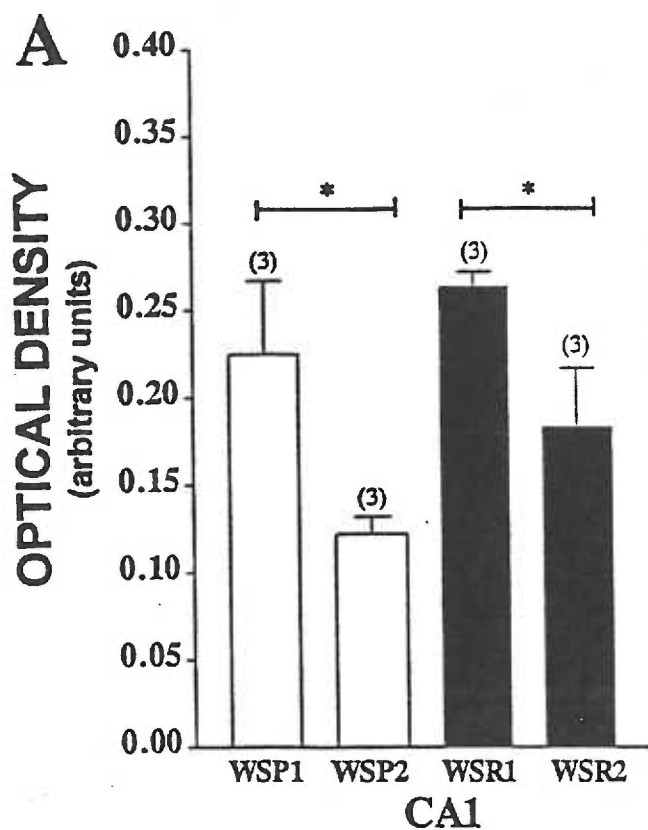


Figure 24

GFAP immunoreactivity within single glial cells from the CA1 region of the hippocampus

(A) the mean number of glial cells (\pm SEM) in an area of interest ($280 \times 140\mu\text{m}$) within the stratum radiatum of the CA1 region of the hippocampus, (B) the area of the glial cell bodies (\pm SEM), in arbitrary units, within this area and (C) the mean optical density (\pm SEM), in arbitrary units, of GFAP immunolabeling within these cell bodies from naive WSP and WSR mice from both replicate lines. The number of tissue slices per group used in each analysis is presented above each bar. Significant differences between the replicate lines was observed in the mean optical density of cell body immunolabeling (C), but no differences in the number or area of the cell bodies were detected. Analysis of the number of immunopositive cells in the CA1 revealed: selected line ($F_{(1,8)}=2.0$, NS); replicate line ($F_{(1,8)}=1.3$, NS); selected x replicate line interaction: ($F_{(1,8)}=2.3$, NS). Analysis of the area of immunopositive glial cell bodies revealed: selected line ($F_{(1,8)}=1.0$, NS); replicate line ($F_{(1,8)}=0.9$, NS); selected x replicate line interaction: ($F_{(1,8)}=0.11$, NS). Analysis of the mean optical density of immunopositive cell bodies revealed: selected line ($F_{(1,8)}=0.07$, NS); replicate line ($F_{(1,8)}=8.9$, $p=0.018$); selected x replicate line interaction: ($F_{(1,8)}=0.6$, NS). [$* p < 0.05$, WSP-1 vs. WSP-2 and WSR-1 vs. WSR-2].

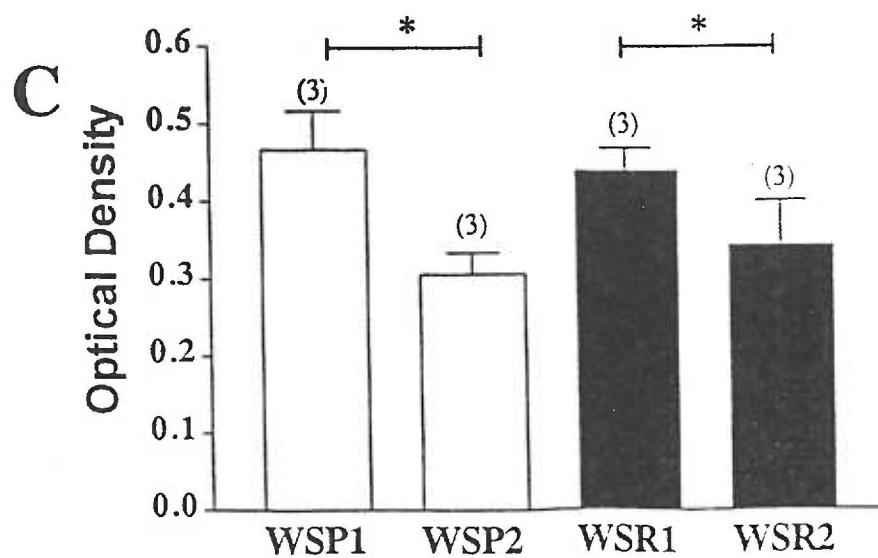
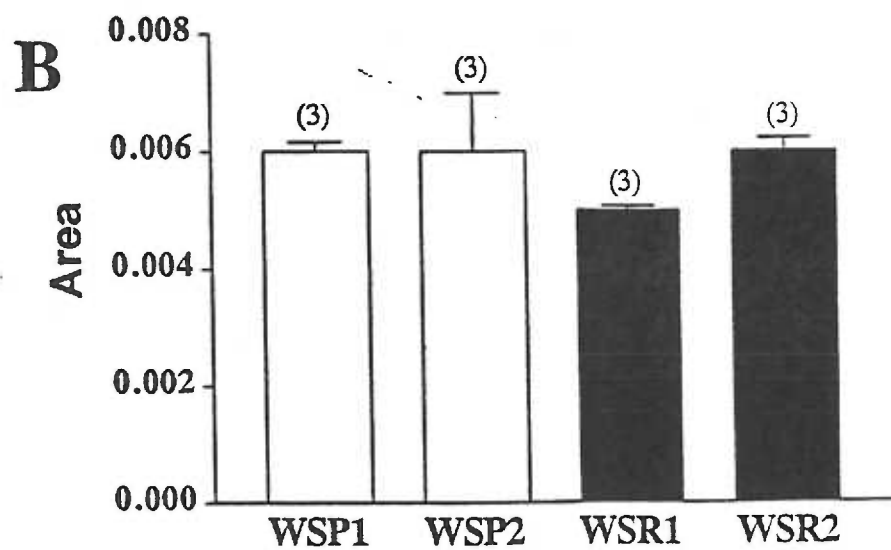
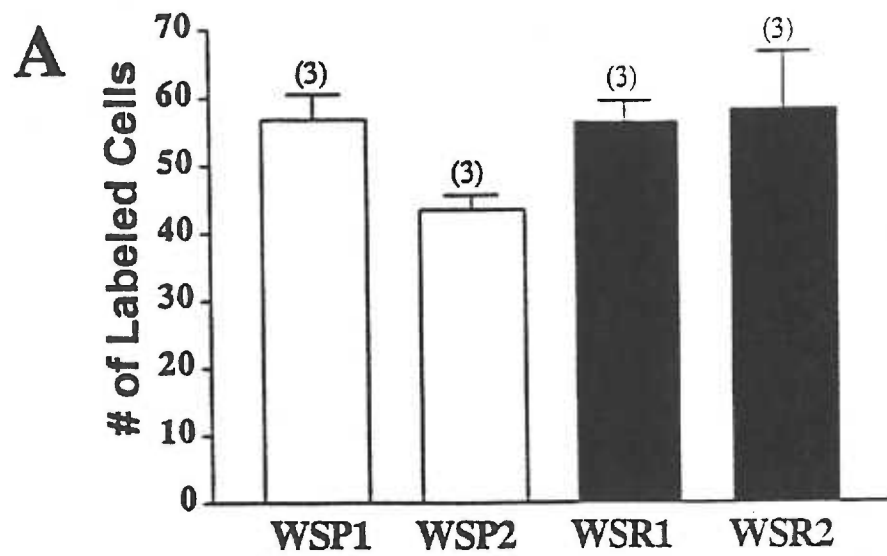
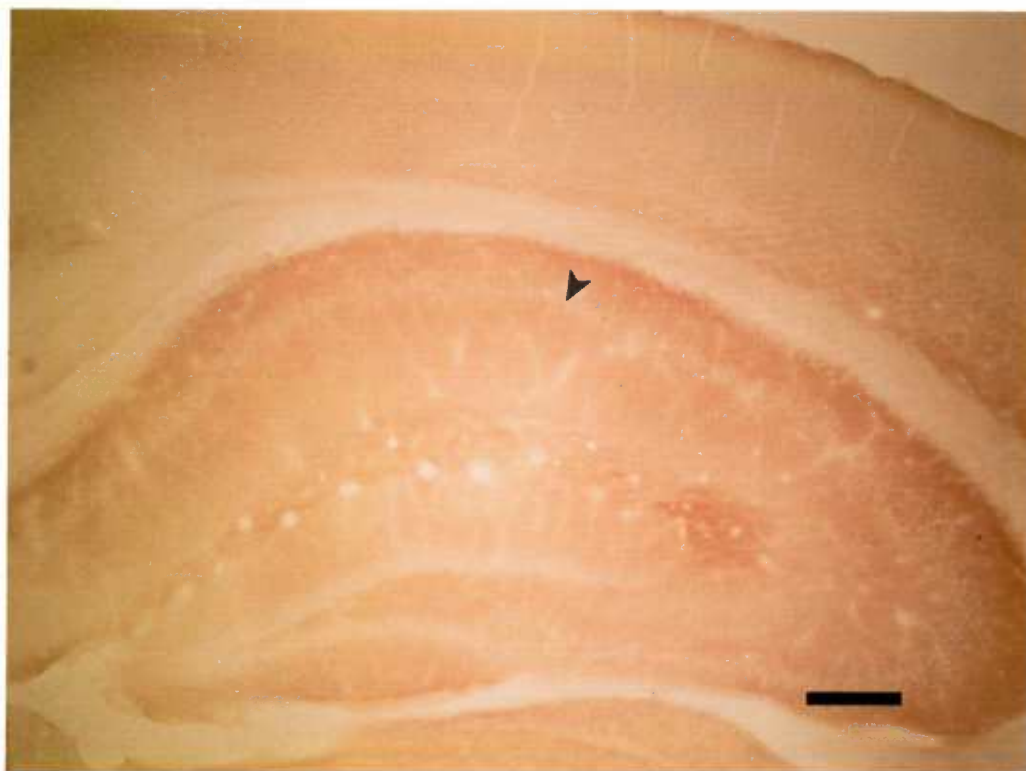


Figure 25

Cytochrome oxidase activity assessed by peroxidase reactivity in naive WSP and WSR mice

Presented is a representative 100 μm slice from one (A) WSP-2 and (B) WSR-2 mouse following a 15 minute incubation in cytochrome c (cytochrome oxidase substrate) and diaminobenzidine (DAB, the reaction product visualizing agent). The reaction is observable as an orange-brown stain seen throughout the hippocampus and cortex. Note the lack of staining seen in the neuronal cell bodies in the stratum pyramidale (*arrowhead*). Cytochrome oxidase activity in the stratum radiatum of the CA1 and CA3 was analyzed, as was the molecular layer of the dentate gyrus and the somatosensory cortex (Figs. 2 and 13). Scale bar, 200 μm .

A



B



Figure 26

Cytochrome oxidase activity in hippocampus and cortex

(A) stratum radiatum of the CA1 (CA1), (B) stratum radiatum of the CA3 (CA3), (C) molecular layer of the dentate gyrus (DG), (D) somatosensory cortex (SSC). Depicted is the mean optical density (\pm SEM), in arbitrary units, representing the activity of the mitochondrial enzyme cytochrome oxidase in naive WSP and WSR mice from both replicate lines. The number of tissue slices per group used in each analysis is presented above each bar. No significant differences between any groups were observed in any brain region tested. CA1: selected line: ($F_{(1,48)}=0.4$, NS); replicate line: ($F_{(1,48)}=0.3$, NS); selected x replicate line interaction: ($F_{(1,48)}=0.1$, NS). CA3: selected line: ($F_{(1,49)}=1.0$, NS); replicate line: ($F_{(1,49)}=0.8$, NS); selected x replicate line interaction: ($F_{(1,49)}=0.9$, NS). DG: selected line: ($F_{(1,48)}=1.3$, NS); replicate line: ($F_{(1,48)}=0.3$, NS); selected x replicate line interaction: ($F_{(1,48)}=0.2$, NS). SSC: selected line: ($F_{(1,49)}=0.04$, NS); replicate line: ($F_{(1,49)}=0.4$, NS); selected x replicate line interaction: ($F_{(1,49)}=0.4$, NS). Data were collapsed across replicate line but no significant differences were observed.

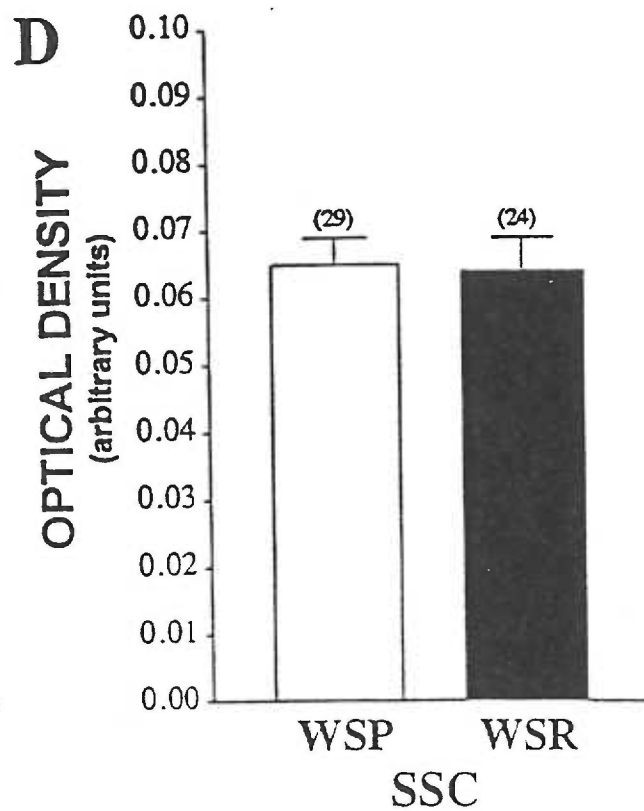
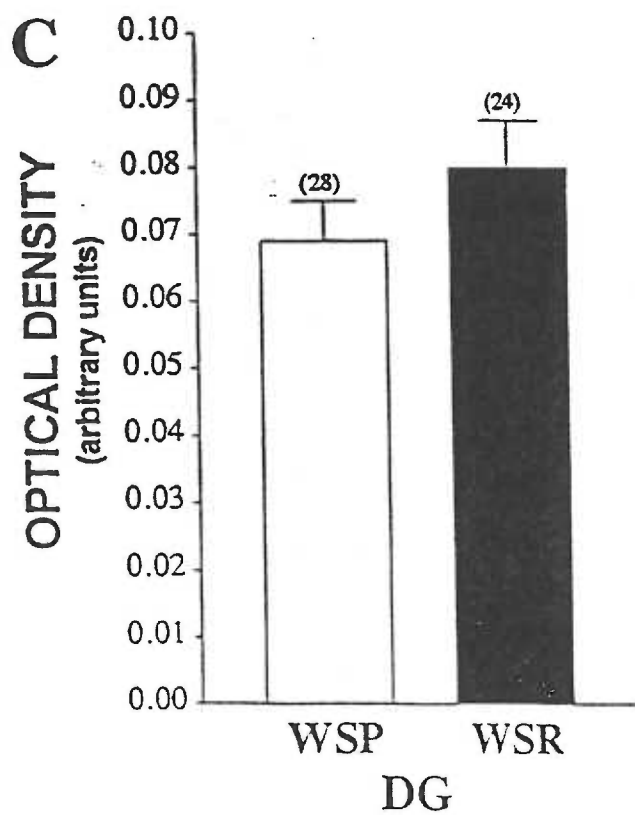
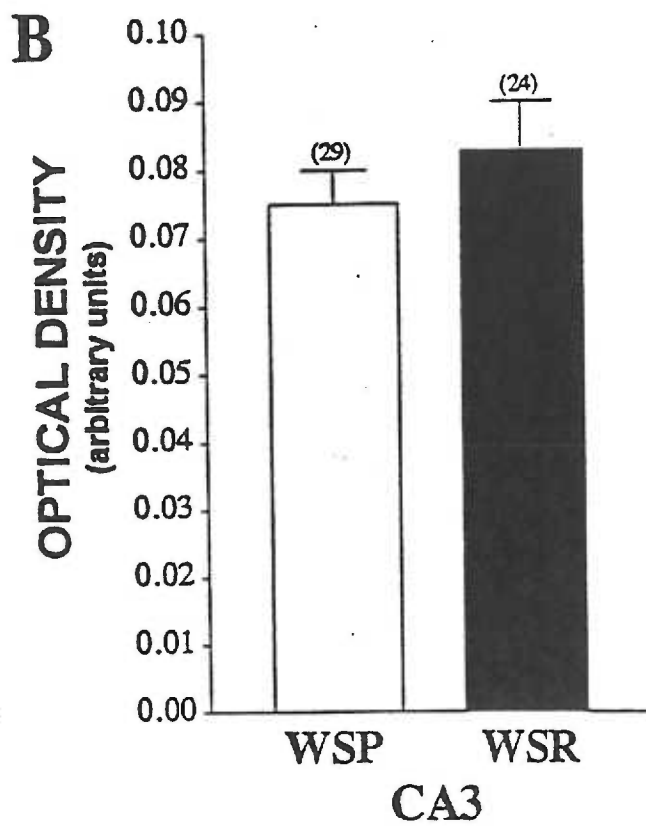
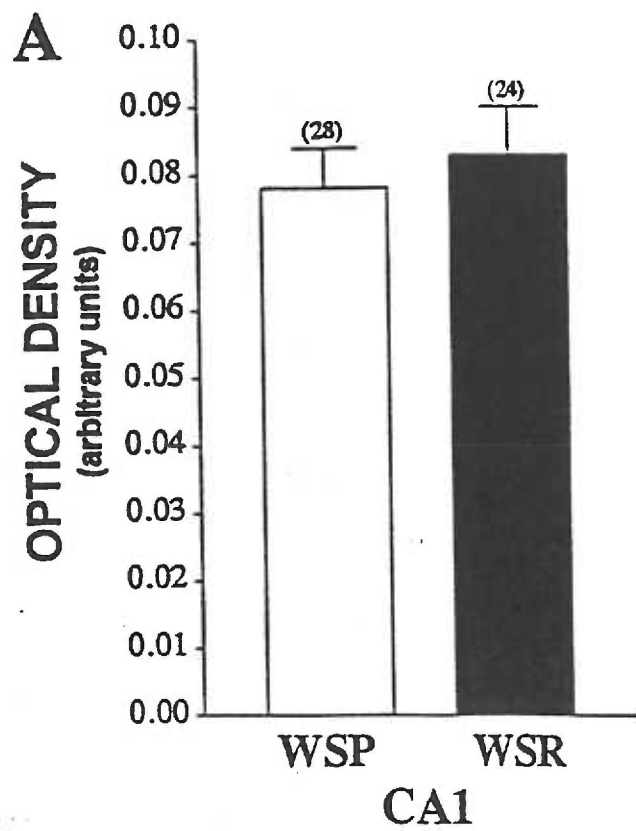


Table 4

Summary of results from experiments performed in drug- and convulsion-naïve WSP and WSR mice

Experiment	Brain Region	Results
L-[³ H]glutamate uptake	Hippocampus Cortex	WSP = WSR WSP = WSR
GLAST immunocytochemistry	CA1 CA3 DG SSC	WSP2 > WSR2** WSP = WSR WSP = WSR WSP = WSR
GLT-1 immunocytochemistry	CA1 CA3 DG SSC	WSP = WSR WSP > WSR ⁺ WSP = WSR WSP = WSR
EAAC1 immunocytochemistry	CA1	WSP = WSR
Glutamine Synthetase	CA1 CA3 DG SSC	WSP2 > WSR2 ⁺ WSP = WSR WSP = WSR WSP2 > WSR2 ⁺
GFAP immunocytochemistry	CA1 CA3 DG SSC	Replicate-1 > Replicate-2* WSP < WSR [#] WSP < WSR ⁺ WSP < WSR ⁺ WSP < WSR ⁺
Glial cell body area	CA1	Replicate-1 > Replicate-2*
Cytochrome oxidase	CA1 CA3 DG SSC	WSP = WSR WSP = WSR WSP = WSR WSP = WSR

p = 0.11
+ p < 0.1
* p < 0.05
** p < 0.01

Table 5Summary of results from L-[³H]glutamate uptake experiments

Experiment	Brain Region	V _{max}	K _m
Handling (effect of handling throughout lifetime)	Hippocampus	WSP < WSR [#] <i>no treatment effect</i>	WSP = WSR <i>no treatment effect</i>
	Cortex	WSP = WSR <i>no treatment effect</i>	WSP = WSR <i>no treatment effect</i>
Acute HIC activity	Hippocampus	WSP2 = WSR2 <i>no treatment effect</i>	WSP2 < WSR2 [#] <i>no treatment effect interaction⁺</i>
	Cortex	WSP2 = WSR2 <i>no treatment effect</i>	WSP2 = WSR2 <i>no treatment effect</i>
Acute EtOH intoxication	Hippocampus	WSP2 = WSR2 <i>no treatment effect interaction[#]</i>	WSP2 = WSR2 <i>no treatment effect</i>
	Cortex	WSP2 = WSR2 <i>no treatment effect</i>	WSP2 = WSR2 <i>no treatment effect</i>
<i>In vitro</i> EtOH exposure	Hippocampus	<i>no dose-response curve</i>	
EtOH withdrawal	Hippocampus	WSP = WSR ↑ by withdrawal**	WSP = WSR <i>no treatment effect</i>

p < 0.15

+ p < 0.1

** p < 0.01